UNIVERSIDADE FEDERAL DO RIO GRANDE DO SUL

INSTITUTO DE PESQUISAS HIDRÁULICAS

PROGRAMA DE PÓS-GRADUAÇÃO EM RECURSOS HÍDRICOS E SANEAMENTO AMBIENTAL

JOÃO PAULO LYRA FIALHO BRÊDA

IMPACTOS DAS MUDANÇAS CLIMÁTICAS SOBRE OS RECURSOS HÍDRICOS DA AMÉRICA DO SUL ATRAVÉS DE PROJEÇÕES DO CMIP5

PORTO ALEGRE

2021

JOÃO PAULO LYRA FIALHO BRÊDA

IMPACTOS DAS MUDANÇAS CLIMÁTICAS SOBRE OS RECURSOS HÍDRICOS DA AMÉRICA DO SUL ATRAVÉS DE PROJEÇÕES DO CMIP5

Tese apresentada ao Programa de Pós-graduação em Recursos Hídricos e Saneamento Ambiental da Universidade Federal do Rio Grande do Sul, como requisito parcial à obtenção do grau de doutor.

Orientador: Rodrigo Cauduro Dias de Paiva

Coorientador: Walter Collischonn

PORTO ALEGRE

2021

Brêda, João Paulo L. F.
Impactos das Mudanças Climáticas sobre os Recursos Hídricos da América do Sul através de Projeções do CMIP5 / João Paulo L. F. Brêda. -- 2021.
110 f.
Orientador: Rodrigo C. D. Paiva.

Coorientador: Walter Collischonn.

Tese (Doutorado) -- Universidade Federal do Rio Grande do Sul, Instituto de Pesquisas Hidráulicas, Programa de Pós-Graduação em Recursos Hídricos e Saneamento Ambiental, Porto Alegre, BR-RS, 2021.

1. Mudanças Climáticas. 2. América do Sul. 3. Disponibilidade Hídrica. 4. Vazão de Cheia. 5. Precipitação Extrema. I. Paiva, Rodrigo C. D., orient. II. Collischonn, Walter, coorient. III. Título.

JOÃO PAULO LYRA FIALHO BRÊDA

IMPACTOS DAS MUDANÇAS CLIMÁTICAS SOBRE OS RECURSOS HÍDRICOS DA AMÉRICA DO SUL ATRAVÉS DE PROJEÇÕES DO CMIP5

Tese apresentada ao Programa de Pós-graduação em Recursos Hídricos e Saneamento Ambiental da Universidade Federal do Rio Grande do Sul, como requisito parcial à obtenção do grau de doutor.

Aprovado em: Porto Alegre, 14 de dezembro de 2021.

Prof. Dr Rodrigo Cauduro Dias de Paiva – IPH/UFRGS
Orientador

Prof. Dr Walter Collischonn – IPH/UFRGS
Coorientador

Prof. Dr Francisco de Assis de Souza Filho – UFC
Examinador

Dr André de Arruda Lyra – INPE
Examinador

Prof. Dr Juan Martin Bravo – IPH/UFRGS
Examinador

AGRADECIMENTOS

Agradeço

aos meus amigos do IPH e HGE que fizeram com que minha vida em Porto Alegre fosse tão especial. Sentirei muita falta de todos, os que permanecem e os que já passaram por esses 7 incríveis anos nesse instituto;

à minha família que me deu uma segurança enorme, que sempre me amou e me apoiou apesar da minha teimosia e rigidez;

e aos meus orientadores que me deram oportunidade de pesquisar temas excelentes e foram essenciais no meu desenvolvimento. Sem a empolgação, ideias e o conhecimento de vocês minha tese teria sido medíocre.

RESUMO

As mudanças climáticas são comuns e recorrentes na história do planeta. Atualmente passamos por um período de aquecimento principalmente devido a ações antrópicas. Esse aquecimento já se encontra acima de 1ºC em média se comparado ao começo do século XX e há tendência de aumentar entre 1 e 4ºC segundo as projeções de modelos climáticos para o final desse século. Essas mudanças na temperatura tem um impacto direto no ciclo hidrológico e vale a pena buscar entender como o clima vai se comportar para que possamos nos preparar para o futuro.

Esse trabalho procurou explorar especificamente os efeitos das mudanças climáticas sobre os recursos hídricos no continente sul-americano. Isso foi feito observando as projeções de modelos climáticos e usando esses dados como entrada em um modelo hidrológico. Especificamente utilizamos o modelo hidrológico MGB-SA para simular os impactos nas vazões. Já os dados de projeções climáticas foram obtidos através de 25 modelos climáticos globais para se analisar médias de longo termo e dados do modelo climático regional Eta para se avaliar eventos extremos. Dessa forma, conseguimos analisar tanto as projeções para disponibilidade hídrica como para as vazões de cheia.

Foi observado que as regiões centrais e ao norte da América do Sul, particularmente as bacias da margem direita do rio Amazonas, e do rio Orinoco, Tocantins e Paraguai tem projeções de diminuição de vazão. Apenas o sudeste do continente, mais especificamente a região da bacia do rio Uruguai, deve apresentar aumento de vazão média de longo termo. Também observamos que em maior parte as inundações em grandes rios estão projetadas para diminuir, muito devido à diminuição da umidade do solo antecedente ao evento do que necessariamente devido à redução de chuva extrema.

Palavras-chave: Mudanças Climáticas. Recursos Hídricos. América do Sul.

ABSTRACT

Climate change is common and recurrent in the world's history. We are currently going through a warming period mainly due to human actions. This warming is already above 1ºC on average when compared to the beginning of the twentieth century and there is a tendency to increase between 1 and 4ºC according to the projections of climate models for the end of this century. These changes in temperature have a direct impact on the hydrological cycle and it is worthwhile try to understand how the climate will behave so that we can prepare for the future.

This work sought to explore specifically the effects of climate change on water resources in South America. This was done by observing climate model projections and using these data as input to a hydrological model. Specifically, we used the MGB-SA hydrological model to simulate the impacts on river discharge. It was used climate projections from 25 global climate models to analyze long-term averages and from the regional climate model Eta to evaluate extreme events. Therefore, we were able to analyze both projections for water availability and flood discharge.

It is expected that the central and northern regions of South America, particularly the basins of the right bank of the Amazon River, and the Orinoco, Tocantins, and Paraguay Rivers present reduced average discharge. Only on the Southeastern South America, more specifically around the Uruguay River basin, it is expected an increase in the long-term mean discharge. We also observed that flooding in large rivers is projected to decrease, much due to the decrease in soil moisture preceding the event than to the reduction in extreme rainfall.

Keywords: Climate Change. Water Resources. South America.

SUMÁRIO

INTRODUÇÃO

Prólogo

Mudanças Climáticas. Um termo que, como vários outros, ganhou significados além do que suas palavras remontam. Fruto da criatividade humana e de sua capacidade de atribuir sentimentos a coisas abstratas, de desenrolar histórias a partir de um simples ponto. Quantas emoções e pensamentos nos suscitam desse termo? Quantos textos inteiros surgem em nossa mente ao se confrontar com apenas essas duas palavras. Incômodo e fantasioso para alguns; grandioso e catastrófico para outros.

Peço perdão e um pouco de paciência caso o leitor disponha de conceitos avançados sobre o tema. Começarei abordando questões simples que talvez sejam óbvias, repetitivas e até entediantes aos leitores mais especializados. Além do mais, estarei conduzindo o texto sobre um ponto de vista particular, mas com toda a boa intenção de um pesquisador iniciante, ousado e com conhecimento limitado. Por si só, a defesa de uma tese é uma ação de ousadia.

Solicito que esqueça por um curto período o sentido inflado – porém não necessariamente incorreto – existente e apague as histórias construídas ao longo deste século. A partir de um conceito mais limpo será mais fácil para o leitor deglutir as intenções dadas a essa Introdução. Ao longo do texto nós vamos construir nossas definições, nossas histórias e atribuir nossos significados. Não me repreenda ainda. O termo não vai se desligar do que o leitor já está acostumado. Embora esteja totalmente conectado às definições científicas, nosso termo terá o sabor particular desse trabalho.

Clima e Sua Dinâmica

Clima são as condições atmosféricas médias sobre uma área durante um determinado período. A Organização Meteorológica Mundial (WMO) adota um intervalo de 30 anos para se avaliar o clima e estabelecer um padrão de normais climatológicas (Arguez and Vose, 2011). Essa avaliação é feita através de centenas de variáveis meteorológicas que incluem informações médias anuais e sazonais, além de registro de extremos, de temperatura, chuva, umidade e pressão atmosférica, velocidade e direção do vento etc. A cada vez que essa janela temporal muda, as normais climatológicas também se alteram. **Logo compreende-se que o clima é naturalmente variável, então há motivo de tanta preocupação?**

De fato, existe uma grande dinâmica no clima terrestre em diversas escalas temporais. O período do Pleistoceno (últimos 2 milhões de anos) é composto por ciclos glaciais que duram cerca de 100 mil anos e apresentam uma variação térmica em torno de 7ºC (Snyder, 2016). Estima-se que o último período glacial se encerrou há 12 mil anos e deu lugar ao período interglacial no qual nos encontramos hoje, denominado Holoceno. Também existem períodos climáticos de menor duração, como as recentes “pequena era do gelo” (Little Ice

Age) e o “período quente medieval” (Medieval Warm Period) que abrangem poucos séculos e tendências de mudanças médias de temperatura em torno de 1ºC (Nesje and Dahl, 2003).

No entanto, atravessamos atualmente uma situação bem particular. Reconstruções da temperatura global indicam que os séculos mais quentes do Holoceno ocorreram por volta de 6.000 a 7.000 anos atrás (Kaufman et al., 2020a). Estima-se que a temperatura média de alguns séculos consecutivos desse período foi aproximadamente 1ºC mais quente do que nos anos 1850 a 1900[1]. Trazendo para os dias atuais, pesquisas demonstram que, em breve, podemos alcançar uma condição no mínimo parecida. O planeta vem esquentando de forma progressiva e sem perspectiva de estabilização. A temperatura média global teve uma taxa de crescimento de 0,08ºC por década a partir de 1880, sendo que se mudarmos a referência inicial para 1980, essa taxa aumenta para 0,18ºC por década (ver o “2020 Annual Climate Report” da NOAA disponível online). Os anos de 2011-2020 já apresentaram temperatura média cerca de 1,1ºC mais alta que 1850-1900. E ainda por cima, as projeções climáticas indicam que a temperatura será entre 1,5ºC e 4,8ºC mais alta ao final do século XXI em comparação a esse mesmo período (1850-1900) (Tebaldi et al., 2021), dependendo das políticas adotadas para controle de emissões de gases de efeito estufa (GEE) e mitigação. Pode parecer um crescimento gradativo, porém num ponto de vista geológico, climatológico, ecológico etc. é uma mudança bastante abrupta. Considerando o alcance dessas projeções, é provável que estejamos compondo os séculos mais quentes desse Holoceno, em outras palavras, o período mais quente dos últimos 100 mil anos se incluirmos a última era glacial.

Embora essa última sentença seja forte, existem grandes possibilidades disso se concretizar. Logo há motivos evidentes para que esse tema seja explorado e exaustivamente estudado pela comunidade científica. Não tenho intenção de alarmar o leitor, afinal esse aumento de temperatura dificilmente ameaçará a sobrevivência da espécie humana e pode até ser pouco impactante numa sociedade com grandes capacidades de adaptação. No entanto, temos no mínimo a obrigação de tentar entender o quão diferente será o clima para ficarmos cientes da urgência da situação, já que iremos enfrentar condições climáticas sem precedentes na história moderna.

Não me alongarei aqui quanto à responsabilidade humana sobre o aquecimento global. Essa é uma questão muito extensa e já temos tópicos suficientes para nos ocupar. Existem diversos estudos que fazem essa conexão, comprovando a influência antrópica no clima (e.g. Bindoff et al., 2013; Gillett et al., 2021; Ribes et al., 2017; Schurer et al., 2018). Apresento a seguir apenas algumas observações que sustentam essa hipótese: i) existe uma grande correlação entre temperatura e concentração de GEE (principalmente CO_2) na atmosfera; ii) as concentrações de CO_2 atuais aumentaram em mais de 100 ppm desde o começo do século passado, o que equivale a um aumento de 33%; iii) e muito

[1] Geralmente tomado como referência pois é o período mais antigo com alta confiança nos registros de temperatura e que se deu no início da 2ª Revolução Industrial.

provavelmente (*high confidence* utilizando a nomenclatura e a referência do AR6[2]) as concentrações atuais de CO_2 na atmosfera são as maiores dos últimos 2 milhões de anos.

Incertezas das Projeções

Ao contrário do que a seção anterior deixa transparecer, o clima não é exclusivamente composto de temperatura. As demais variáveis meteorológicas também assumiram diferentes faixas de valores ao longo da história e também têm sofrido influências antrópicas (Carmichael et al., 2017; Scussolini et al., 2019). Em minha defesa, mencionei apenas temperatura por se tratar de um índice referência para o clima e que tem uma grande quantidade de registros e pesquisas relacionadas (Kaufman et al., 2020b; Smerdon and Pollack, 2016). Além disso, os impactos causados pelo desenvolvimento industrial são mais diretos sobre essa variável, o que a torna uma via mais simples para se abordar e contextualizar o problema. As séries históricas observadas, sua relação com a concentração de GEE na atmosfera e as projeções oriundas de modelos matemáticos constituem grandes indicativos do aquecimento global, porém são menos conclusivos quanto a outras variáveis como precipitação (Flato et al., 2013). Ou seja, ainda existe muita incerteza quanto às alterações esperadas para outras variáveis atmosféricas que não temperatura (Knutti and Sedláček, 2013).

Isso ocorre devido às deficiências das atuais ferramentas de previsão e à nossa limitada compreensão de processos físicos, que não permitem antever todas as consequências do aquecimento global. Os fenômenos atmosféricos são desenvolvidos por relações complexas e não-lineares entre variáveis que atravessam múltiplas escalas, formando um sistema extremamente caótico e apenas parcialmente compreendido (Xubin Zeng et al., 1993). Em seu famoso discurso no ano de 1972, Edward Lorenz deu um exemplo da alta sensibilidade do sistema atmosférico ao mencionar a possibilidade de um bater das asas de uma borboleta no Brasil causar um tornado no Texas (Ott, 2008). O caso denominado de Efeito Borboleta se tornou um dos exemplos mais citados da Teoria do Caos, inspirando até filmes hollywoodianos. Ou seja, estamos falando de um sistema incrivelmente sensível e que está sujeito a interferência humana. Logo se torna necessário procurar entender as consequências de se incluir uma nova variável nesse complexo conjunto de equações. **Mas se atualmente nosso conhecimento e ferramentas são limitados, por que então nos damos ao trabalho de fazer projeções?**

Peço perdão ao leitor pois meus argumentos no parágrafo anterior acabaram misturando os conceitos de clima e tempo. Tempo são condições atmosféricas no instante e o clima, em um intervalo. Enquanto o tempo (*weather*) tem horizontes de previsão muito curtos (dias) por se tratar de componentes atmosféricos bastante dinâmicos, o clima

[2] Sixth Assessment Report – Sexto relatório do IPCC (Intergovernmental Panel on Climate Change) que faz um apanhado dos maiores avanços relacionados às mudanças climáticas. Consiste na maior referência existente sobre o assunto.

compreende horizontes de previsão maiores e incluem processos lentos que ocorrem na interação com os oceanos, terra e gelo (Toth and Buizza, 2018). Então, embora não sejamos capazes de prever eventos com grande antecedência (Slingo and Palmer, 2011; Smith, 2002), podemos ter uma estimativa do aumento ou diminuição da sua probabilidade de ocorrência e assim fazer projeções para o clima futuro. A modelagem é uma importante ferramenta para essas previsões, e que será abordada logo mais.

Além disso, existem consequências simples e diretas de impactos antrópicos sobre o clima que são previstas em teoria. O próprio aumento de temperatura devido às emissões de GEE é um exemplo. A próxima seção exemplifica alguns desses impactos, dessa vez, sobre os recursos hídricos.

Impactos Gerais sobre os Recursos Hídricos

Várias hipóteses sustentam impactos diretos das mudanças climáticas sobre o ciclo hidrológico.

Uma delas é que o aquecimento global deve contribuir com o aumento da quantidade de água na atmosfera, porém não necessariamente com um clima mais úmido (Feng and Zhang, 2015). As relações de Clausius-Clapeyron indicam que, a cada ^{o}C mais quente, a atmosfera é capaz de reter entre 6 e 7% mais vapor d'água. Dessa forma, entende-se que os eventos extremos de chuva serão mais intensos pois existe mais água disponível para precipitação em condições de saturação (Donat et al., 2016; Lenderink and Fowler, 2017; Myhre et al., 2019). Ao mesmo tempo, onde existe limitação de disponibilidade de água, a umidade relativa tende a diminuir com o aumento de temperatura (Byrne and O'Gorman, 2016; Mendoza et al., 2021) fazendo com que as chuvas sejam menos frequentes apesar de haver uma maior quantidade de água na atmosfera.

Um outro exemplo é o efeito do aquecimento global sobre a umidade do solo. O aumento de temperatura está fortalecendo o potencial de evaporação deixando o solo mais seco (Asadi Zarch et al., 2017; Samaniego et al., 2018). Isso tem consequências diretas na geração de escoamento e frequência de inundações (Sharma et al., 2018; Wasko et al., 2020), além de aumentar o uso consumptivo da água por criar uma maior necessidade de irrigação para agricultura (Meza et al., 2020).

Modelos Climáticos

Entretanto existe uma heterogeneidade climática enorme no planeta e cada região será impactada de forma particular. Através de modelos climáticos podemos ter respostas em um campo espaço-temporal e alcançar projeções em diferentes cenários que são imprevisíveis apenas com teoria. Esses modelos constituem ferramentas matemáticas que calculam transferências de massa e calor na atmosfera e suas iterações com o oceano, terra e gelo (Flato et al., 2013). Atualmente a maioria dos modelos climáticos globais (MCG) também representam importante ciclos biogeoquímicos, como o ciclo do carbono e do

enxofre, constituindo o que chamamos de modelos do sistema terrestre (“Earth System Models”).

Diversas instituições internacionais desenvolvem seu próprio MCG e fazem projeções de maneira independente. Logo se tornou conveniente padronizar as simulações dos MCG para possibilitar comparações de variáveis e cenários entre os diversos modelos. Isso foi alcançado graças ao “Coupled Model Intercomparison Project” (CMIP) coordenado pelo “World Climate Research Program” (WRCP[3]) (Eyring et al., 2016). Assim é possível avaliar as incertezas das projeções, entender defeitos e pontos fortes de cada MCG e contribuir com avanços consistentes nessas ferramentas. Ou seja, o CMIP nos permite entender onde temos mais segurança nas projeções climáticas e onde elas são ainda incertas e necessitam de melhorias.

Atualmente nos encontramos na sexta fase do CMIP (CMIP6), que é relativo ao sexto relatório do IPCC[4] (AR6). Para se ter uma ideia da quantidade de MCG sendo desenvolvidos, no atlas iterativo do AR6 (https://interactive-atlas.ipcc.ch/) são apresentados os resultados de um ensemble de 36 modelos do CMIP6 e 29 modelos do CMIP5. E essas ferramentas vêm sendo aprimoradas desde o CMIP3 (Flato et al., 2013). Atualmente a resolução horizontal dos MCG está entre 100 e 250 km, embora também tenham surgido projetos dentro do escopo do CMIP6 de estudar modelos globais de alta resolução (HighResMIP), com células de ao menos 50 x 50 km (Haarsma et al., 2016).

De qualquer forma, os MCG ainda apresentam resoluções muito grosseiras para representar componentes mais detalhados da superfície como gradientes topográficos, corpos d’água, costa litorânea e áreas urbanas, que acabam impactando o clima regional (Feser et al., 2011; Giorgi, 2019). Sua resolução horizontal os torna de certa forma incompatíveis para estudos hidrológicos de média escala que são influenciados pela topografia local e cujo campo de precipitação é heterogêneo. Por isso, normalmente se adota ferramentas de downscaling dinâmico denominadas de modelos climáticos regionais (MCR) que são essenciais principalmente para investigações em bacias hidrográficas específicas (Teutschbein and Seibert, 2010).

Os MCR são modelos matemáticos que tem uma resolução horizontal superior aos MCG (<20 km), porém abrangem um domínio menor (e.g. continentes). Os MCR utilizam dados de MCG como condição de contorno nas bordas do domínio, na temperatura dos oceanos e como condições iniciais (Chou et al., 2014b). Sua resolução permite representar fenômenos atmosféricos de mesoescala e até ventos induzidos por orografia (Antico et al.,

[3] Programa sob a direção da World Meteorological Organization (WMO) responsável por coordenar as pesquisas climáticas, principalmente modelagem, incluindo projetos como o CMIP e o CORDEX.
[4] Intergovernmental Panel on Climate Change (IPCC) é uma organização criada pelas Nações Unidas em parceria com a WMO que define o estado da arte sobre mudanças climáticas dando suporte aos tomadores de decisões ao redor do mundo.

2020), no entanto a resolução ainda não é suficiente para representar, por exemplo, chuvas convectivas explicitamente.

É importante salientar que da mesma forma que existem esforços por MCG de alta resolução também existem iniciativas semelhantes para MCR. Esses estudos buscam alcançar modelos regionais com resoluções < 3 km e que permitam simular convecção de forma explícita (Prein et al., 2015). Logo podemos dizer que a comunidade científica se dedica ao desenvolvimento de modelos no limite da atual capacidade computacional, mas a todo momento fazendo pressão sobre essa barreira tecnológica e se preparando para conquistar maiores avanços.

Portanto, gostaria de encerrar essa seção passando uma mensagem positiva. Já existem diversos sinais de mudança indicados pelos modelos, e esses sinais tendem a ficar cada vez mais nítidos pois temos uma grande expectativa de que essas ferramentas se tornem mais completas e precisas no futuro. A comunidade científica tem trabalhado bastante no desenvolvimento tanto de MCG quanto de MCR, e os testes e avaliações propostos dentro dos CMIPs tem se tornado cada vez mais abrangentes (Eyring et al., 2016).

Impactos nos Recursos Hídricos da América do Sul

Quanto aos impactos das mudanças climáticas nos recursos hídricos, diversos trabalhos já foram desenvolvidos em bacias específicas da América do Sul e os modelos climáticos são as principais ferramentas metodológicas para isso. Borges de Amorim et al. (2020) faz um interessante compilado dos trabalhos que foram realizados para bacias hidrográficas brasileiras em uma plataforma online denominada YARA (https://www.labhidro.ufsc.br/yara/).

No geral, os trabalhos normalmente utilizam dados de MCG ou MCR para alimentar um modelo hidrológico e detectar as mudanças através de comparações entre um período futuro e um período de base. Destaco aqui 3 trabalhos que acho relevante por se tratar de uma escala compatível com a que estamos abordando. Sorribas et al. (2016) estudaram a Bacia Amazônica e notou que os modelos projetam uma tendência de maior umidade no oeste da bacia, porém menores vazões ao leste, principalmente nos afluentes da margem direita do rio. Já Ribeiro Neto et al. (2016) avaliaram todas as bacias hidrográficas brasileiras – as quais representam uma grande percentual das bacias sul-americanas – usando dados de MCR e concluiu que existirá uma diminuição geral da disponibilidade hídrica exceto no sul do país. Esses resultados também foram alcançados por da Silva et al. (2020) ao avaliar os impactos das mudanças climáticas sobre a Energia Natural Afluente no Sistema Interligado Nacional (SIN).

Devo informar que nosso trabalho tem uma essência parecida. Nós fazemos simulações hidrológicas usando como forçantes tanto dados de MCR como de MCG. Porém, o estudo em questão tem várias particularidades que contribuem de maneira

significativa para o avanço do tema na América do Sul. Nós propusemos avaliar o continente sul-americano utilizando uma metodologia padrão que nos permite comparar os impactos de maneira sistemática em diferentes regiões do continente. Utilizamos também um modelo hidrológico construído e calibrado para a América do Sul que apresentou resultados superiores a modelos hidrológicos globais (Vinicius A. Siqueira et al., 2018). Além disso, quando avaliamos os efeitos das mudanças climáticas sobre a disponibilidade hídrica na América do Sul, procuramos utilizar o maior número de MCG disponível (25), para podermos apresentar resultados considerando as incertezas associadas. E por fim, não apenas nos restringimos a observar as projeções de vazão, como também analisamos sua relação com outras variáveis hidrológicas como umidade do solo, precipitação e evapotranspiração, buscando explicar a causa dos sinais e tendências.

Arrisco dizer que esse trabalho vai proporcionar uma visão completa e abrangente dos impactos das mudanças climáticas nos recursos hídricos na América do Sul, porém focando apenas em dados quantitativos e sem entrar em questões socioeconômicas e ecológicas. Sem mais delongas, os resultados dessas investigações e análises serão apresentados através de 3 artigos nas próximas seções.

Referências

Antico, P.L., Chou, S.C., Brunini, C.A., 2020. The foehn wind east of the Andes in a 20-year climate simulation. Meteorol. Atmos. Phys. https://doi.org/10.1007/s00703-020-00752-3

Arguez, A., Vose, R.S., 2011. The definition of the standard WMO climate normal: The key to deriving alternative climate normals. Bull. Am. Meteorol. Soc. 92, 699–704. https://doi.org/10.1175/2010BAMS2955.1

Asadi Zarch, M.A., Sivakumar, B., Malekinezhad, H., Sharma, A., 2017. Future aridity under conditions of global climate change. J. Hydrol. 554, 451–469. https://doi.org/10.1016/j.jhydrol.2017.08.043

Bindoff, N.L., Stott, P.A., AchutaRao, K.M., Allen, M.R., Gillett, N., Gutzler, D., Hansingo, K., Hegerl, G., Hu, Y., Jain, S., 2013. Detection and attribution of climate change: from global to regional.

Borges de Amorim, P., Silva de Souza, K.I., Borges Chaffe, P.L., 2020. A web-based tool for synthesis assessments of the impacts of climate change on water resources. Environ. Model. Softw. 133, 104848. https://doi.org/10.1016/j.envsoft.2020.104848

Byrne, M.P., O'Gorman, P.A., 2016. Understanding decreases in land relative humidity with global warming: Conceptual model and GCM simulations. J. Clim. 29, 9045–9061. https://doi.org/10.1175/JCLI-D-16-0351.1

Carmichael, M.J., Inglis, G.N., Badger, M.P.S., Naafs, B.D.A., Behrooz, L., Remmelzwaal, S., Monteiro, F.M., Rohrssen, M., Farnsworth, A., Buss, H.L., Dickson, A.J., Valdes, P.J., Lunt, D.J., Pancost, R.D., 2017. Hydrological and associated biogeochemical consequences of rapid global warming during the Paleocene-Eocene Thermal Maximum. Glob. Planet. Change 157, 114–138. https://doi.org/10.1016/j.gloplacha.2017.07.014

Chou, S.C., Lyra, A., Mourão, C., Dereczynski, C., Pilotto, I., Gomes, J., Bustamante, J., Tavares, P., Silva, A., Rodrigues, D., Campos, D., Chagas, D., Sueiro, G., Siqueira, G., Nobre, P., Marengo, J., 2014. Evaluation of the Eta Simulations Nested in Three Global Climate Models. Am. J. Clim.

Chang. 03, 438–454. https://doi.org/10.4236/ajcc.2014.35039

da Silva, M.V.M., Silveira, C. da S., da Silva, G.K., Pedrosa, W.H. de V., Marcos Júnior, A.D., Souza Filho, F. de A., 2020. Projections of climate change in streamflow and affluent natural energy in tbrazilian hydroelectric sector of cordex models. Rev. Bras. Recur. Hidricos 25, 1–15. https://doi.org/10.1590/2318-0331.252020200020

Donat, M.G., Lowry, A.L., Alexander, L. V., O'Gorman, P.A., Maher, N., 2016. More extreme precipitation in the world's dry and wet regions. Nat. Clim. Chang. 6, 508–513. https://doi.org/10.1038/nclimate2941

Eyring, V., Bony, S., Meehl, G.A., Senior, C.A., Stevens, B., Stouffer, R.J., Taylor, K.E., 2016. Overview of the Coupled Model Intercomparison Project Phase 6 (CMIP6) experimental design and organization. Geosci. Model Dev. 9, 1937–1958. https://doi.org/10.5194/gmd-9-1937-2016

Feng, H., Zhang, M., 2015. Global land moisture trends: Drier in dry and wetter in wet over land. Sci. Rep. 5, 1–6. https://doi.org/10.1038/srep18018

Feser, F., Rrockel, B., Storch, H., Winterfeldt, J., Zahn, M., 2011. Regional climate models add value to global model data a review and selected examples. Bull. Am. Meteorol. Soc. 92, 1181–1192. https://doi.org/10.1175/2011BAMS3061.1

Flato, G., Marotzke, J., Abiodun, B., Braconnot, P., Chou, S.C., Collins, W., Cox, P., Driouech, F., Emori, S., Eyring, V., Forest, C., Gleckler, P., Guilyardi, E., Jakob, C., Kattsov, V., Reason, C., Rummukainen, M., 2013. Evaluation of Climate Models. Clim. Chang. 2013 Phys. Sci. Basis. Contrib. Work. Gr. I to Fifth Assess. Rep. Intergov. Panel Clim. Chang. 741–866. https://doi.org/10.1017/CBO9781107415324

Gillett, N.P., Kirchmeier-Young, M., Ribes, A., Shiogama, H., Hegerl, G.C., Knutti, R., Gastineau, G., John, J.G., Li, L., Nazarenko, L., Rosenbloom, N., Seland, Ø., Wu, T., Yukimoto, S., Ziehn, T., 2021. Constraining human contributions to observed warming since the pre-industrial period. Nat. Clim. Chang. 11, 207–212. https://doi.org/10.1038/s41558-020-00965-9

Giorgi, F., 2019. Thirty Years of Regional Climate Modeling: Where Are We and Where Are We Going next? J. Geophys. Res. Atmos. 124, 5696–5723. https://doi.org/10.1029/2018JD030094

Haarsma, R.J., Roberts, M.J., Vidale, P.L., Catherine, A., Bellucci, A., Bao, Q., Chang, P., Corti, S., Fučkar, N.S., Guemas, V., Von Hardenberg, J., Hazeleger, W., Kodama, C., Koenigk, T., Leung, L.R., Lu, J., Luo, J.J., Mao, J., Mizielinski, M.S., Mizuta, R., Nobre, P., Satoh, M., Scoccimarro, E., Semmler, T., Small, J., Von Storch, J.S., 2016. High Resolution Model Intercomparison Project (HighResMIP v1.0) for CMIP6. Geosci. Model Dev. 9, 4185–4208. https://doi.org/10.5194/gmd-9-4185-2016

Kaufman, D., McKay, N., Routson, C., Erb, M., Dätwyler, C., Sommer, P.S., Heiri, O., Davis, B., 2020a. Holocene global mean surface temperature, a multi-method reconstruction approach. Sci. Data 7, 1–13. https://doi.org/10.1038/s41597-020-0530-7

Kaufman, D., McKay, N., Routson, C., Erb, M., Davis, B., Heiri, O., Jaccard, S., Tierney, J., Dätwyler, C., Axford, Y., Brussel, T., Cartapanis, O., Chase, B., Dawson, A., de Vernal, A., Engels, S., Jonkers, L., Marsicek, J., Moffa-Sánchez, P., Morrill, C., Orsi, A., Rehfeld, K., Saunders, K., Sommer, P.S., Thomas, E., Tonello, M., Tóth, M., Vachula, R., Andreev, A., Bertrand, S., Biskaborn, B., Bringué, M., Brooks, S., Caniupán, M., Chevalier, M., Cwynar, L., Emile-Geay, J., Fegyveresi, J., Feurdean, A., Finsinger, W., Fortin, M.C., Foster, L., Fox, M., Gajewski, K., Grosjean, M., Hausmann, S., Heinrichs, M., Holmes, N., Ilyashuk, B., Ilyashuk, E., Juggins, S., Khider, D., Koinig, K., Langdon, P., Larocque-Tobler, I., Li, J., Lotter, A., Luoto, T., Mackay, A., Magyari, E., Malevich, S., Mark, B., Massaferro, J., Montade, V., Nazarova, L., Novenko, E., Pařil, P., Pearson, E., Peros, M., Pienitz,

R., Płóciennik, M., Porinchu, D., Potito, A., Rees, A., Reinemann, S., Roberts, S., Rolland, N., Salonen, S., Self, A., Seppä, H., Shala, S., St-Jacques, J.M., Stenni, B., Syrykh, L., Tarrats, P., Taylor, K., van den Bos, V., Velle, G., Wahl, E., Walker, I., Wilmshurst, J., Zhang, E., Zhilich, S., 2020b. A global database of Holocene paleotemperature records. Sci. Data 7, 1–34. https://doi.org/10.1038/s41597-020-0445-3

Knutti, R., Sedláček, J., 2013. Robustness and uncertainties in the new CMIP5 climate model projections. Nat. Clim. Chang. 3, 369–373. https://doi.org/10.1038/nclimate1716

Lenderink, G., Fowler, H.J., 2017. Hydroclimate: Understanding rainfall extremes. Nat. Clim. Chang. 7, 391–393. https://doi.org/10.1038/nclimate3305

Mendoza, V., Pazos, M., Garduño, R., Mendoza, B., 2021. Thermodynamics of climate change between cloud cover, atmospheric temperature and humidity. Sci. Rep. 11, 1–11. https://doi.org/10.1038/s41598-021-00555-5

Meza, I., Siebert, S., Döll, P., Kusche, J., Herbert, C., Rezaei, E.E., Nouri, H., Gerdener, H., Popat, E., Frischen, J., Naumann, G., Vogt, J. V., Walz, Y., Sebesvari, Z., Hagenlocher, M., 2020. Global-scale drought risk assessment for agricultural systems. Nat. Hazards Earth Syst. Sci. 20, 695–712. https://doi.org/10.5194/nhess-20-695-2020

Myhre, G., Alterskjær, K., Stjern, C.W., Hodnebrog, Marelle, L., Samset, B.H., Sillmann, J., Schaller, N., Fischer, E., Schulz, M., Stohl, A., 2019. Frequency of extreme precipitation increases extensively with event rareness under global warming. Sci. Rep. 9, 1–10. https://doi.org/10.1038/s41598-019-52277-4

Nesje, A., Dahl, S.O., 2003. The “Little Ice Age” - Only temperature? Holocene 13, 139–145. https://doi.org/10.1191/0959683603hl603fa

Ott, E., 2008. Edward N. Lorenz (1917–2008) 453, 20742.

Prein, A.F., Langhans, W., Fosser, G., Ferrone, A., Ban, N., Goergen, K., Keller, M., Tölle, M., Gutjahr, O., Feser, F., Brisson, E., Kollet, S., Schmidli, J., Van Lipzig, N.P.M., Leung, R., 2015. A review on regional convection-permitting climate modeling: Demonstrations, prospects, and challenges. Rev. Geophys. 53, 323–361. https://doi.org/10.1002/2014RG000475

Ribeiro Neto, A., da Paz, A.R., Marengo, J.A., Chou, S.C., 2016. Hydrological Processes and Climate Change in Hydrographic Regions of Brazil. J. Water Resour. Prot. 08, 1103–1127. https://doi.org/10.4236/jwarp.2016.812087

Ribes, A., Zwiers, F.W., Azaïs, J.M., Naveau, P., 2017. A new statistical approach to climate change detection and attribution. Clim. Dyn. 48, 367–386. https://doi.org/10.1007/s00382-016-3079-6

Samaniego, L., Thober, S., Kumar, R., Wanders, N., Rakovec, O., Pan, M., Zink, M., Sheffield, J., Wood, E.F., Marx, A., 2018. Anthropogenic warming exacerbates European soil moisture droughts. Nat. Clim. Chang. 8, 421–426. https://doi.org/10.1038/s41558-018-0138-5

Schurer, A., Hegerl, G., Ribes, A., Polson, D., Morice, C., Tett, S., 2018. Estimating the transient climate response from observed warming. J. Clim. 31, 8645–8663. https://doi.org/10.1175/JCLI-D-17-0717.1

Scussolini, P., Bakker, P., Guo, C., Stepanek, C., Zhang, Q., Braconnot, P., Cao, J., Guarino, M.V., Coumou, D., Prange, M., Ward, P.J., Renssen, H., Kageyama, M., Otto-Bliesner, B., Aerts, J.C.J.H., 2019. Agreement between reconstructed and modeled boreal precipitation of the last interglacial. Sci. Adv. 5, 1–12. https://doi.org/10.1126/sciadv.aax7047

Sharma, A., Wasko, C., Lettenmaier, D.P., 2018. If Precipitation Extremes Are Increasing, Why Aren’t

Floods? Water Resour. Res. 54, 8545–8551. https://doi.org/10.1029/2018WR023749

Siqueira, V.A., Paiva, R.C.D., Fleischmann, A.S., Fan, F.M., Ruhoff, A.L., Pontes, P.R.M., Paris, A., Calmant, S., Collischonn, W., 2018. Toward continental hydrologic-hydrodynamic modeling in South America. Hydrol. Earth Syst. Sci. 22, 4815–4842. https://doi.org/10.5194/hess-22-4815-2018

Slingo, J., Palmer, T., 2011. Uncertainty in weather and climate prediction. Philos. Trans. R. Soc. A Math. Phys. Eng. Sci. 369, 4751–4767. https://doi.org/10.1098/rsta.2011.0161

Smerdon, J.E., Pollack, H.N., 2016. Reconstructing Earth's surface temperature over the past 2000 years: the science behind the headlines. Wiley Interdiscip. Rev. Clim. Chang. 7, 746–771. https://doi.org/10.1002/wcc.418

Smith, L.A., 2002. What might we learn from climate forecasts? Proc. Natl. Acad. Sci. U. S. A. 99, 2487–2492. https://doi.org/10.1073/pnas.012580599

Snyder, C.W., 2016. Evolution of global temperature over the past two million years. Nature 538, 226–228. https://doi.org/10.1038/nature19798

Sorribas, M.V., Paiva, R.C.D., Melack, J.M., Bravo, J.M., Jones, C., Carvalho, L., Beighley, E., Forsberg, B., Costa, M.H., 2016. Supplementary Material: Projections of climate change effects on discharge and inundation in the Amazon basin.

Tebaldi, C., Debeire, K., Eyring, V., Fischer, E., Fyfe, J., Friedlingstein, P., Knutti, R., Lowe, J., O'Neill, B., Sanderson, B., Van Vuuren, D., Riahi, K., Meinshausen, M., Nicholls, Z., Tokarska, K., Hurtt, G., Kriegler, E., Meehl, G., Moss, R., Bauer, S., Boucher, O., Brovkin, V., Yhb, Y., Dix, M., Gualdi, S., Guo, H., John, J., Kharin, S., Kim, Y.H., Koshiro, T., Ma, L., Olivié, D., Panickal, S., Qiao, F., Rong, X., Rosenbloom, N., Schupfner, M., Séférian, R., Sellar, A., Semmler, T., Shi, X., Song, Z., Steger, C., Stouffer, R., Swart, N., Tachiiri, K., Tang, Q., Tatebe, H., Voldoire, A., Volodin, E., Wyser, K., Xin, X., Yang, S., Yu, Y., Ziehn, T., 2021. Climate model projections from the Scenario Model Intercomparison Project (ScenarioMIP) of CMIP6. Earth Syst. Dyn. 12, 253–293. https://doi.org/10.5194/esd-12-253-2021

Teutschbein, C., Seibert, J., 2010. Regional climate models for hydrological impact studies at the catchment scale: A review of recent modeling strategies. Geogr. Compass 4, 834–860. https://doi.org/10.1111/j.1749-8198.2010.00357.x

Toth, Z., Buizza, R., 2018. Weather forecasting: What sets the forecast skill horizon?, Sub-seasonal to Seasonal Prediction: The Gap Between Weather and Climate Forecasting. Elsevier Inc. https://doi.org/10.1016/B978-0-12-811714-9.00002-4

Wasko, C., Nathan, R., Peel, M.C., 2020. Changes in Antecedent Soil Moisture Modulate Flood Seasonality in a Changing Climate. Water Resour. Res. 56, no. https://doi.org/10.1029/2019WR026300

Xubin Zeng, Pielke, R.A., Eykholt, R., 1993. Chaos theory and its applications to the atmosphere. Bull. Am. Meteorol. Soc. 74, 631–644. https://doi.org/10.1175/1520-0477(1993)074<0631:ctaiat>2.0.co;2

ORGANIZAÇÃO DA TESE

Essa tese está organizada em formato de artigos que foram escritos em inglês. Serão apresentados 3 manuscritos que já foram publicados, submetidos ou em processo de revisão interna que estão diretamente relacionados ao tema de “Impactos das Mudanças Climáticas nos Recursos Hídricos da América do Sul”.

Primeiro gostaria de traçar os pontos comuns, as particularidades e a lógica por trás da sequência de apresentação. Todos os estudos foram construídos a partir da análise de resultados de modelos climáticos (destaca-se a precipitação) do CMIP5. Em seguida esses resultados foram usados como dados de entrada em um modelo hidrológico para poder simular o impacto das mudanças climáticas sobre os recursos hídricos (artigos 1 e 3), ou apenas para entender o efeito das incertezas das chuvas extremas na vazão (artigo 2). Em todas as situações o modelo hidrológico escolhido foi o Modelo de Grandes Bacias para América do Sul / MGB-SA (Vinicius A. Siqueira et al., 2018) que consiste numa ferramenta capaz de fornecer boas estimativas de vazão, armazenamento de água no solo e evaporação para o continente sul-americano.

O objetivo do trabalho foi de avaliar tanto os impactos sobre mudanças médias de longo prazo como sobre eventos extremos. Como são informações distintas, esses assuntos foram estudados de forma separada. No **artigo 1** avaliamos o balanço hídrico, destacando as mudanças médias nas bacias hidrográficas esperadas para o final do século. Assim, foi possível trabalhar com um número grande de modelos climáticos globais (25) que forneceram dados mensais dos quais removemos o viés e forçamos o modelo hidrológico. Já para analisar as projeções de eventos extremos (**artigo 3**) tivemos que utilizar dados diários numa resolução espacial mais alta através do modelo climático regional Eta, o que acabou reduzindo nosso leque de simulações (4). Antes de fazer essa avaliação de vazões de cheia, resolvemos testar a performance do Eta em simular chuvas extremas comparando com curvas IDFs em pontos e dados de chuva em grade. Assim pudemos entender as incertezas do modelo antes de entrar nas projeções. Esse estudo prévio resultou no **artigo 2**. Figura 1 e a Tabela 1 trazem uma apresentação compacta da organização dos artigos.

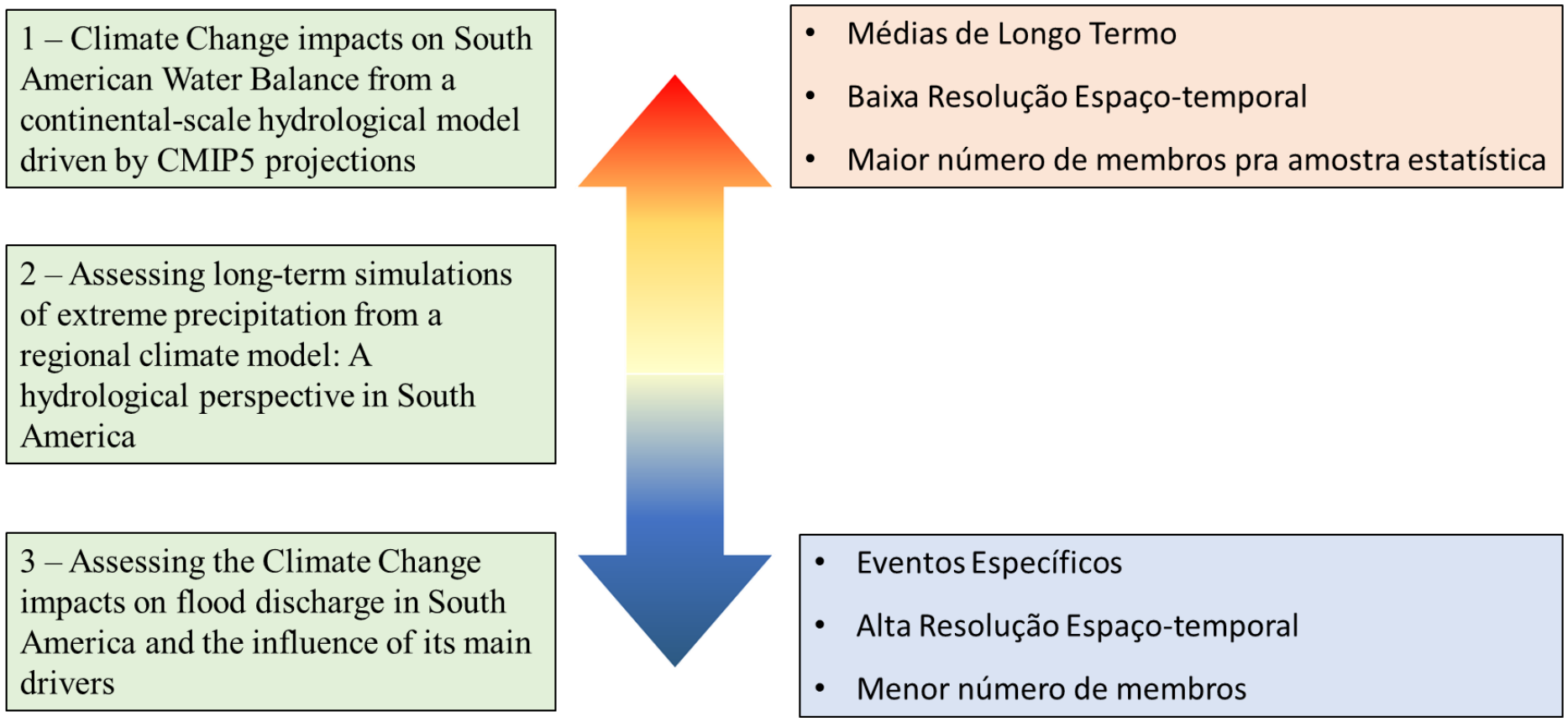

Figura 1. Apresentação e organização dos artigos da tese caracterizados pelo nível de detalhamento

Tabela 1. Artigos da tese e o resumo de suas principais características metodológicas.

Título (Inglês)	Objetivo	Modelos Climáticos	Remoção de Viés	Modelo Hidrológico	Variáveis Analisadas	Status
1– Climate Change impacts on South American Water Balance from a continental-scale hydrological model driven by CMIP5 projections	Avaliar projeções de mudanças médias nas bacias hidrográficas	Ensemble de 25 Modelos Globais	Delta Change	MGB-SA	Evaporação Média, Precipitação Média, Vazão Média	Publicado na revista “Climatic Change” (2020)
2– Assessing long-term simulations of extreme precipitation from a regional climate model: A hydrological perspective in South America	Avaliar a capacidade do Eta de representar eventos extremos	Downscaling com o Eta de 4 Modelos Globais	Não se aplica	MGB-SA	Precipitação Extrema, Vazão de Cheia	Submetido à revista “International Journal of Climatology”
3– Assessing the Climate Change impacts on flood discharge in South America and the influence of its main drivers	Avaliar projeções de mudanças sobre vazões de cheia	Downscaling com o Eta de 4 Modelos Globais	Quantile Mapping	MGB-SA	Precipitação Extrema, Umidade do Solo, Vazão de Cheia	Ainda em processo de revisão interna

CONCLUSÕES

Embora tenham sido avaliados tópicos diferentes, os artigos foram ao mesmo tempo convergentes e complementares. Utilizando os dados de diferentes modelos climáticos globais e do Eta como entrada do MGB-SA, fomos capazes de analisar: **art. 1**) projeções de balanço hídrico no continente; **art. 2**) as incertezas dos dados climáticos (precipitação) e **art. 3**) projeções de vazões extremas. Isso foi feito de forma padronizada para todo o continente possibilitando comparações entre regiões e análises de incerteza. Observamos que os sinais e a distribuição espacial dos eventos extremos e de vazões médias de longo termo tiveram semelhanças, mas fizemos avaliações correspondentes a cada tipo de variável. As conclusões mais relevantes e os artigos referidos estão postos a seguir:

1) O sudeste da América do Sul (e.g. bacia do rio Uruguai) é a única região do continente que apresenta projeções claras de aumento da vazão e maior umidade (o oeste da bacia Amazônica com menor evidência). Isso vale também para vazões de inundação com baixo tempo de retorno. Para vazões extremas de tempo de retorno mais alto, outras regiões também podem indicar um aumento. **(art. 1 e 3)**

2) Bacias na região central do Brasil, margem direita do rio Amazonas, rio Orinoco, rio Tocantins-Araguaia e alto Paraguai (Pantanal) vão sofrer redução significativa na vazão. As projeções apontam para um alto impacto com sinais bem claros nessas bacias principalmente porque são regiões úmidas com alta disponibilidade de água para evaporação e ao mesmo tempo apresentam projeções de redução na chuva média anual. O impacto sobre vazões de cheia de baixo tempo de retorno é parecido. **(art. 1 e 3)**

3) Para bacias com maior apelo socioeconômico como São Francisco, Magdalena, Parnaíba e alto Paraná, os sinais indicam uma diminuição da vazão média de longo-prazo, porém não tão claros como nas bacias do item anterior. A bacia do Paraná é uma região particular que perde o sinal negativo a jusante da foz do rio Iguaçu, onde começa a entrar numa região que se projeta maior umidade. **(art. 1)**

4) As vazões mais extremas (tempo de retorno ≈ 20 anos) apresentaram sinais positivos em mais lugares do que as medianas das vazões máximas anuais (tempo de retorno de 2 anos). Ou seja, existem locais em que os eventos mais extremos apresentam projeções de aumento enquanto vazões máximas anuais recorrentes tendem a diminuir (em torno de 10% dos casos). Isso é algo apontado na literatura, que os eventos mais extremos serão impactados de forma diferente. **(art. 3)**

5) Espera-se que a umidade do solo diminua em quase toda a América do Sul, exceto no sudeste do continente que vai ficar mais úmido. Isso significa que o solo vai estar mais seco previamente a um evento de cheia. Detectamos que a influência da umidade do solo

antecedente deve ser maior que a influência da precipitação extrema quanto ao sinal dos eventos de inundação no futuro. **(art. 3)**

6) Os resultados do cenário mais extremo (RCP8.5) possuem praticamente a mesma disposição espacial do cenário menos extremo (RCP4.5), porém com uma intensidade maior. **(art. 1 e 3)**

7) O modelo climático regional Eta subestima as precipitações extremas de um dia de duração em praticamente todo o continente, exceto na costa oeste da Patagônia. Porém, quando se faz uma agregação temporal para média de 5 dias, por exemplo, esse erro é reduzido. Da mesma forma, os erros de vazão acabam diminuindo à medida que se aumenta o tamanho da bacia hidrográfica. **(art. 2)**

É importante salientar que as conclusões relacionadas a eventos extremos se referem exclusivamente aos rios com área de drenagem maior que 1,000 km2, que são os rios simulados pelo modelo hidrológico. É discutido na literatura que os impactos das inundações sobre bacias pequenas são diferentes dos impactos sobre bacias grandes, as quais são exploradas nesse trabalho. Acredito que até o momento a escala que trabalhamos seja a mais adequada em relação aos dados de projeções climáticas, pois estes ainda apresentam muitas incertezas nas escalas menores, principalmente na representação de chuvas convectivas.

Gostaria de ressaltar que esse trabalho foi capaz de cobrir de maneira sistemática mudanças médias de longo-termo e eventos de vazão extrema para o continente sul-americano. No entanto, o tema dos impactos sobre os recursos hídricos na América do Sul ainda não foi completamente esgotado. Nem de perto. Trabalhos futuros e de forma complementar são essenciais. Gostaríamos, mas não chegamos a avaliar os eventos extremos relacionados às secas. Sua duração, intensidade e o déficit hídrico na agricultura. Além disso, muito trabalho ainda pode ser realizado em menores escalas conforme ocorra o avanço na capacidade computacional e no desenvolvimento dos modelos climáticos para representar o microclima. É importante lembrar que nosso trabalho foi realizado no escopo do CMIP5, e atualmente já estamos na 6ª fase desse projeto. Logo a expectativa é que trabalhos posteriores apresentem previsões mais acuradas.

Para concluir, destaco que, embora simulações e estudos futuros consigam atingir previsões mais confiáveis, é importante olhar para os resultados atuais e começar o planejamento para reduzir os impactos. As mudanças climáticas são uma realidade e devemos propor técnicas e alternativas viáveis para fornecer maior segurança à população. É necessário observar onde está previsto aumento das intensidades de cheias para evitar desastres recorrentes causados por inundações e fazer uma administração adequada do volume d'água observando seus múltiplos usos principalmente nas diversas bacias que apresentam uma diminuição da vazão média de longo termo. Por fim, gostaria de mencionar que a pesquisa dos impactos é apenas um primeiro passo rumo ao fortalecimento do tema diante dos tomadores de decisão. A importância desse assunto é indiscutível e a população deve ser devidamente orientada para lidar com o problema.

ARTIGO 1

Climate Change impacts on South American Water Balance from a continental-scale hydrological model driven by CMIP5 projections

Authors:

João Paulo Lyra Fialho Brêda
Rodrigo Cauduro Dias de Paiva
Walter Collischon
Juan Martín Bravo
Vinicius Alencar Siqueira
Elisa Bolzan Steinke

Abstract

South America contributes around 30% of the global runoff to the oceans. As the regional economy and biodiversity extremely depend on its water resources, assessing the potential climate change impacts on the continental water balance is crucial to support water management planning. Here we evaluate the mean alterations on water budget variables and river discharge in South America by the end of this century testing two different GHG scenarios (RCP4.5 and RCP8.5). An ensemble composed by 25 Global Climate Models (GCM) from CMIP5 was used to force a continental-scale hydrologic-hydrodynamic model developed for that region. A negative signal with respect to changes on precipitation, evapotranspiration and runoff was observed on most of the continent. Major decreases in the annual mean discharge are expected on the Orinoco, Tocantins and Amazon basins, which would be around 8% - 14% at least (statistically significant - RCP4.5 and RCP8.5, respectively). Only the Uruguay Basin presented a positive trend on the mean discharge.

Keywords: Water Resources, South America, Impacts, Climate Change

1. INTRODUCTION

Climate models' projections indicate temperature rise above 1.5 ºC by the end of this century and considerable changes on precipitation patterns around the globe (Flato et al., 2013). In South America, the mean precipitation is likely to increase in southeast and decrease in most areas between latitudes 5 to 20 degrees south (Chou et al., 2014). These climate trends will affect the occurrence of hydrological events (e.g. floods and droughts) and consequently socio-economic and environmental aspects in the continent (Reyer et al., 2017). Predicted water related impacts include reduction of long-term water supply due to glacier melts on tropical Andes (Chevallier et al., 2011; Vuille et al., 2018), drying on Andean Basins of subtropical (Vicuña et al., 2011) and Mediterranean (Bozkurt et al., 2018) climate types on Chile, decrease on hydroelectric production (Silveira et al., 2017), modifications on biogeochemical properties of Amazon floodplains (Melack and Coe, 2012), increased flood risk on western Amazonia and southeast South America due to extreme events (Marengo et al., 2009) and increased desertification risks in Northeast Brazil (Marengo and Bernasconi, 2015).

Climate projections are derived from Global Climate Models (GCM) driven by different scenarios of greenhouse gas (GHG) emissions. These outcomes provide atmospheric conditions to force hydrological models and consequently predict the climate change impact on water resources. The state-of-the-art GCMs are Land Surface Models which simulates not only the interaction between atmosphere, land, ocean and sea ice but also various biogeochemical processes as carbon, Sulphur and ozone cycles (Flato et al., 2013). However, GCMs are still limited by actual computational power (which defines modelling resolution), current physical understanding and mathematical/numerical representation of the Earth systems dynamics (Zhao et al. 2016), which reflects on model uncertainty (Flato et al., 2013). In order to increase climate projections performance and reliability, the World Climate Research Programme conducts the Coupled Models Intercomparison Project (CMIP) which involves a continuous and combined assessment and data availability of a broad set of GCMs (Eyring et al., 2016).

GCM multimodel approaches are appropriate for impact studies as there are considerable uncertainties in climate projections, especially related to precipitation (Flato et al., 2013; Gulizia and Camilloni, 2015; Knutti and Sedláček, 2013; Torres and Marengo, 2013), and an ensemble of GCMs helps identify the magnitude of the uncertainties, increasing confidence where GCMs results converge. This is particularly important because precipitation is the main driver of hydrological models, and hydrological variables such as streamflow can be very sensitive to rainfall variations (Chiew 2006; Ribeiro Neto et al., 2016).

In this context, several studies in South American basins have used hydrological models forced by outputs from GCM ensembles to evaluate climate change impacts (Adam et al., 2015; Bravo et al., 2014; Buytaert and Bievre, 2012; Guimberteau et al., 2017; Nóbrega et al., 2011; Siqueira Júnior et al., 2015; Sorribas et al., 2016a). However, independent studies on specific basins are often characterized by differences in the adopted methods (e.g. hydrological model selection, parameterization, bias-correction, downscaling), climatological data (i.e. number of

selected GCMs and different CMIP phases), scenario, and evaluation period, which hinders a comprehensive assessment of how the impacts on water resources vary across different regions and how reliable the projections are.

At the same time, other studies have assessed the effects of climatic trends on a larger scale through global hydrological models – GHM (Arnell and Gosling, 2013; Koirala et al., 2014; Sperna Weiland et al., 2012). A broader perspective offered by GHMs is an alternative to easily identify the spatial distribution of climate change impacts at larger scales, permitting an integrated water resources planning at the continental level. However, GHM uncertainties could be as significant as GCM uncertainties (Guimberteau et al., 2017; Hagemann et al., 2013; Schewe et al., 2014), which leads to the adoption of a multimodel approach not only for GCMs but for GHMs as well, in order to increase confidence in the overall results. Ensembles composed by several GHMs and GCMs are being increasingly used to address the uncertainty in climate change related impacts, and some examples include the effects on runoff trends (Hagemann et al., 2013), flood hazard (Dankers et al., 2014), water scarcity (Schewe et al., 2014) and streamflow extremes (Asadieh and Krakauer, 2017).

More recently, attention has been given to the cross-scale comparison of global and regional hydrological modeling approaches. Despite the former may be useful to provide large-scale projections of climate change impacts, it lacks confidence when specific rivers or regions are of interest due to the absence of calibration and consequent poor performances in the historical period (Hattermann et al., 2017; Krysanova et al., 2018). Moreover, in large South American basins subject to extensive flat areas, it is also important to account for vertical processes in floodplains and its related hydrodynamics to achieve reasonable results (Vinícius A Siqueira et al., 2018), which are usually not represented by GHMs.

The objective of this paper is to assess the impacts of climate change on South American water resources according to CMIP5 projections. We use a continental-scale, hydrologic-hydrodynamic model specifically calibrated for South America to provide insights on where alterations of water budget variables and river discharge are expected, and how they compare to the uncertainties of projections. This article is organized in the following sections: i) Methodology – which contains descriptions of the hydrological model, climatological data, bias correction method and assessment approach; ii) a summary of the South America hydrology; iii) results and discussion about the main impacts of climate change on water resources which was divided as: impacts on precipitation, evapotranspiration and runoff, specific impacts on discharge and overall water balance on the continent.

2. METHODOLOGY

2.1. Hydrological Model - MGB

The *Modelo de Grandes Bacias* – MGB (Paulo Rï¿½genes Monteiro Pontes et al., 2017) was selected for this study due to: (i) its capability to represent the main South America hydrological processes as it was developed through experiences in this region (Siqueira et al., 2018), (ii) its

performance demonstrated in previous validation studies and (iii) its successful application in several climate change studies in specific South American basins (Adam et al., 2015; Bravo et al., 2014; Nóbrega et al., 2011; Sorribas et al., 2016a).

The MGB is a conceptual, distributed hydrological model, in which the river basin is divided into unit-catchments following the terrain, and into Hydrological Response Units (HRU) defined by land use, land cover, geological features and soil types. The HRU classification was based on the soil and land use map for South America provided by Fan et al. (2015). The water balance is calculated on each HRU within a unit-catchment and evapotranspiration is calculated through the Penman-Monteith equation. The water stored on the soil layer heads to three different linear reservoirs per unit-catchment: surface, subsurface and groundwater reservoirs. The water flows to the surface reservoir following the ARNO model (Todini, 1996) while the subsurface and groundwater flows are respectively non-linearly and linearly related to the water storage in the soil layer. The water volume that heads to the river channel is proportional to the volume stored on each reservoir. The flow routing on the river channel is computed using a hydrodynamic model (Paulo Rï¿½genes Monteiro Pontes et al., 2017), accounting for inundation and infiltration from flooded areas into the unsaturated soil column in floodplains (Fleischmann et al., 2018).

The MGB has been frequently used for assessing climate impacts in South American basins (Adam et al., 2015; Bravo et al., 2014; Nóbrega et al., 2011; Sorribas et al., 2016a). In a broader scale, Ribeiro Neto et al. (2016) used MGB to simulate climate change effect in the main Brazilian basins, although with no streamflow routing between cells. Here we used the same continental scale, hydrodynamic model setup from Siqueira et al. (2018), which was developed for South America region (hereafter named as MGB-SA) and enables to obtain discharges along the drainage networks in addition to runoff. MGB-SA has been manually calibrated by linking parameters to HRUs, large basins and geology/lithology maps instead of applying automatic calibration at specific gauge stations, aiming to reduce model overfitting (Siqueira et al., 2018). This model has been validated with hundreds of in situ gauges and compared favorably to GHMs with respect to river discharges (daily data KGE and NSE > 0.6 in 70% and 55% of the gauges, respectively). MGB-SA was also validated with terrestrial water storage from the Gravity Recovery and Climate Experiment (GRACE) and evapotranspiration from multiple datasets, which increases confidence to simulate general hydrological processes and consequently climate change impacts (Krysanova et al., 2018). Nonetheless the model does not include snowmelt processes and present unsatisfactory performances on arid regions, as discussed in the model development and validation (Siqueira et al., 2018).

2.2. GCM data

The GCM data used in this study is a subset of the CMIP5 multi-model ensemble snapshot of March 15, 2013, which was discussed on the IPCC Working Group I AR5 report. This dataset consists of monthly means of climate variables from 1850 to 2100. Our assessment was conducted considering two distinct periods of 20 years, baseline period (1986-2005) and future (2081-2100), and two different scenarios, RCP 4.5 and RCP 8.5. The scenarios are named after the radiative

forcing increment in W/m² by the end of the 21st century compared to the pre-industrial era, and those are specially related to GHG emissions policies. RCP 8.5 (Riahi et al., 2011) represents a scenario with no concern about GHG emissions on a highly industrial society, while the RCP 4.5 represents a more moderate scenario (Thomson et al., 2011).

We selected the GCMs that provide the prescribed MGB-SA input variables, simulation periods and GHG emission scenarios. The hydrological model MGB-SA requires as climate inputs: air surface temperature, relative humidity, wind speed, atmospheric pressure, income shortwave solar radiation (evapotranspiration variables) and precipitation. Except for rainfall data, climate variables used as input for MGB-SA were long-term monthly means. The 25 selected GCMs are listed in the supporting material.

2.3. Bias Correction

Raw GCM data are limited as input to hydrological models due to existing biases. Instead, climatological databases derived from system observations are taken as reference to reduce the GCM biases by means of bias correction methods (Christensen et al. 2008; Pierce et al. 2015; Teutschbein and Seibert 2012). Although discussions have arisen about the effectiveness of these methods and how they represent a new source of uncertainty (Ehret et al. 2012; Muerth et al. 2013; Zhao et al. 2017), bias correction is still necessary on hydrological modeling, since streamflow sensitivity to precipitation depends on the precipitation volume itself, i.e., a precipitation bias could cause an significantly higher bias on streamflow (variable runoff coefficient).

The delta change method is simple and robust since the model projection is built over the current climate; however it ignores simulated climate dynamics as extreme events or number of wet days (Teutschbein and Seibert, 2012). As we are dealing with a continental scale and monthly means of climate variables from GCMs, specific events were ignored and only annual means were analyzed. The delta change method can be either additive or relative as described below:

Relative: $P_f^* = P_p^* \times \left(\frac{P_f}{P_p}\right)$ Additive: $P_f^* = P_p^* + (P_f - P_p)$

where P_p and P_f are the simulated monthly means of GCM variables for the baseline and future periods, respectively; P_p^* is the observed variable value from a climatological database; P_f^* represents the bias-corrected variable for the future period.

The relative delta change was used for precipitation while the additive method was used for the remaining climate variables. The climate model variables (P_p and P_f) refers to the 20-yr mean for each calendar month. As the water balance component of the MGB-SA is run with a daily time step, the daily precipitation of the climatological database (P_p^*) was multiplied by the P_f/P_p ratio of the respective month. However, some limiting conditions were imposed to the delta change method due to relative precipitation changes on very dry areas (described on the supporting information text).

The reference climatological databases used are: (i) the MSWEP v1.1 (Beck et al., 2017) daily precipitation dataset from 1990 to 2009 and (ii) the CRU Global Climate v.2 (New et al., 2002), which provides monthly means of the 1961-1990 period for the remaining climate variables needed to estimate evapotranspiration (see section 2.2). The delta change and MSWEP data were interpolated to the MGB-SA unit-catchments centroids using the inverse distance squared method, while the CRU data is interpolated using the nearest neighbor method. There are 33,749 unit-catchments on the MGB-SA model, which gives an average of 4 km distance between the downstream and upstream unit-catchments centroid. The CRU and MSWEP databases have a spatial resolution of approximately 18 and 25 km respectively, while climate projections' spatial resolution ranges from 100-300 km depending on the GCM. On heterogenous areas, e.g. the steep regions of the Andes Cordillera, climate can be substantially different within a GCM grid cell. In those regions, a downscaling approach based on delta change interpolation ignores the climate heterogeneity which is a clear limitation of the current method.

2.4. Assessment (significance and quantiles)

The MGB-SA was driven by bias corrected climate data of different GCMs, constituting an ensemble (25 simulations per scenario) of hydrological conditions, i.e., runoff, evapotranspiration and river discharge for the future period. This ensemble was compared with a model run of the baseline period (named hereafter as the **reference simulation)**, which refers to the MGB-SA model forced with the climatological databases (MSWEP and CRU).

The GCMs projections present high uncertainties which are transferred and even amplified on the impact models outputs. Thus, a statistical evaluation becomes necessary to adequately address uncertainties. It was assumed that each member of the ensemble is independent and compose a random sample of 25 individuals.

The statistical relevance of the climate change projections was addressed by means of ensemble quartiles, ensemble agreement, coefficient of variation and a two-sample t-test. The coefficient of variation (CV) measure the future projections ensemble spread normalized by the ensemble mean. It was assumed that there is an agreement if 2/3 of the ensemble members present the same change signal, indicating either a drier or wetter condition for the future.

The two-sample t-test evaluates to what extent the reference and future mean variables differ in a specific location using two samples of unknown and unequal variances. The sample 1 (p) was composed by annual means of the reference simulation, to account the natural interannual variability (n_p=18, warm-up period of 2 years), while the sample 2 (f) was composed by the long period mean of each ensemble member (n_f=25). We assumed a null hypothesis (H_o) that the samples' means are equal ($\overline{x_p} = \overline{x_f}$) within a 5% level of significance (α). If test fails to reject H_o, then it is assumed that there is no significant change. However, if H_o is rejected, then we quantify how much the sample 1 mean should increase/decrease (Δ_p) in order to avoid the null hypothesis rejection:

$$\Delta_p = \overline{x_f} - \overline{x_p} \ \pm \ |Z^*(\alpha, d)| \left[\frac{S_p^2}{n_p} + \frac{S_f^2}{n_f}\right]^{1/2}$$

where $\overline{x_p}$ and $\overline{x_f}$ represents sample 1 (reference/present) and sample 2 (future) means respectively; S and n are related to the sample standard deviation and number of individuals respectively. Z^* is the limiting test statistic value for no rejection of H_o, which is a function of the level of significance α and the degrees of freedom (d); and its term signal is positive if $\overline{x_p} > \overline{x_f}$ and negative otherwise.

That increase/decrease of $\overline{x_p}$ on a relative basis (Δ_p / $\overline{x_p}$) is called **significant change**. This index was used further to indicate the minimum variation on $\overline{x_p}$ to avoid the null hypothesis rejection within a 5% level of significance, i.e. how much a hydrological variable is likely to change at least.

This statistic test is built on the assumption of randomly selected independent variables from a normal distribution. Although the different GCMs responses are not necessarily independent as they share similar physical and numerical features (Flato et al., 2013), the combination of the ensemble members outputs approximates to normality (supporting information).

3. HYDROLOGY OF SOUTH AMERICA

South America drains around 30% of the continental freshwater that reach the oceans (Clark et al., 2015a). Half of this water flows through the Amazon River (mean annual flow ≈ 200,000 m³/s), whose basin occupies 1/3 of the continent area and has a significant environmental importance since it holds the world's largest rainforest (land use and soil map can be seen in Fan et al. 2015). The Amazon Basin is formed by the steep regions of the tropical Andes on west, the Brazilian and Guyanese shields on east, and the Amazon plain, which occupies nearly half of the basin area. In the Amazon plain, the low slope causes backwater effects and floodplains to largely influence the river dynamics (Paiva et al. 2013).

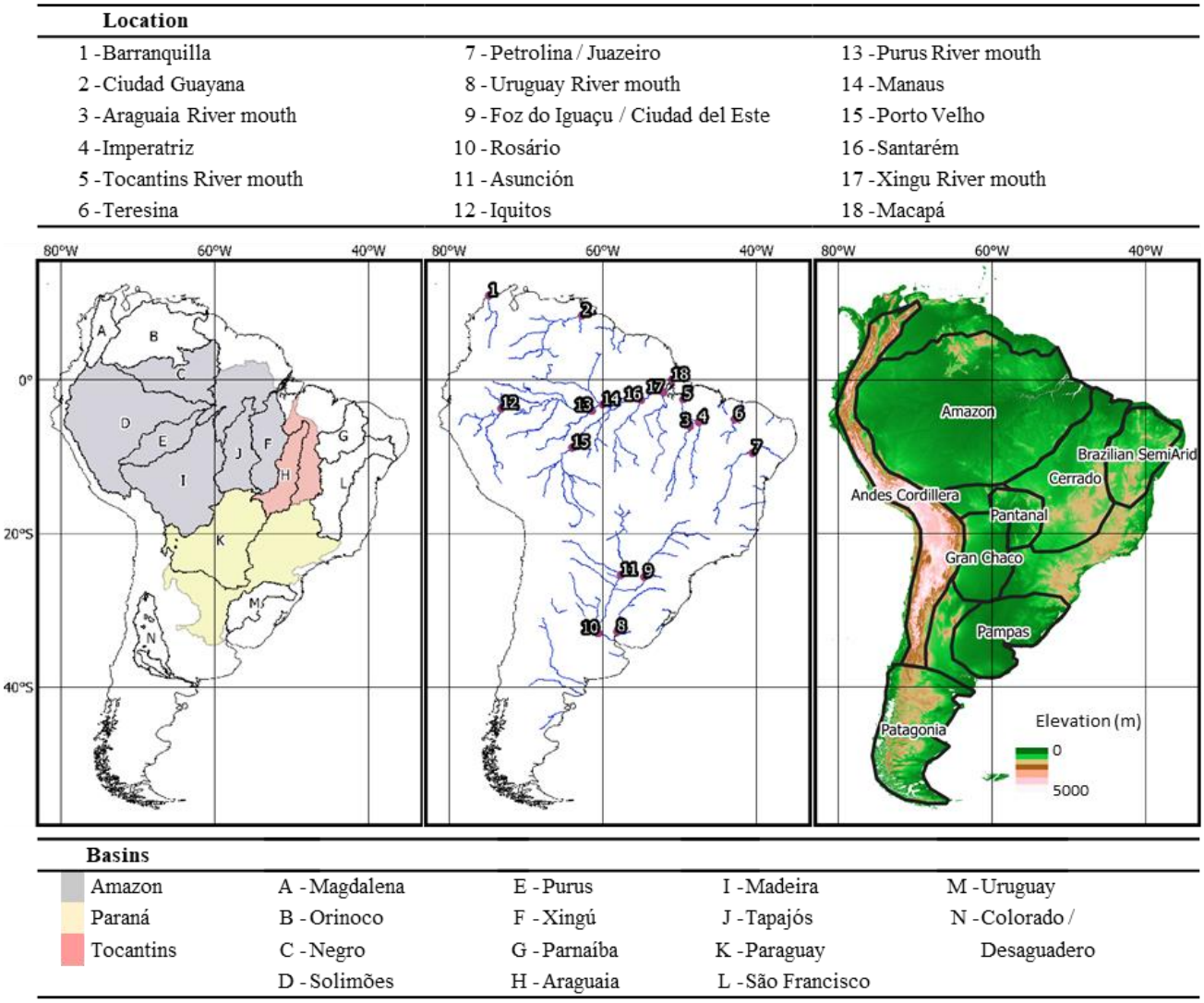

Figure 1 - South American larger basins, hydrography estimated by flow direction maps from the Hydrosheds database, relief from SRTM DEM and regions classification for this article.

We might also cite other important basins as the Orinoco, which is a tropical basin that occupies a third of the Paraná Basin area but has a higher annual mean discharge; or the São Francisco and Parnaíba Rivers, which cross the Brazilian Semiarid and are essential for regional subsistence. The South America basins larger than 200,000 km² are illustrated on Figure 1.

The annual precipitation distribution along the South American continent on present days (MSWEP, 1990-2010) is shown on Figure 2.c. Low annual precipitation is observed on the south Andes, Patagonia and Brazilian Semiarid while a higher annual precipitation occurs on the Pampas and mainly surrounding the Equatorial line, especially on the west Amazon. This precipitation pattern over the continent reflects on aridity and consequently on the runoff coefficient, since runoff is highly related to soil moisture.

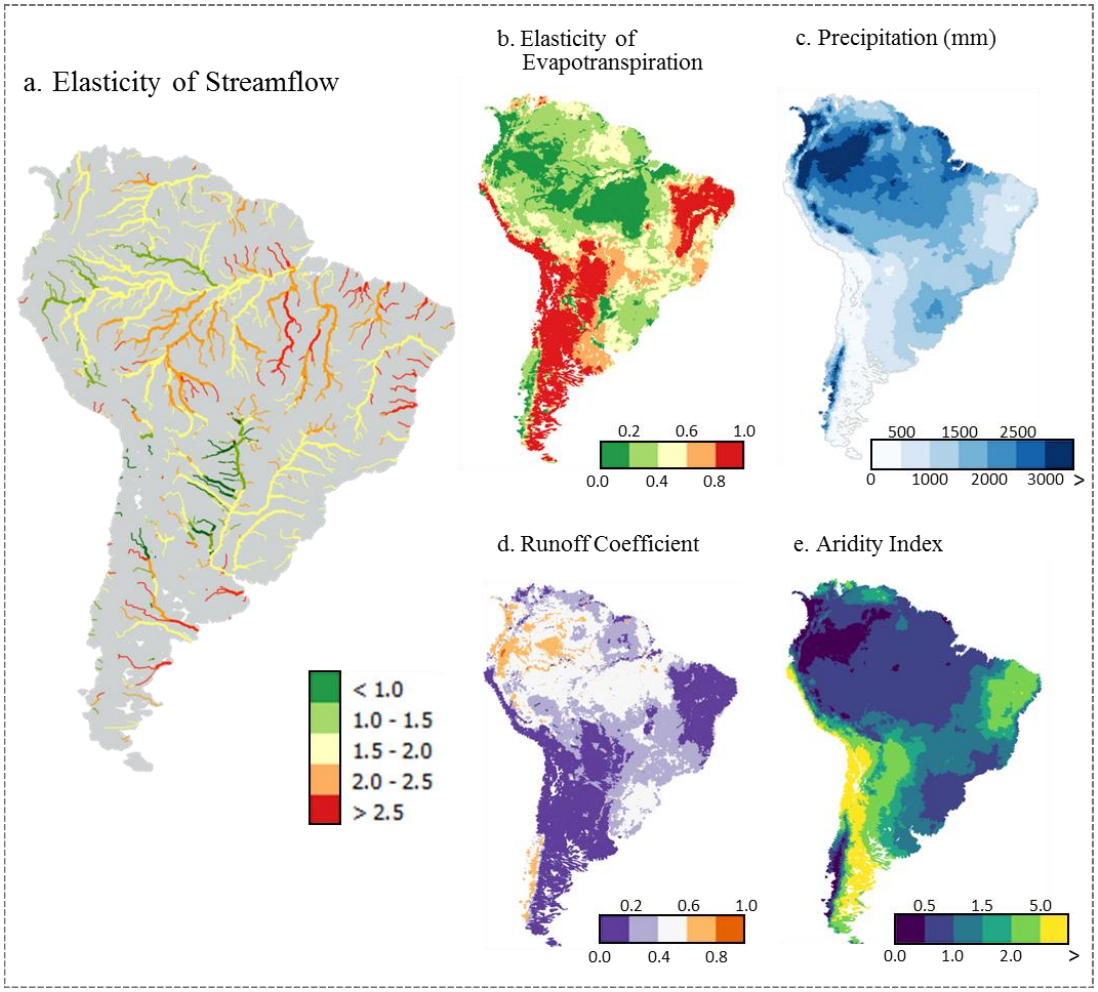

Figure 2 - Hydrological characteristics of South America. a. Elasticity of Streamflow which represents the relative sensibility of streamflow to precipitation; b. Elasticity of Evapotranspiration which represents the sensibility of evapotranspiration to precipitation; c. South America annual precipitation from the MSWEP 1.1 database; d. Runoff Coefficient which indicates how much of the Precipitation volume flows through the surface; e. Aridity Index which measure the ratio between PET and annual Precipitation.

The Aridity Index (AI) is given by the ratio between potential evapotranspiration (PET) and precipitation of a specific area. PET was calculated based on the open water Penman equation (Shuttleworth, 1993). The World Atlas Desertification (Middleton and Thomas, 1997) defines regions with AI above 5.0 as arid, AI between 2.0 and 5.0 as semi-arid, AI between 1.5 and 2.0 as dry subhumid and below 1.5 as humid. As climate change is expected to affect precipitation and evapotranspiration rates (e.g. through raise on temperature), this coefficient becomes a proxy of the climate change impacts on water resources although it does not necessarily indicates the runoff change signal (Yang et al., 2018). We might classify central-south Andes (latitude between 20º S and 35º S) and east Patagonia as arid regions, mainly due to a very low annual precipitation rather than PET intensity; the Brazilian Semiarid and part of the Gran Chaco as semi-arid regions; and the Pampas, Amazon and west Patagonia as humid areas. On the center of South America there is a transitional zone between the semi-arid and humid areas, mainly dominated by the biome called “Cerrado”, which is equivalent to the African Savanna.

The long-term mean discharge sensitivity to precipitation changes can be analyzed in terms of elasticity (Chiew, 2006). The rainfall elasticity of streamflow is given by the ratio between the relative

change of streamflow (evapotranspiration) and precipitation ($\epsilon = \Delta Q(\%)/\Delta P(\%)$). It shows how much a change on annual precipitation could affect the mean discharge/ evapotranspiration. Due to the non-linearity relation between rainfall and streamflow, the elasticity coefficient becomes a fair sensitivity indicator only for small changes in precipitation. The discharge and evapotranspiration sensitivity to rainfall was estimated by forcing the hydrological model with precipitation values 20% higher/lower. The elasticity of streamflow is mostly related to the runoff coefficient, as higher values occurs on dry regions as discussed on previous studies (Chiew, 2006; Ribeiro Neto et al., 2016). However, a low elasticity can be noticed on the right-bank tributaries of the Paraguay River (Gran Chaco) and a high elasticity is observed on the humid Xingu Basin, which indicates high sensibility to precipitation changes.

4. IMPACTS ON WATER BUDGET VARIABLES

Precipitation, evapotranspiration, runoff and AI projections were evaluated in terms of the difference between mean annual values of the reference simulation and the 20-yr ensemble mean of the future projections (Figure 3). The precipitation data refers directly to the bias corrected data from the GCM ensemble, while evapotranspiration and runoff are outputs of the hydrological model.

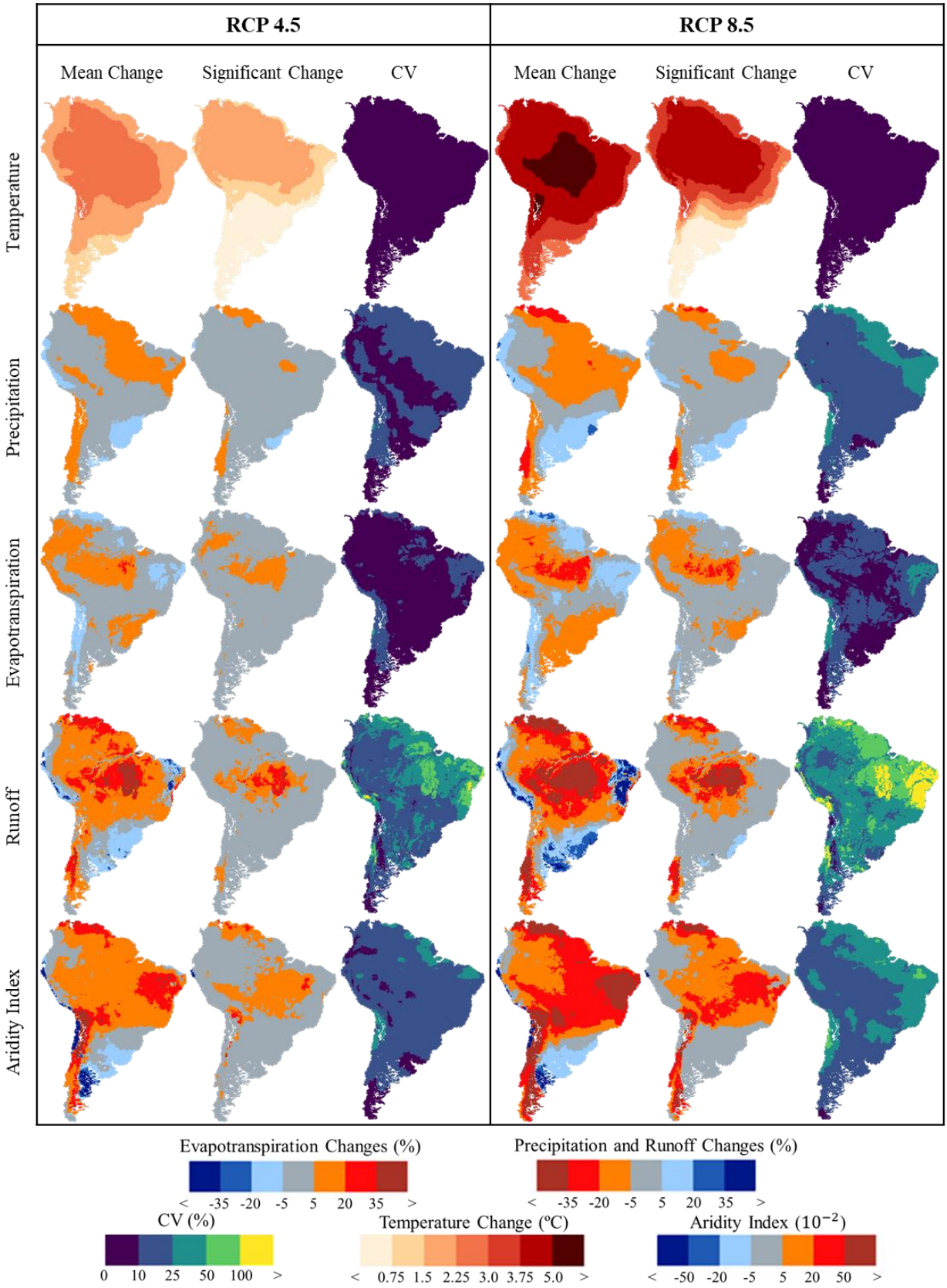

Figure 3 – Projected impacts on water budget components in South America (in terms of mean values). It is presented relative changes (mean and statistically significant) of precipitation, evapotranspiration and runoff, and absolute changes on aridity index and temperature in both scenarios (RCPs 4.5 and 8.5). The Coefficient of Variation (CV) is related to the projection's ensemble (it is not applicable to temperature, because of ocasional 0 mean values if considering the Celsius scale and larger mean values compared to standard deviation if its on Kelvin scale).

It can be seen two main regions of precipitation/runoff reduction: north to northeast and southwest of South America which embraces mainly the Amazon, Tocantins and Orinoco Basins and west Patagonia. Precipitation increase is mostly observed on the southeast and northwest of the continent which corresponds to the north Andes and the Pampas, although with almost any statistically significant change in runoff.

The overall results of both RCP4.5 and RCP8.5 scenarios were similar. Equal spatial patterns and change signals are identified among the scenarios, however with different intensities. As expected, the RCP8.5 scenario is likely to cause higher impacts. These results are particularly interesting because it suggests a direct relation between GHG concentrations and climate change impacts, at least on a mean annual basis (i.e. higher GHG concentrations implies on higher impacts with same sign at the same areas).

The highest emission scenario is likely to cause a higher impact but is also more uncertain. The coefficient of variation of the ensemble projections on the RCP8.5 scenario is consistently higher than RCP4.5, which implies on a larger uncertainty (figure 3). However, the statistical tests show that the RCP8.5 scenario is still associated to higher statistically significant impacts.

Figure 3 shows a direct relation between changes on precipitation and evapotranspiration. Lower precipitation volumes reduce the soil moisture, and consequently, the evapotranspiration rate. As the opposite is also true, changes on evapotranspiration and precipitation often have the same signal. This pattern is detected on most of the continent except in some parts of the Amazon. The Amazon Basin is very humid as 14% of the basin area consists of wetlands (Hess et al., 2015), thus precipitation anomalies do not limit the amount of water available for evapotranspiration (less sensitive to rainfall, as shown on Figure 2.b) and changes in other climatological variables as temperature becomes predominant in this process. As the mean temperature is likely to increase across the continent (Chou et al., 2014; Marengo et al., 2012), evapotranspiration rate in the Amazon would follow the temperature change signal while annual mean precipitation is expected to reduce.

Peculiarly on the Brazilian Semiarid, which includes the Parnaíba Basin and part of the São Francisco Basin, a negative change signal on the mean precipitation is observed together with a positive signal on the mean runoff. These results were mainly consequence of the rainfall elasticity, which ranges from 4 to 10 in that region (Ribeiro Neto et al., 2016). High elasticity on the Brazilian Semiarid (Figure 2.a) means that a small variation on precipitation causes a large variation on the streamflow. Actually a few ensemble members projected highly positive precipitation anomalies that pushed up the mean runoff, thus amplifying the ensemble spread. This means that the normal distribution assumption is not adequate on the Brazilian Semiarid since the runoff mean of the GCM ensemble is significantly different from the runoff median. Although a significant change signal of the runoff could not be predicted with the present methodology and current GCM data, the AI indicates that the Brazilian Semiarid is likely to become larger and dryer on the RCP 8.5 scenario. These results agree with Marengo and Bernasconi (2015), who used a Regional Climate Model to estimate projections of the arid region expansion on the Northeast Brazil.

Climate change on the Andes Cordillera is clearly divided in two regions. On the Tropical Andes the change signal is positive and from the latitude 18º S of the Andes Cordillera to Patagonia it is predicted a negative trend. However, only on Patagonia the runoff change signal was statistically significant. It is important to remark that there are high uncertainties due to the misrepresentation of snow melting by the hydrological model, which is an important hydrological feature on Patagonian and Andean basins.

Despite of the high impacts indicated by the GCM ensemble mean runoff across the continent, only on few basins they were statistically significant. It is expected a negative signal of precipitation and runoff on the Orinoco, Tocantins and South Amazon (Tapajós, Xingu, Madeira and Purus) basins. The combination of precipitation decrease and evapotranspiration increase leads to an intense climate change effect on the South Amazon, where it is estimated the higher impacts – at least 20% of runoff reduction on the Tapajós and Xingu basins. Only on a small region placed between the Uruguay basin and the Atlantic coast (southeast South America) it is expected a statistically significant increase in annual precipitation and runoff.

Negative trends in the east Amazon and Patagonia and positive trends in southeast South America and Tropical Andes have been announced for a while (Marengo et al., 2009; Milly et al., 2005). The mean changes results are similar to studies with no bias-correction (Koirala et al., 2014), studies that used the Eta regional climate model (Chou et al., 2014b) on South America (Ribeiro Neto et al., 2016) and GCM data from CMIP3 (Arnell and Gosling, 2013). However some disagree especially about the Amazon Basin change signal (Guimberteau et al., 2017; Hagemann et al., 2013; Sperna Weiland et al., 2012) and even about the wetting trend in the southeastern South America (Schewe et al., 2014). This paper described to which extent the results from CMIP5 GCMs agree and the change signal was clear especially on the South Amazon.

5. IMPACTS ON RIVER DISCHARGE

Future anomalies in river discharge are presented in Figure 4 and Table 1. Similar to the other hydrological variables, the discharge projections of both GHG scenarios present the same change signal, with higher impacts related to the RCP8.5 scenario.

From north to south, a significant negative trend is observed on the Orinoco, Tocantins, Paraguay Rivers and on all Southern tributaries of the Amazon. On the Orinoco Basin, reduced discharges are expected mainly downstream. The mean annual discharge at Ciudad Guayana is likely to decrease in 14% (9%) at least on the RCP8.5 (RCP4.5) scenario, which is equivalent to nearly 5.000 m³/s. Climate change impact in the Tocantins River is similar to the Orinoco River in relative terms. Higher changes are expected on the west side of the basin, mainly in the Araguaia River. On the Paraguay Basin, main discharge variation is likely to occur upstream, on Pantanal. These results are different from Bravo et al. (2014) findings that presented an equal probability of positive and negative trends, although using the same hydrological model. It is worth mentioning that waters flowing from river channels to the floodplains are considered in the vertical water balance of this current MGB-SA model (i.e., evapotranspiration and infiltration, the latter specifically

in Pantanal) (Siqueira et al., 2018) while Bravo et al. (2014) used the HEC-RAS (Brunner, 2010) hydrodynamic model as a routing component disconnected to the MGB. This physical representation has a considerable impact on the Paraguay Basin discharges due to the amount of floodplains areas. At Asunción, it is expected a mean discharge reduction of 6% and a decrease of 15% on the 30-days minimum on the RCP8.5 scenario.

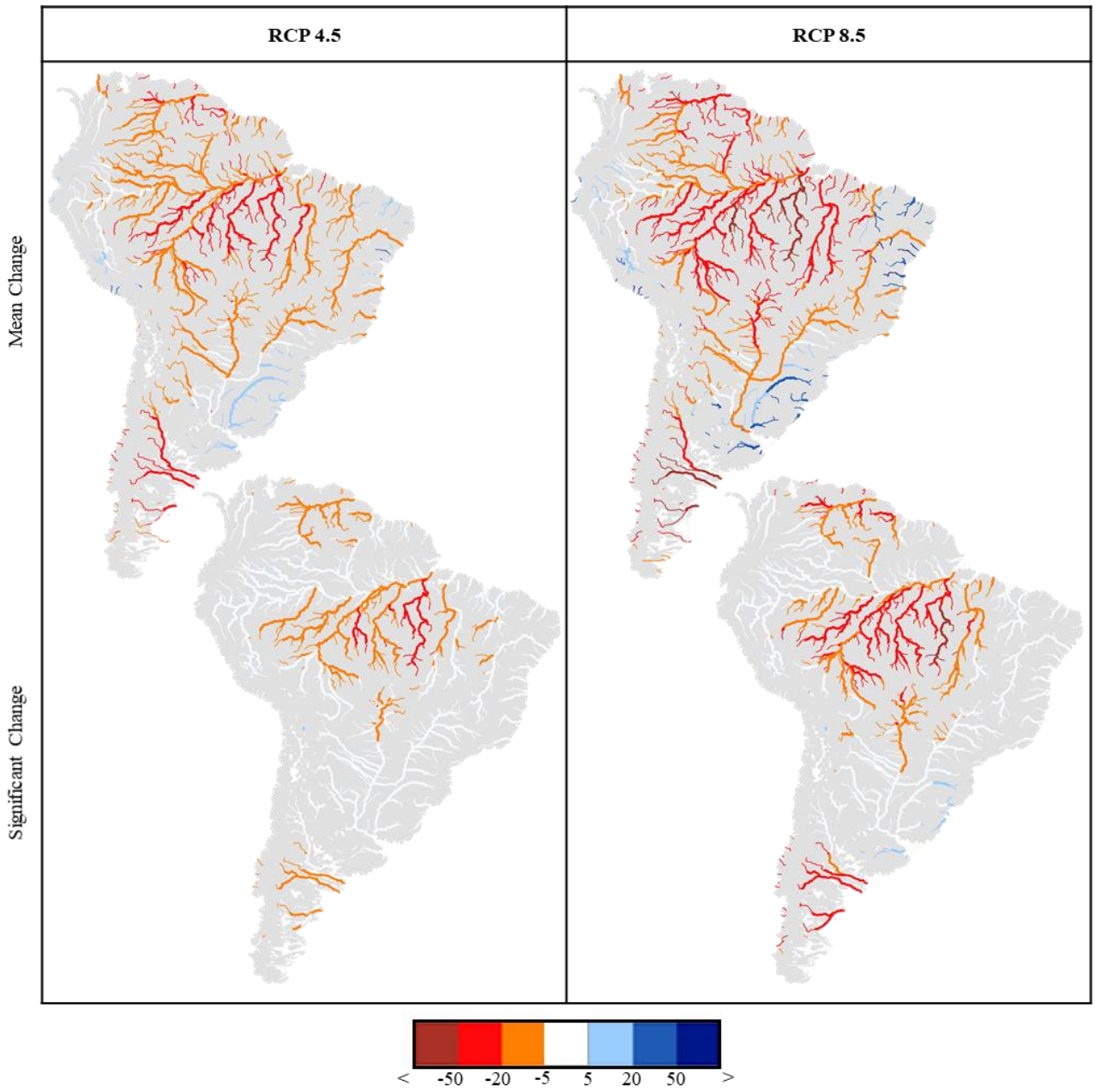

Figure 4 - Expected relative discharge anomalies (%) due to climate change. Top: Mean changes on annual discharge. Bottom: Significant changes on the mean discharge.

The most significant impact is likely to take place in the Amazon Basin. Over 18 % (34%) of discharge reduction is expected on the Tapajós and Xingu basins for the RCP4.5 (RCP8.5) scenario. Considerable impacts are also expected on the Madeira and Purus basins. The overall negative trend over the Amazon Basin, especially on the southeast, affects the Amazon River mean discharge, which is likely to decrease in at least 8% (15%) on the RCP4.5 (RCP8.5) scenario. A

discharge reduction of 8% does not seem excessive; however, it is equivalent to nearly 17,000 m³/s while the annual mean discharge of the Paraná Basin is around 24,000 m³/s.

The results on the Amazon Basin are very similar to those obtained by Sorribas et al. (2016), who found a moderate discharge decrease on the Negro, Purus and Madeira Rivers (over 5%) and a considerable reduction on the Tapajós (over 20%) and Xingu Rivers (over 50%) on the RCP8.5 scenario. However, changes were only statistically significant on the Xingu River, which is probably due to the small sample of GCM (5) to support their results. The authors also indicated a statistically significant and moderate discharge increase on the West Amazon (Tropical Andes), while our projections indicate only a slight increase on the maximum discharge.

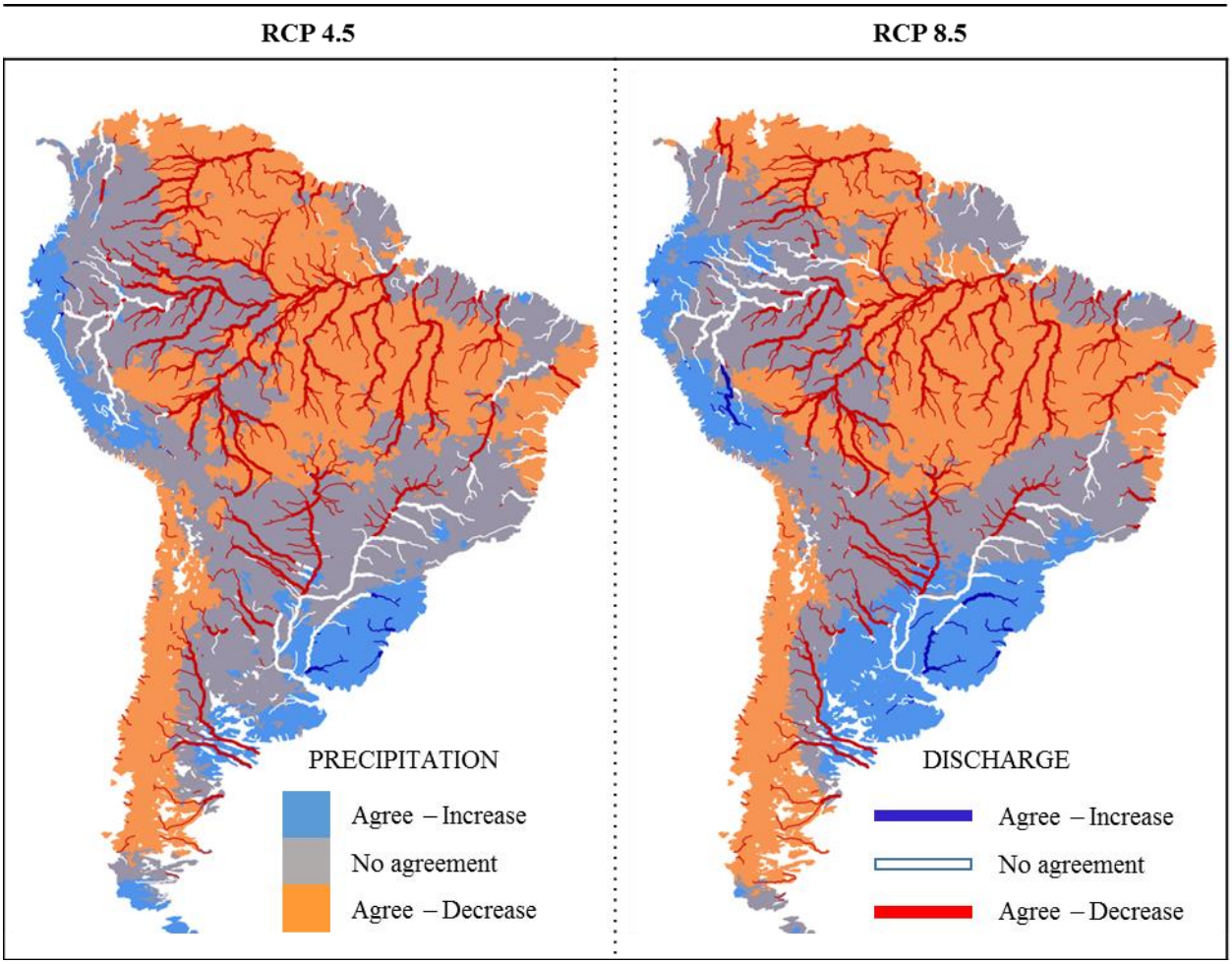

Figure 5 – Agreement of GCM ensemble members on precipitation/discharge change signal. Agree means that at least 2/3 of the ensemble members indicate same signal.

The Uruguay Basin was the only large basin (over 200,000 km²) that presented a positive trend, although statistical significance was only detected on the RCP8.5 scenario. Near to the river mouth, significant discharge change was negligible (1% - Table 1), although the GCM ensemble members clearly agree on a positive signal (Figure 5).

Table 1 - Climate change impact on specific locations of South America. $\boldsymbol{A}$ – drainage area; $\boldsymbol{Q}$ – current mean discharge; $\boldsymbol{\Delta Q}$ – ensenble mean discharge change; $\boldsymbol{sg\Delta Q}$ – signicant mean change.

River	Location	A (10^3 km²)	Q (10^3 m3/s)	RCP 4.5				RCP 8.5			
				ΔQ (%)	sg**Δ**Q (%)	Quartiles (10^3 m3/s)		**Δ**Q (%)	sg**Δ**Q (%)	Quartiles (10^3 m3/s)	
						1st	3rd			1st	3rd
Magdalena	Barranquilla	261	7.7	-5	0	6.6	8.3	-11	0	5.3	7.7
Orinoco	Ciudad Guayana	927	34.6	-16	-9	26.9	31.8	-25	-14	18.7	32.5
Araguaia	River mouth	387	6.5	-21	-11	4.4	5.9	-34	-19	3.2	5.2
Tocantins	Imperatriz	302	5.1	-16	-5	3.5	5.2	-26	-8	2.6	4.3
Tocantins	River mouth	774	14.5	-19	-8	10.2	13.3	-30	-14	7.3	12.1
Parnaíba	Teresina	291	0.7	-13	0	0.5	0.7	-12	0	0.4	0.6
São Francisco	Petrolina / Juazeiro	521	3.2	-10	0	2.6	3.3	-11	0	2.2	3.3
Uruguay	River mouth	267	6.7	11	0	6.5	8.3	20	1	6.5	9.4
Paraná	Foz do Iguaçu	911	15.7	-3	0	13.6	17.3	-6	0	11.9	18
Paraná	Rosário	2540	23.2	-3	0	20.1	25.2	-6	0	18	24.5
Paraguay	Asunción	907	4	-8	0	3.3	4.1	-17	-6	2.7	3.7
Solimões	Iquitos	745	27.9	-4	0	25.8	28.4	-1	0	25.3	30.5
Purus	River mouth	379	11.5	-22	-13	8.3	10.2	-38	-29	5.6	8.6
Negro	Manaus	716	35	-10	-2	30	33.3	-13	-2	24.1	36.2
Solimões	Manaus	2222	94.8	-9	-3	84.3	93.3	-12	-5	76.2	93.3
Madeira	Porto Velho	982	16.3	-14	-8	13	15	-26	-18	9.9	13.7
Tapajós	Santarém	496	15.7	-27	-18	9.3	13.4	-46	-34	5.1	10.5
Xingu	River mouth	515	14.6	-40	-25	4.5	11.2	-58	-41	1.4	7.3
Amazonas	Macapá	5927	206.6	-15	-8	164.8	191.5	-22	-15	131.3	189.4

No significant change was observed on the mean discharge of São Francisco and Parnaíba basins (Brazilian Semiarid). As previously discussed, the high rainfall elasticity of streamflow leads to a large spread of the discharge ensemble which directly affects the statistical significance. However, the ensemble quartiles under both scenarios indicate a negative trend, especially on the Parnaíba Basin (Figure 6). Also the ensemble members agree on a negative trend on the Brazilian Semiarid (Figure 5), which is consistent to the current literature (Asadieh & Krakauer, 2017; Marengo & Bernasconi, 2015; Ribeiro Neto et al., 2016).

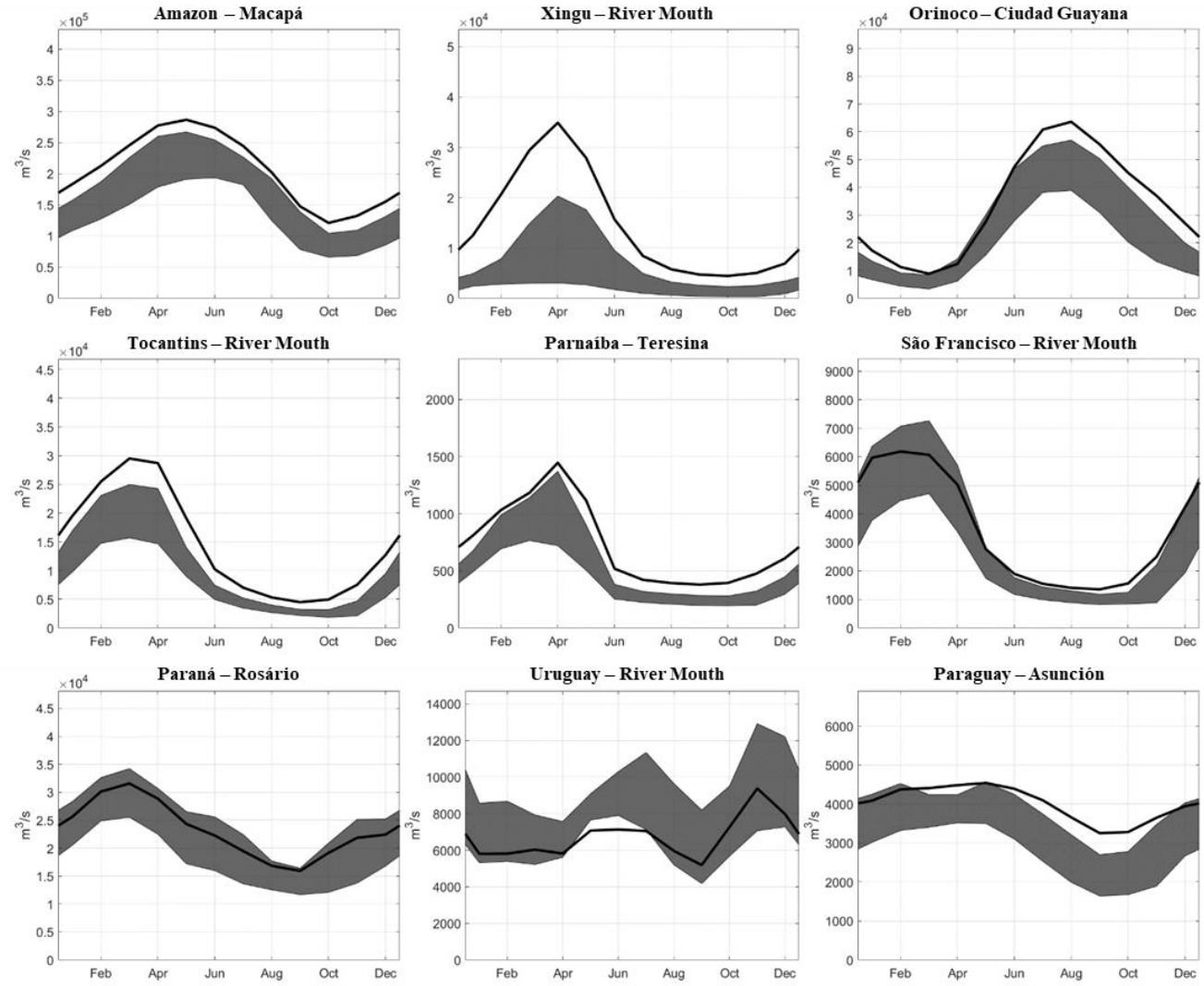

Figure 6 - Discharge climatology of some South American large basins under the RCP8.5 scenario. The black line refers to the reference period discharge and the grey swath refers to the GCM ensemble interquartile range.

On the Paraná and Magdalena basins there is a negative trend although not statistically significant. The GCM models show an agreement only on the downstream Magdalena under the RCP8.5 scenario. Nóbrega et al. (2011), Adam et al. (2015) and Ribeiro Neto et al. (2016) have used a fewer number of climate models and have pointed out the uncertainty related to discharge projections on the Paraná Basin. Our results indicate a

slight negative trend on the Paraná Basin mainly due to the Paraguay Basin. The precipitation agreement indicates that the Paraná Basin is a transitional region; where the upstream area is projected to become dryer while the downstream, wetter.

Discharge changes on basins in the south of the continent, are not addressed as the MGB-SA presented an unsatisfactory performance on that area (Vinícius A Siqueira et al., 2018). Snowmelt is an important hydrological process in basins of Patagonia and those draining the Central Andes of Argentina. In addition to snowmelt, consumptive water use plays a significant role, for example, on the Desaguadero River Basin water balance (Scarpati et al., 2014), but neither of them are considered in the MGB-SA. By studying models in a global scale, Schewe et al. (2013) and Dankers et al. (2013) have shown that uncertainties related to hydrological modelling is higher than climate modelling in the south of the continent. This paper results indicate a negative trend on basins of the south of the continent due to GCMs precipitation and aridity index projections, but discharge quantification or relative changes estimate with current assumptions and modelling choices is not trustworthy.

6. IMPACTS ON THE CONTINENTAL WATER BALANCE

Figure 7 presents how the continent water balance is likely to change on the RCP4.5 and RCP8.5 scenarios by the end of this century.

Like the previous analyses, projections on the continental water balance are more uncertain under the RCP8.5 scenario as the ensemble interquartile range of the RCP4.5 scenario is narrower compared with the former. Basically, the 3rd quartile of discharge projections is similar among the scenarios, but the 1st quartile under RCP8.5 presents lower values, which implies on a drier condition.

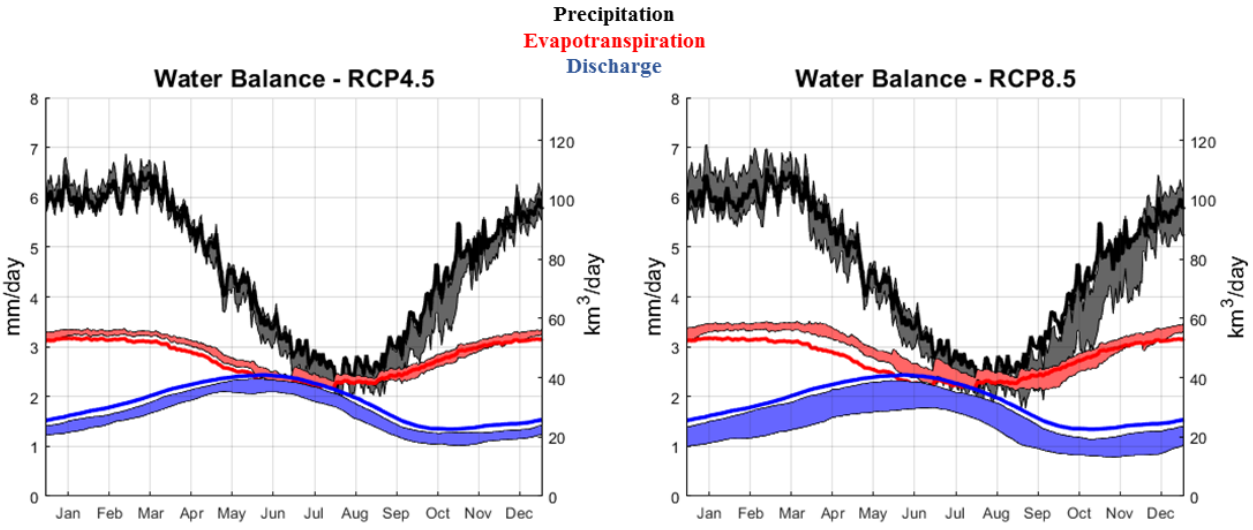

Figure 7 – Water balance over the South American continent. The darker lines represent precipitation, evapotranspiration and discharge annual means of the reference simulation and the colored swath

refers to the interquartile range of the ensemble projections under climate change for the end of the 21st century.

It is clear that the climate projections indicate a drier continent by the end of this century. On wet periods (December to March) mean precipitation is unlikely to change, but less average rainfall amounts are expected on dry periods (June to September). Actually, it seems that the dry period will be extended to include October as well. In addition, as temperature is likely to increase in South America, evapotranspiration is expected to be higher in the wet periods especially on the RCP8.5 scenario.

The combination of precipitation decrease and evapotranspiration increase is responsible for major changes on the expected river discharge. The total amount of water flowing to the oceans is likely to be equally reduced along the year. The ensemble median discharge under the RCP8.5 scenario is in average 0.3 mm/day lower compared with the reference simulation. In that condition, 1,800 km³ less water is likely to reach the ocean every year, which correspond to 15% of South American current fluxes to the ocean and it is equivalent to the annual amount of freshwater drained from the Australian continent (Global Runoff Data Centre (GRDC), 2014).

A lag between the peaks of precipitation and discharge is also noticed. This lag refers to the “time of concentration” of the continental waters, which is about 4 months in average. On the other hand, evapotranspiration response to precipitation is almost immediate. It is important to remark that the “continental hydrograph” is largely influenced by the Amazon Basin as it drains half of the continent freshwaters. Thus, a discharge decrease of the same magnitude as the Amazon River was already expected.

7. CONCLUSIONS

Climate change impacts on South American water resources were estimated by a continental hydrological-hydrodynamic model forced with an ensemble of bias corrected GCM data under two scenarios: RCP4.5 and RCP8.5. We conducted a comparison between mean values of the reference (1986-2005) and future (2081-2100) periods, which means that specific events were not addressed in this study.

It was assessed the expected alterations in water budget and river discharges across the continent, and to what extent these impacts are statistically significant. It is important to clarify that the significant change does not represent the expected variation of hydrological variables; neither areas that the mean change were not statistically significant are unlikely to be impacted. The significant change refers to the minimum variation of a hydrological variable in order to not reject the hypothesis that the reference and future period have same means.

Results shown no significance regarding discharge alterations in large basins such as the Parnaíba, São Francisco, Paraná and Magdalena. On the other hand, positive trends are

expected on the Tropical Andes and southeast South America, although only at the Uruguay Basin the runoff increase was significant. On the Uruguay River, the mean discharge is expected to increase in 20% under the RCP8.5, but only an increase of 1% on mean discharge was statistically significant.

Negative trends were found to be much more expressive. Runoff is expected to decrease in most of the South American large basins. Under the RCP8.5 scenario, the Orinoco, Tocantins and Madeira basins are likely to present at least a moderate discharge decrease (10% - 20%) while on the Tapajós, Xingu and Purus basins, water resources are expected to be highly impacted (over 29% of discharge reduction at least). On the RCP4.5 scenario, the same change signal is expected but with a lower impact.

It was assumed that GCMs projections are right to some extent and the ensemble mean and median would be an acceptable indicative of what would be the climate in the future. However, poor understanding on some land surface processes (e.g. cloud feedback, Zhao et al. 2016) and shared representation of physical and numerical aspects among different GCMs (Flato et al., 2013) may lead to common errors that affect the change signals, as well as the randomness and independence assumptions of the statistical analysis.

In addition, the modelling options and bias-correction approach brought different sources of uncertainty to the results. For example, there is a high climate variability on Andes with the horizontal distance, and interpolating coarse GCM grid cells might not be the most accurate alternative. Also, the MGB-SA does not represent snowmelt processes neither consider water consumptive uses, which are very important for discharge estimate on snow melting dependent basins (e.g. east Patagonian basins) and on semi-arid regions, respectively. Land use alterations were not evaluated, which is an important aspect considering current pressure on mineral extraction and agriculture expansion over Amazon (Guimberteau et al., 2017; Siqueira Júnior et al., 2015), for example.

In conclusion, the majority of GCM projections predict similar climate change impacts on many South American basins as the Amazon, Tocantins and Uruguay basins, despite of recognized modeling limitations. This information should be considered by decision makers on planning hydroelectric power plants, supply reservoirs or agricultural expansion. Upcoming enhancements from CMIP phase 6 combined to a multi hydrological model and bias correction approaches are paths of improvements on projections robustness and uncertainty understanding.

ACKNOWLEDGEMENTS

This work is part of the project "*Desenvolvimento do Modelo Regional do Sistema Terrestre ETA e Geração de Cenários de Mudanças Climáticas e de Usos da Terra visando Estudos de Impacto Sobre os Recursos Hídricos*" funded by the Brazilian National Water Agency (ANA) and the "*Coordenação de Aperfeiçoamento de Pessoal de Nível Superior*"

(CAPES). It is also included on the project SAFAS “South America Flood Awareness System” funded by the “*Conselho Nacional de Desenvolvimento Científico e Tecnológico* (CNPq)”. We acknowledge the World Climate Research Programme’s Working Group on Coupled Modelling, which is responsible for CMIP, and we thank the climate modeling groups for producing and making available their model output. This paper results related to streamflow are summarized on the South America Climate Change Impacts on water resources (SACCI) available at https://www.ufrgs.br/hge/modelos-e-outros-produtos/sacci/.

REFERENCES

Adam K, Fan F, Pontes P, et al (2015) Mudanças climáticas e vazões extremas na Bacia do Rio Paraná / Climate Change and Extreme Streamflows in Paraná River Basin. Rev Bras Recur Hídricos 20:999–1007. doi: 10.21168/rbrh.v20n4.p999-1007

Arnell NW, Gosling SN (2013) The impacts of climate change on river flow regimes at the global scale. J Hydrol 486:351–364. doi: 10.1016/j.jhydrol.2013.02.010

Asadieh B, Krakauer NY (2017) Global change in streamflow extremes under climate change over the 21st century. Hydrol Earth Syst Sci 21:5863–5874. doi: 10.5194/hess-21-5863-2017

Beck HE, Van Dijk AIJM, Levizzani V, et al (2017) MSWEP: 3-hourly 0.25° global gridded precipitation (1979-2015) by merging gauge, satellite, and reanalysis data. Hydrol Earth Syst Sci 21:589–615. doi: 10.5194/hess-21-589-2017

Bozkurt D, Rojas M, Boisier JP, Valdivieso J (2018) Projected hydroclimate changes over Andean basins in central Chile from downscaled CMIP5 models under the low and high emission scenarios. Clim Change 150:131–147. doi: 10.1007/s10584-018-2246-7

Bravo JM, Collischonn W, da Paz AR, et al (2014) Impact of projected climate change on hydrologic regime of the Upper Paraguay River basin. Clim Change 127:27–41. doi: 10.1007/s10584-013-0816-2

Brunner GW (2010) HEC-RAS river analysis system: hydraulic reference manual. US Army Corps of Engineers, Institute for Water Resources, Hydrologic …

Buytaert W, Bievre B De (2012) Water for cities: The impact of climate change and demographic growth in the tropical Andes. Water Resour Res 48:1–13. doi: 10.1029/2011WR011755

Chevallier P, Pouyaud B, Suarez W, Condom T (2011) Climate change threats to environment in the tropical Andes: Glaciers and water resources. Reg Environ Chang 11:179–187. doi: 10.1007/s10113-010-0177-6

Chiew FHS (2006) Estimation of rainfall elasticity of streamflow in Australia. Hydrol Sci J 51:613–625. doi: 10.1623/hysj.51.4.613

Chou SC, Lyra A, Mourão C, et al (2014a) Assessment of Climate Change over South America under RCP 4.5 and 8.5 Downscaling Scenarios. Am J Clim Chang 03:512–527. doi: 10.4236/ajcc.2014.35043

Chou SC, Lyra A, Mourão C, et al (2014b) Evaluation of the Eta Simulations Nested in Three Global Climate Models. Am J Clim Chang 03:438–454. doi: 10.4236/ajcc.2014.35039

Clark EA, Sheffield J, van Vliet MTH, et al (2015) Continental Runoff into the Oceans (1950–2008). J Hydrometeorol 16:1502–1520. doi: 10.1175/JHM-D-14-0183.1

Dankers R, Arnell NW, Clark DB, et al (2014) First look at changes in flood hazard in the Inter-Sectoral Impact Model Intercomparison Project ensemble. Proc Natl Acad Sci 111:3257–3261. doi: 10.1073/pnas.1302078110

de Paiva RCD, Buarque DC, Collischonn W, et al (2013) Large-scale hydrologic and hydrodynamic modeling of the Amazon River basin. Water Resour Res 49:1226–1243. doi: 10.1002/wrcr.20067

Eyring V, Bony S, Meehl GA, et al (2016) Overview of the Coupled Model Intercomparison Project Phase 6 (CMIP6) experimental design and organization. Geosci Model Dev 9:1937–1958. doi: 10.5194/gmd-9-1937-2016

Flato G, Marotzke J, Abiodun B, et al (2013) Evaluation of Climate Models. Clim Chang 2013 Phys Sci Basis Contrib Work Gr I to Fifth Assess Rep Intergov Panel Clim Chang 741–866. doi: 10.1017/CBO9781107415324

Fleischmann A, Siqueira V, Paris A, et al (2018) Modelling hydrologic and hydrodynamic processes in basins with large semi-arid wetlands. J Hydrol 561:943–959. doi: 10.1016/j.jhydrol.2018.04.041

Global Runoff Data Centre (GRDC) (2014) Global Freshwater Fluxes into the World Oceans. Koblenz

Guimberteau M, Ciais P, Pablo Boisier J, et al (2017) Impacts of future deforestation and climate change on the hydrology of the Amazon Basin: A multi-model analysis with a new set of land-cover change scenarios. Hydrol Earth Syst Sci 21:1455–1475. doi: 10.5194/hess-21-1455-2017

Gulizia C, Camilloni I (2015) Comparative analysis of the ability of a set of CMIP3 and CMIP5 global climate models to represent precipitation in South America. Int J Climatol 35:583–595. doi: 10.1002/joc.4005

Hagemann S, Chen C, Clark DB, et al (2013) Climate change impact on available water resources obtained using multiple global climate and hydrology models. Earth Syst Dyn 4:129–144. doi: 10.5194/esd-4-129-2013

Hattermann FF, Krysanova V, Gosling SN, et al (2017) Cross-scale intercomparison of climate change impacts simulated by regional and global hydrological models in eleven large river basins. Clim Change 141:561–576. doi: 10.1007/s10584-016-1829-4

Hess LL, Melack JM, Affonso AG, et al (2015) Wetlands of the Lowland Amazon Basin: Extent, Vegetative Cover, and Dual-season Inundated Area as Mapped with JERS-1 Synthetic Aperture Radar. Wetlands 35:745–756. doi: 10.1007/s13157-015-0666-y

Knutti R, Sedláček J (2013) Robustness and uncertainties in the new CMIP5 climate model projections. Nat Clim Chang 3:369–373. doi: 10.1038/nclimate1716

Koirala S, Hirabayashi Y, Mahendran R, Kanae S (2014) Global assessment of agreement among streamflow projections using CMIP5 model outputs. Environ Res Lett 9:. doi: 10.1088/1748-9326/9/6/064017

Krysanova V, Donnelly C, Gelfan A, et al (2018) How the performance of hydrological models relates to credibility of projections under climate change. Hydrol Sci J 00:1–25. doi: 10.1080/02626667.2018.1446214

Marengo JA, Bernasconi M (2015) Regional differences in aridity/drought conditions over Northeast Brazil: present state and future projections. Clim Change 129:103–115. doi: 10.1007/s10584-014-1310-1

Marengo JA, Chou SC, Kay G, et al (2012) Development of regional future climate change

scenarios in South America using the Eta CPTEC/HadCM3 climate change projections: Climatology and regional analyses for the Amazon, São Francisco and the Paraná River basins. Clim Dyn 38:1829–1848. doi: 10.1007/s00382-011-1155-5

Marengo JA, Jones R, Alves LM, Valverde MC (2009) Future change of temperature and precipitation extremes in South America as derived from the PRECIS regional climate modeling system. Int J Climatol 29:2241–2255. doi: 10.1002/joc.1863

Melack J, Coe M (2012) Climate change and the floodplain lakes of the Amazon basin. Clim Chang Glob Warm … 295–310. doi: 10.1002/9781118470596.ch17

Middleton N, Thomas D (1997) World Atlas of Desertification, 2nd edn. Oxford Univ. Press

Milly PCD, Dunne KA, Vecchia A V. (2005) Global pattern of trends in streamflow and water availability in a changing climate. Nature 438:347–350. doi: 10.1038/nature04312

New M, Lister D, Hulme M, Makin I (2002) A high-resolution data set of surface climate over global land areas. Clim Res 21:1–25. doi: 10.3354/cr021001

Nóbrega MT, Collischonn W, Tucci CEM, Paz AR (2011) Uncertainty in climate change impacts on water resources in the Rio Grande Basin, Brazil. Hydrol Earth Syst Sci 15:585–595. doi: 10.5194/hess-15-585-2011

Pontes PRM, Fan FM, Fleischmann AS, et al (2017) MGB-IPH model for hydrological and hydraulic simulation of large floodplain river systems coupled with open source GIS. Environ Model Softw 94:1–20. doi: 10.1016/j.envsoft.2017.03.029

Reyer CPO, Adams S, Albrecht T, et al (2017) Climate change impacts in Latin America and the Caribbean and their implications for development. Reg Environ Chang 17:1601–1621. doi: 10.1007/s10113-015-0854-6

Riahi K, Rao S, Krey V, et al (2011) RCP 8.5-A scenario of comparatively high greenhouse gas emissions. Clim Change 109:33–57. doi: 10.1007/s10584-011-0149-y

Ribeiro Neto A, da Paz AR, Marengo JA, Chou SC (2016) Hydrological Processes and Climate Change in Hydrographic Regions of Brazil. J Water Resour Prot 08:1103–1127. doi: 10.4236/jwarp.2016.812087

Scarpati O, Kruse E, Gonzalez M, et al (2014) Updating the Hydrological. In: Handbook of Engineering Hydrology: Environmental Hydrology and Water Management. CRC Press, p 445

Schewe J, Heinke J, Gerten D, et al (2014) Multimodel assessment of water scarcity under climate change. Proc Natl Acad Sci 111:3245–3250. doi: 10.1073/pnas.1222460110

Shuttleworth WJ (1993) Evaporation. In: Maidment DR (ed) Handbook of Hydrology. McGraw-Hill

Silveira C da S, Souza Filho F de A de, Vasconcelos Júnior F das C (2017) Streamflow projections for the Brazilian hydropower sector from RCP scenarios. J Water Clim Chang 8:114–126. doi: 10.2166/wcc.2016.052

Siqueira Júnior JL, Tomasella J, Rodriguez DA (2015) Impacts of future climatic and land cover changes on the hydrological regime of the Madeira River basin. Clim Change 129:117–129. doi: 10.1007/s10584-015-1338-x

Siqueira VA, Paiva RCD, Fleischmann AS, et al (2018) Toward continental hydrologic – hydrodynamic modeling in South America. 1–50. doi: 10.5194/hess-2018-225

Sorribas MV, Paiva RCD, Melack JM, et al (2016) Supplementary Material: Projections of climate change effects on discharge and inundation in the Amazon basin

Sperna Weiland FC, Van Beek LPH, Kwadijk JCJ, Bierkens MFP (2012) Global patterns of change in discharge regimes for 2100. Hydrol Earth Syst Sci 16:1047–1062. doi: 10.5194/hess-16-1047-2012

Teutschbein C, Seibert J (2012) Bias correction of regional climate model simulations for hydrological climate-change impact studies: Review and evaluation of different methods. J Hydrol 456–457:12–29. doi: 10.1016/j.jhydrol.2012.05.052

Thomson AM, Calvin K V., Smith SJ, et al (2011) RCP4.5: A pathway for stabilization of radiative forcing by 2100. Clim Change 109:77–94. doi: 10.1007/s10584-011-0151-4

Todini E (1996) The ARNO rainfall-runoff model. J Hydrol 175:339–382. doi: 10.1016/S0022-1694(96)80016-3

Torres RR, Marengo JA (2013) Uncertainty assessments of climate change projections over South America. Theor Appl Climatol 112:253–272. doi: 10.1007/s00704-012-0718-7

Vicuña S, Garreaud RD, McPhee J (2011) Climate change impacts on the hydrology of a snowmelt driven basin in semiarid Chile. Clim Change 105:469–488. doi: 10.1007/s10584-010-9888-4

Vuille M, Carey M, Huggel C, et al (2018) Rapid decline of snow and ice in the tropical Andes – Impacts, uncertainties and challenges ahead. Earth-Science Rev 176:195–213. doi: 10.1016/j.earscirev.2017.09.019

Yang Y, Zhang S, McVicar TR, et al (2018) Disconnection Between Trends of Atmospheric Drying and Continental Runoff. Water Resour Res 54:4700–4713. doi: 10.1029/2018WR022593

Zhao M, Golaz JC, Held IM, et al (2016) Uncertainty in model climate sensitivity traced to representations of cumulus precipitation microphysics. J Clim 29:543–560. doi: 10.1175/JCLI-D-15-0191.1

SUPPORTING INFORMATION

List of the CMIP5 GCMs that included all inputs required by MGB on both scenarios (RCP 4.5 and 8.5) at the snapshot of March 15, 2013. The required MGB inputs are: air surface temperature, relative humidity, wind speed, atmospheric pressure, income shortwave solar radiation (evapotranspiration variables) and precipitation.

Model	Institution	Country	Resolution* (degrees)	
			Longitude	Latitude
ACCESS1.0	Commonwealth Scientific and Industrial Research Organisation/Bureau of Meteorology (CSIRO-BOM)	Australia	1.25	1.875
ACCESS1.3			1.25	1.875
BCC-CSM1.1	Beijing Climate Center (BCC)	China	2.7906	2.8125
BCC-CSM1.1 (m)			1.1215	1.125
BNU-ESM	Beijing Normal University (BNU)		2.7906	2.8125
CanESM2	Canadian Centre for Climate Modelling and Analysis (CCCma)	Canada	2.7906	2.8125
CNRM-CM5	Centre National de Recherches Météorologiques (CNRM-CERFACS)	France	1.4008	1.40625
CSIRO-Mk3-6-0	Commonwealth Scientific and Industrial Research Organisation (CSIRO)	Australia	1.8653	1.875
GFDL-CM3	Geophysical Fluid Dynamics Laboratory (GFDL)	USA	2	2.5
GFDL-ESM2G			2.0225	2.5
GFDL-ESM2M			2.0225	2.5
GISS-E2-H	NASA Goddard Institute for Space Studies (NASA-GISS)		2	2.5
GISS-E2-R			2	2.5
HadGEM2-CC	Met Office Hadley Centre (MOHC)	United Kingdom	1.25	1.875
HadGEM2-ES			1.25	1.875
HadGEM2-AO	MOHC + National Institute of Meteorological Research, Korea Meteorological Administration (NIMR-KMA)	UK + South Korea	1.25	1.875
INM-CM4	Russian Academy of Sciences, Institute of Numerical Mathematics (INM)	Russia	1.5	2
IPSL-CM5A-LR	Institut Pierre Simon Laplace (IPSL)	France	1.8947	3.75
IPSL-CM5A-MR			1.2676	2.5
IPSL-CM5B-LR			1.8947	3.75
MIROC-ESM-CHEM	Atmosphere and Ocean Research Institute (The University of Tokyo), National Institute for Environmental Studies, and Japan Agency for Marine-Earth Science and Technology (MIROC)	Japan	2.7906	2.8125
MIROC-ESM			2.7906	2.8125
MIROC5			1.4008	1.40625
MRI-CGCM3	Meteorological Research Institute (MRI)		1.12148	1.125
NorESM1-M	Bjerknes Centre for Climate Research, Norwegian Meteorological Institute (NCC)	Norway	1.8947	2.5

BIAS CORRECTION

A relative delta change method was used to correct supposed bias errors of GCM simulated precipitation. This method was conducted as follow:

$$P_f^* = P_p^* \times \left(\frac{P_f}{P_p}\right)$$

where p and f subscripts indicates reference and future periods respectively; P_p and P_f represents monthly means of accumulated precipitation estimated by GCMs; P_p^* is the MSWEP daily precipitation and P_f^* is the “unbiased” daily precipitation of the future period.

This method is simple and robust for most situations. However, on very dry areas as the Dry Andes (e.g. Atacama Desert), the relative change ratio (P_f/P_p) can be too large although it only means few millimeters increase on absolute value. For example, GCM simulations could estimate a mean accumulated precipitation of 0.05 mm for June on the reference period and 1.00 mm for the same month in the future period, which implies on a change ration of 20. This situation was frequently found among the GCM outcomes (Figure 8) and it can significantly compromises impact studies as a reference rain event (P_p^*) of 10 mm would imply on a 200 mm event for a bias corrected future period (P_f^*).

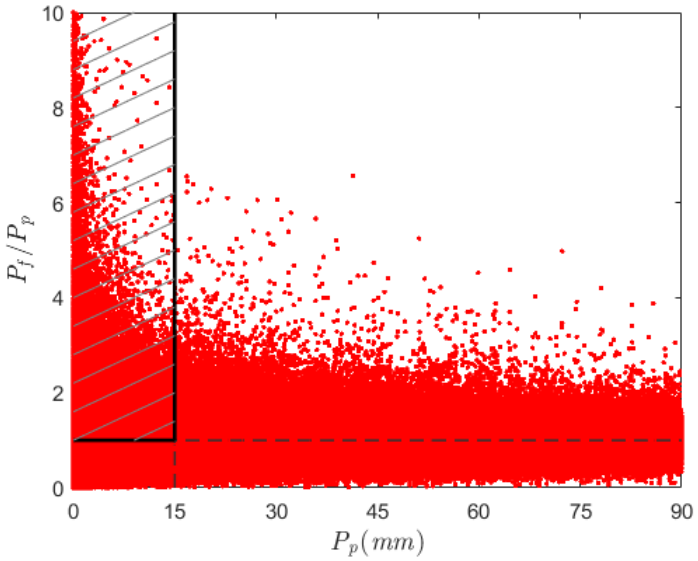

Figure 8 – Delta change ratio related to the accumulated precipitation of a specific GCM grid point. The dashed area marks the region selected for an additive delta change method.

It can be confirmed on Figure 8 that the highest delta change ratios are found on the driest months/areas. To work around this issue, it was proposed a monthly accumulated precipitation threshold of 15 mm as shown on Figure 8. When the accumulated precipitation in the reference period (P_p) was under 15 mm, and if the change ratio was larger than 1 ($P_f > P_p$), the delta change bias correction would be no longer relative, but additive:

$$P_f^{**} = P_p^{**} + \left(P_f - P_p\right)$$

As P_f and P_p represents the accumulated precipitation of a specific month, the rain increment ($P_f - P_p$) was added to the first rainy day of the month (P_p^{**}) or the last day of the month if no precipitation was registered.

ASSESSMENT

The two-sample t-test, used in this study for a significance assessment, requires independent and normally distributed variables, which cannot be inferred about GCMs outputs as they share many numerical features and modelling approaches. However, the

combination of 25 GCM along the South American continent approximated to a normal distribution as can be observed below.

The South American MGB is composed by 33,479 unit-catchments. For the statistical test, two samples are needed: the Sample 1 refers to annual variability of the reference period (n_p=18) and the Sample 2 refers to the period mean of each ensemble member (n_f=25). As the samples size are small (n = 18 and 25), they easily pass on normality tests as Kolmogorov-Smirnov. Therefore, we evaluated normality with standardized samples of all unit-catchments combined. On standardization, each individual is subtracted by the sample mean and divided by the sample standard deviation. The figure bellow presents the approximated distribution formed by the standardized samples:

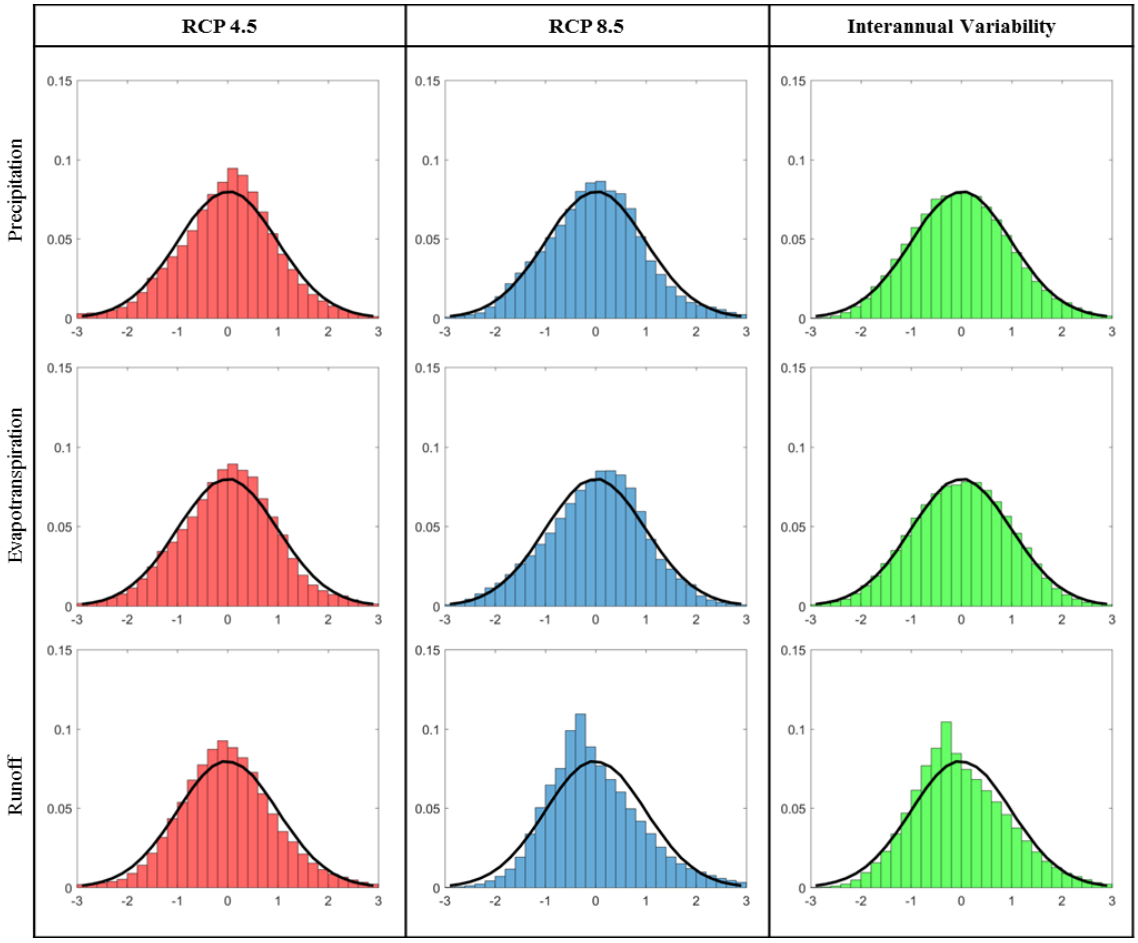

Figure 9 - Standardized samples histogram. The black line represents the standard normal distribution. The X-axis refers to the standardized value and the Y-axis represents its respective probability.

It can be seen in the Figure 9 that the samples distribution highly approximates to a normal distribution. Thus, it was assumed that the two-sample t test could be used to provide reasonable estimates about climate projections uncertainty. When the distribution was notably different from the normal distribution, it was discussed on the manuscript, e.g. on the Brazilian Semi-arid. Nevertheless, it was used other approaches to assess uncertainty (ensemble quantiles and agreement) that have supported significance conclusions.

ARTIGO 2

Assessing long-term simulations of extreme precipitation from a regional climate model: A hydrological perspective in South America

Authors:

João Paulo Lyra Fialho Brêda
Rodrigo Cauduro Dias de Paiva
Walter Collischon
Sin Chan Chou

Abstract

Global and Regional Climate Models (GCM and RCM respectively) are the current mathematical tools used to project alterations on precipitation regimes given different greenhouse gases emissions scenarios. However, these models have specific resolutions, physical equations and numerical approaches that provide a diverse set of performances across different regions and spatial-temporal scales. In South America, most hydrological impact studies have used the Eta RCM to yield precipitation projections without a proper uncertainty analysis. It is important to acknowledge its uncertainties prior to any hydrological assessment to adequately support climate change investigations and related water decision making. Here we evaluate the extreme precipitation generated by the Eta RCM driven by 4 different GCMs. It is investigated Eta biases across different temporal (3 hours to 5 days) and spatial scales (0.2 to 1.0 degrees) and how those errors affect river streamflow simulations of various spatial scales. It is used local IDF curves and a gridded precipitation dataset (MSWEP) as references for Eta assessment. In general, Eta underestimates sub-daily extreme precipitation across South America, regardless of the driven GCM. Eta presented high spatial dependence for extreme events of 1-day duration compared to MSWEP, which might indicate a poor representation of short-scale processes. However, the relative errors reduce with temporal and spatial aggregation. For example, the average bias of extreme precipitation decreases 8.4 percentage points from 1-day to 5-days duration. The negative biases observed for precipitation (≈20%) are propagated to the flood discharges (≈40%); and these errors reduce with the drainage area. In general, there are greater biases in extreme discharges for small basins, but these errors considerably reduce for basins larger than 30,000 km² (≈ 25%). Those results indicate that the RCM biases are scale dependent, and the uncertainties of hydrological impact studies should be adequately addressed considering the size of the respective basin.

1. INTRODUCTION

Observed trends point towards higher frequency of extreme events, indicating wetter conditions on the southeastern South America and western Amazon and increase of warming nights consistently through the continent (Ávila et al., 2016; Marengo et al., 2010; Skansi et al., 2013; Valverde and Marengo, 2014). An increased frequency of extreme rainy events is often unwelcome since those are associated with natural disasters such as flooding and landslides (Debortoli et al., 2017). Other alterations in climatic features, either in space or intensity, are expected due to the continuous growth of greenhouse gases concentration in the atmosphere (Stocker et al., 2013). Identifying extreme precipitation trends and understanding climate projections is essential to guide management decisions, such as urban, coastal, and fluvial infra-structure projects, water resources planning (Iglesias and Garrote, 2015; Mortazavi-Naeini et al., 2015; Neumann et al., 2015).

Global climate models (GCM) are the most common tools used to simulate future climate given different scenarios of greenhouse gases (GHG) emissions and mitigation policies (Hirabayashi et al., 2013; Milly et al., 2005). GCMs are numerical models that calculate Earth's energy and mass balance, simulate the interaction between ocean, atmosphere, land surface and sea ice, estimate heat and water exchange horizontally and vertically. These models provide precipitation projections that can be used to infer about future water availability and flood risks on continental scales (Brêda et al., 2020; Hirabayashi et al., 2021; Lehner et al., 2006). However, GCMs are limited by current computational power, which often constrain the grid spatial resolution from 0.5 to 2 degrees horizontally (Bador et al., 2020; Flato et al., 2013; Haarsma et al., 2016). Such a coarse resolution precludes the representation of local landscape features such as topography gradient, inland water bodies, urban areas, etc. Thus, downscaling approaches become alternatives to improve regional phenomena representation.

Dynamical downscaling refers to Regional Climate Models (RCM) which calculates mass and energy balance on a finer resolution compared to GCMs. RCMs are applied to a limited domain, e.g. continents (Giorgi et al., 2009), using GMCs outputs as initial and lateral boundary conditions – process called nesting. RCMs generally add value to GCM simulations (Falco et al., 2019; Llopart et al., 2020) as they provide a more accurate representation of orographically induced wind systems (Antico et al., 2020), medium scale temperature fields and mesoscale weather phenomena (Feser et al., 2011; Giorgi, 2019) becoming an important tool for regional hydrological impact assessment (Lee et al., 2019; Teutschbein and Seibert, 2010). However, there is still room for improvement in regional climate modelling. Current RCMs grid resolution (around 10 km horizontal grid spacing) is not sufficient to reproduce cumulus convection explicitly, using parametrization schemes instead (Arakawa, 2004; Prein et al., 2015). These parametrization schemes are among the greatest sources of uncertainties in climate modeling (Sherwood et al., 2014), especially for extreme precipitation (Fosser et al., 2014; Prein et al., 2013). In addition, RCMs inherit

GCMs errors to some extent from lateral boundary forcing. Thus, RCMs become valuable tools for regional impact studies of climate change, but their uncertainties should be adequately acknowledged a priori.

The Eta model (Mesinger et al., 2012) is one of the most used RCM for studies in South America (Chou et al., 2014a, 2000; Pesquero et al., 2010). Its formulation scheme includes the η vertical coordinate (Mesinger, 1984) that enables fairly accurate calculation of horizontal gradients around very steep topography regions such as the Andes Cordillera. Today, there are coordinated Eta simulations for climate research in South America nested in 4 different GCMs with a horizontal resolution of 20 km (Chou et al., 2014a, 2014b), although a more local version (5 km) has been applied for Southeast Brazil (Lyra et al., 2018). The output from this model has been frequently used to project hydrological impacts from climate projections (Lima et al., 2014; Oliveira et al., 2015; Ribeiro Neto et al., 2016; Santos et al., 2019) even in relatively small drainage basins (<5,000 km2) (Alvarenga et al., 2016; Andrade et al., 2020; de Oliveira et al., 2019), but studies testing how well Eta represents precipitation regime focusing on hydrological purposes are rare.

Chou et al. (2014b) evaluated precipitation through long-term monthly and seasonal means discussing average results mostly over 3 large regions in Brazil – North, Northeast and Central-South (area of at least 1,5 million km2). The authors observed negative bias on the North region during summer and overestimation of monthly extreme values compared to CRU TS 3.1 database (New et al., 2002). Later, Almagro et al. (2020) also investigated Eta long-term monthly and seasonal mean precipitation over the six Brazilian main biomes (Amazon, Atlantic Forest, Pantanal, Caatinga, Pampas and Cerrado) and compared against a high resolution grid of observed precipitation (Xavier et al., 2016). On the other hand, Dereczynski et al. (2020) and Avila-Diaz et al. (2020) investigated daily extreme precipitation indices. The former noted that Eta simulated trends do not considerably agree with observation data since there are mixed trend signals and no statistical significance on most gauge stations. The latter observed that Eta consistently underestimate extreme precipitation compared to the precipitation dataset yielded by Xavier et al. (2016). These studies have investigated climatic variables simulated by Eta performing their analysis on cell size or over large regions and extreme events or annual/seasonal averages, however a cross-scale assessment exploring the effects on drainage basins is essential to understand how the climate model biases impact the river streamflow.

Precipitation is by far the most important input variable for water-related impact studies (Biemans et al., 2009; Chiew, 2006), therefore a consistent data analysis should be conducted prior to any hydrological projection. There are considerable uncertainties regarding precipitation on global climate modeling (Flato et al., 2013; Knutti and Sedláček, 2013), as in South America (Gulizia and Camilloni, 2015; Llopart et al., 2020), and these uncertainties are larger than those yielded by hydrological modelling specially for high flow extremes (Meresa and Romanowicz, 2017; Vetter et al., 2017). However, projections from climate models have been used indiscriminately for impact studies in this continent without

adequately addressing their respective uncertainties (Borges de Amorim and Chaffe, 2019). In addition, the spatial and temporal scale of hydrological applications (drainage basin scale) and climate modeling assessments (large climatological regions) do not always match and some studies have reached unreliable results while projecting local extreme precipitation (e.g. Fontolan et al. 2019).

Due to the Clausius-Clapeyron relation climate specialists claim that sub-daily raining events will become more intense (Barbero et al., 2018; Fowler et al., 2021b). The increase in extreme precipitation is already being observed worldwide (Fischer and Knutti, 2016; Papalexiou and Montanari, 2019; Sun et al., 2021) although an inverse trend is observed for temperatures above 24oC (Lenderink and Fowler, 2017; Westra et al., 2014). This theoretical effect is straight-forward and considerably important for small and urban catchments. It has become a consensus on the scientific community that if a model does not have a considerably high-resolution (grid spacing lower than 5 km) or there is no adequate convective physical representation (e.g. superparametrization), short scale extreme precipitation is not well reproduced (Fowler et al., 2021a; Gervais et al., 2014; Knist et al., 2020; Kooperman et al., 2016). However, even GCMs can simulate extreme precipitation of larger areas with errors similar to the uncertainty of global precipitation datasets (Bador et al., 2020). Thus, understanding to what scale a RCM as Eta can represent adequately extreme rainfall for different sizes of watersheds is crucial to support hydrological studies on projections of flood frequency change.

Thus, the objective of this paper is to access Eta simulation of extreme precipitation in South America and to which scale it is reliable for hydrological simulations of flood discharge. We (1) first analyzed how well the regional model Eta, nested in four different GCMs, can represent local scale extreme precipitation of short duration (3 hours to 1 day) through Intensity-Duration-Frequency (IDF) curves. Secondly, (2) the Eta outputs are compared to a relatively high-resolution precipitation dataset and they were submitted to spatial (0.2 to 1 degree) and temporal (1 to 5 days) aggregations to understand how the Eta RCM accuracy varies with different scales. Finally, (3) it is simulated the discharge response to these precipitation time series using a continental hydrological model to investigate how the precipitation biases impact on simulating extreme flooding events across small (1,000 km2) to large (>100,000 km2) river basins.

2. METHODOLOGY

This study focuses on understanding the uncertainties related to extreme precipitation simulated by the Eta RCM and its effect on river flood discharge. It is composed by three main subjects of analysis: (1) the simulated extreme precipitation of short duration compared with IDF curves built from in situ gauges; (2) the simulated extreme precipitation compared with a gridded dataset testing different spatial and temporal scales; and (3) the discharge estimates from a hydrological model forced with Eta precipitation dataset. In this section, we briefly describe the Eta model (section 2.1), the gridded precipitation dataset used as

reference (section 2.2), and the procedure to fit an extreme value distribution to the precipitation data (section 2.3). Then, we provide details on the local IDF curves (section 2.4), we comment about the spatial and temporal scales of the analyses (section 2.5), and finally, we describe the hydrological model used to estimate flood discharge (section 2.6).

2.1. The Eta Regional Climate Model

Eta is an RCM developed by INPE (Brazilian National Institute for Space Research) to simulate mesoscale atmospheric conditions (Chou et al., 2012; Pesquero et al., 2010). This model is named after the vertical coordinate η which is a quasi-horizontal surface and prevents pressure-gradient force errors in areas of steep topography (Mesinger et al., 2012). The Eta RCM has its origins on numerical weather predictions and has been used for climate projections since Chou *et al.* (2012) and Marengo *et al.* (2012).

Here, we used results from Eta nested simulations within four GCMs from CMIP5 (Coupled Model Intercomparison Project phase 5): BESM (Brazilian Earth System Model - Nobre *et al.*, 2013), HadGEM2-ES (Hadley Centre Global Environmental Model - Collins *et al.*, 2011), CanESM2 (Canadian Earth System Model - Chylek *et al.*, 2011) and MIROC5 (Model for Interdisciplinary Research On Climate - Watanabe *et al.*, 2010).

The current Eta version for climate research in South America was set up with 38 vertical levels, horizontal spatial resolution of 20 km and output at 3-hourly temporal intervals. The simulations were taken in two different periods following the CMIP5 protocol: the historical reference period (1961-2005) and the future period (2006-2100). We only assessed the historical reference period comparing it with observed data. Climate data from these simulations are available online at https://projeta.cptec.inpe.br/ and have being used frequently for hydrological assessments in South America, especially in Brazil (de Oliveira et al., 2017; Oliveira et al., 2015; Ribeiro Neto et al., 2016; Santos et al., 2019). Thus, it is essential to understand how well Eta represents precipitation in different temporal and spatial scales to adequately project the climate change impacts on drainage basins.

2.2. Gridded Precipitation Reference

The precipitation dataset used as reference is the Multi-Source Weight-Ensemble Precipitation – MSWEP version 2.2 (Beck et al., 2019). This gridded dataset is based on multiple precipitation products from different sources: gauge stations, satellite, and reanalysis. The daily gauge observations are used to determine the merging weights of the satellite and reanalysis products and for temporal mismatch correction while the monthly gauge-based precipitation products are applied for long-term climatological corrections. In addition, MSWEP uses some river discharge measurements to correct precipitation systematic underestimation due to gauge-undercatch and orographic effects.

MSWEP version 2.2 is a 3-hourly time resolution and 0.1º spatial resolution dataset. This product is available online at http://www.gloh2o.org/ and provides precipitation data for continents and ocean from 1979 to 2017. In this study we used the 1-day time resolution

product upscaled to 0.2 degrees to match the Eta grid resolution for South America. MSWEP was selected as a reference as it is built from multiple products of precipitation and presented a satisfactory performance compared to other global precipitation datasets (Sun et al., 2018).

2.3. Statistic Distribution for Extreme Event

Eta and MSWEP precipitation data were adjusted to a statistical distribution in order to compare extreme events with equivalent probability of occurrence. However, the climate model, the gridded dataset and the local IDF curves were built with precipitation data from different periods. Thus, we assumed stationarity to enable a direct comparison between MSWEP (1979-2017), Eta (1961-2005), and local IDF curves (section 2.4). Although the stationarity assumption is properly questionable (Milly et al., 2008) and it is a good practice to compare data of common periods (1979-2005), using the complete MSWEP and Eta datasets raises the length of the data series in about 30%, considerably increasing the data sample for curve fitting. The main aspects of fitting Eta and MSWEP data into an extreme value distribution is described below.

We selected maximum precipitation values for each hydrological year and each grid cell of Eta and MSWEP datasets. This process was performed for different intervals of precipitation - from 3 hours to 5 days. Then we fitted Gumbel distributions (Generalized Extreme Value – GEV distribution Type-1) to the data through the Method of Moments (Naghettini, 2017):

$$P[Y \leq y] = \exp\big(-exp\big(-\alpha(y-\mu)\big)\big)$$

$$\alpha = 1.2862\ s \qquad \mu = \bar{x} - 0.451\ s$$

where $\bar{x}$ is the average of the maximum precipitations of a respective cell, s is the standard deviation of this sample, y is a specific precipitation event and P is the probability of y not being exceeded in a random year. The Return Period (RP) is given by the inverse of this probability ($1/P$).

2.4. IDF Curves

Intensity-Duration-Frequency curves are empirical curves fitted to an observed series of a rain gauge station that estimate the intensity of a precipitation event based on its duration, which usually has minutes or hours magnitude, and its frequency, given by a return period (Naghettini, 2017). These curves are frequently used in the design of urban drainage and small catchment fluvial structures.

We gathered IDF curves based on automatic ground based rain gauges from 74 cities across South America, more specifically in Argentina (Catalini, 2018), Colombia (IDEAM, 2017), Chile (Ministerio de Vivienda y Urbanismo, 1996), Paraguay (Cuevas and Rolón, 2010), Bolivia (Martinez et al., 2009), Ecuador (INAMHI, 2019) and Brazil (Bertoni and Tucci,

1993; Castro et al., 2011; Distrito Federal, 2009; Fendrich, 1998; Fragoso Jr, 2004; Oliveira et al., 2005; Silva et al., 2013; Silveira et al., 2000; Zahed and Marcellini, 1995).

Then, we compared the gauge based IDF curves to extreme precipitation values obtained from Gumbel distributions fitted to Eta and MSWEP data.

To accomplish direct comparisons between Eta/MSWEP adjusted curves and observed IDF curves, two specific adaptations were necessary. Firstly, Eta recorded total precipitation within 3-hours intervals while the IDF curves are continuous curves which yields rainfall intensity for any duration given its return period. Fixed time measurements may not capture the full intensity of a rainfall event since it may be split between two consecutive recording intervals. Secondly, IDFs normally represent point rainfalls related to a specific gauge station while the Eta model is discretized into 0.2º x 0.2º cells, which characterizes an average rainfall within a relatively large area compared to a rain gauge. As rainfall is barely uniform in space, the intensity of an extreme precipitation on a specific location is generally higher than the average intensity of a larger area for the same return period (Sivapalan and Blöschl, 1998; Skaugen, 1997). Thus, two correction factors were applied to make a proper comparison between Eta simulations and observed IDF curves:

i. True-to-Fixed Interval Ratio Factor (TFIR)

Rainfall measurements are often taken in a fixed time interval, for example, from 8:00 am to 8:00 am of the following day. Thus, if a 24-hour extreme event starts around midday, it would intersect two fixed intervals and, consequently, its intensity would be underestimated. On the other hand, fixed intervals of one hour could almost completely capture this event.

Thus, an estimated extreme rainfall is often multiplied by a coefficient that is based on the relation between the duration of the event and the interval of measurement, namely TFIR. One of the most used methods to estimate TFIR was presented on Weiss (1964):

$$TFIR = \frac{n}{n - 0.125}$$

where n is the number of intervals that contain the event. For example, if a rain gauge provides rainfall data every 3 hours and the rainy event is 12 hours long, n would be 4. As Eta has a 3-hour resolution, if we want to analyze an event of 3 hours long, n would be 1 and the TFIR would be 1.143. There so, TFIR approximates to one the longer the duration of the event compared to the measurement interval. Weiss method is one of the few analytical methods for estimating TFIR (Yoo et al., 2015).

ii. Areal Reduction Factor (ARF)

IDF curves are generally based on data from automatic gages, with catching surface of less than 1 m², while they are used to estimate design storms at the catchment scale. However extreme events are not spatially uniform, and the precipitation intensity tends to

reduce with area. Thus, in order to adequately estimate design storms and optimize hydraulic projects, IDFs are multiplied by a reduction coefficient named ARF. ARF is a multiplication factor, between 1 and 0, that relates a point rainfall to a mean areal rainfall.

However, the estimation of ARF is not as straight-forward as TFIR. ARF strongly depends on the nature of the precipitation event (Allen and DeGaetano, 2005; Breinl et al., 2020; Skaugen, 1997). In South America, there are diverse climate regions and rainy patterns and few studies have explored ARF estimation, e.g. cities of Porto Alegre (Silveira, 2001), Belo Horizonte (Santos and Naghettini, 2003) and Mendoza (Fernández et al., 1999). Investigating, developing, or adopting a single ARF estimation approach for South America seems currently unfeasible specially with the limited precipitation data available. In addition, the ARF can assume a large range of values which depend on the method used to estimate it (Silveira, 2001; Svensson and Jones, 2010; Wright et al., 2014). In the literature there are ARF lower than 0.5 for a 3-hour duration event covering a 400 km² area, mainly through methods based on radar estimates which give precise storm centers of rainfall events (Kim et al., 2019; Wright et al., 2014). However, most commonly used analytical methods (Lebel and Laborde, 1988; Sivapalan and Blöschl, 1998; Weather Bureau, 1958) are more conservative, reaching ARFs around 0.8 for a similar precipitation event – 3-hours duration and a 400 km² area (Silveira, 2001; Wright et al., 2014).

Due to the high uncertainties regarding ARF estimates, we assumed a range of possible IDF curves related to the same area of an Eta cell (≈ 400 km²). It is proposed intensity boundaries that are given by the observed IDF curve multiplied by the following ARFs: 0.5 (0.85) for a 3-hours event and 0.7 (0.95) for a 24-hours event for the inferior (superior) limit (Figure 10). The ARF curve from 3 hours to 1 day is based on Lebel and Laborde (1988) apud Silveira (2001):

$$ARF = 1 - \frac{\sqrt{A}}{a\, t^n} \qquad => \qquad \ln(A)/2 - \ln(1 - ARF) = \ln(a) + n \ln(t)$$

where A is the catchment/cell area, t is the event duration and a and n are parameters. As it was assumed values of ARF for 3 hours and 1 day, it is possible to directly calculate these parameters solving a system of 2 linear equations and 2 variables. So, a is equal to 11.17 (8.58) and n is equal to 0.2457 (0.5283) for the inferior (superior) limit, A in km² and t in minutes.

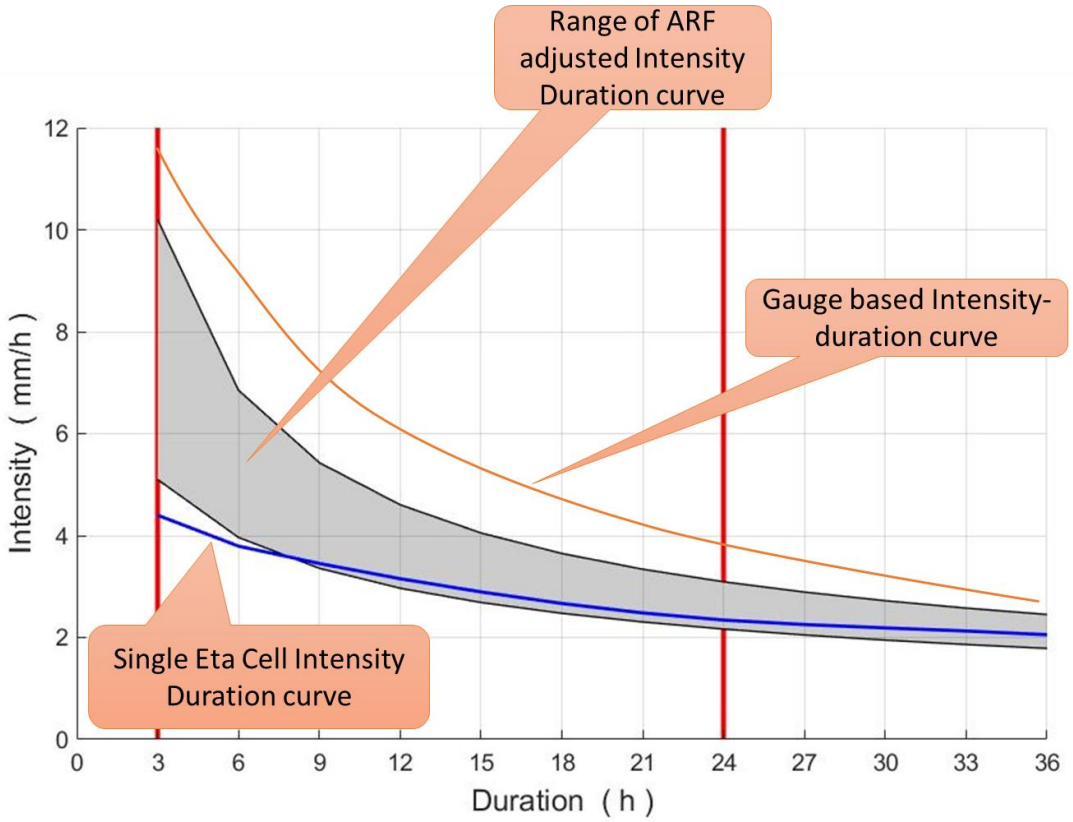

Figure 10. Schematic of the limits of point IDF (orange) expanded to an area size after the ARF multiplication (gray) and a IDF of a specific Eta cell (blue) for a generic return-period.

2.5. Spatial and Temporal Scale Experiments

In addition to the analysis of short-duration local events (< 1 day), we evaluated how extreme precipitation simulated by the Eta model compare with MSWEP at different spatial and temporal scales in South America. The original cell size of 0.2o x 0.2o were aggregated from west to east up to 1.0o x 1.0o. We further evaluated precipitation extreme events of 1- and 5-day duration and annual mean precipitation. Aggregated cells from Eta and MSWEP were directly compared using the nearest neighbor method through the absolute and relative difference between cells and the correlation of the precipitation grid.

2.6. Hydrological Simulation

We generated river discharge time series trough the MGB hydrological model (Paulo Rógenes Monteiro Pontes et al., 2017) using both Eta and MSWEP rainfall data as input.

The MGB, Portuguese acronym for Large Basins Model, have been consistently applied for hydrological assessments in South America for climate change projections (Adam et al., 2015; Bravo et al., 2014; Jati et al., 2020; Ribeiro Neto et al., 2016; Sorribas et al., 2016b; Vergasta et al., 2021). In this study, it is used a continental scale version of this model which was developed for South America by Siqueira et al. (2018), named MGB-SA. As the MGB-SA performed well on multiple hydrological components (e.g. streamflow,

evapotranspiration, water storage anomalies, etc.), the model reliability in simulating the environmental system increased, being used for several purposes such as streamflow forecast (Siqueira et al., 2020), climate change projections (Brêda et al., 2020) and sediments production and transport (Fagundes et al., 2020).

Precipitation data from MSWEP and Eta was used to force the MGB-SA model which yielded daily discharge series for catchments larger than 1,000 km2. South American catchments located south of 50º S were ignored since this region fall out of the Eta domain.

We obtained the daily values of river discharge at over 30,000 river reaches in South America, from year 1961 to 2005 for MGB simulations forced by Eta precipitation, and from year 1979 to 2015 for MGB simulations forced by MSWEP precipitation. From this daily time series, we obtained the annual maximum values, and based on those we estimated the 50%, 10% and 1% exceedance probability in a given year (i.e. return periods of 2, 10 and 100 years respectively) by applying the Gumbel distribution. Then Eta and MSWEP relative differences of discharge and precipitation were compared in terms of catchment drainage area, enabling spatial and temporal scale analysis.

3. RESULTS

3.1. Extreme Precipitation of Short Duration

Eta simulations from the historical period (1961-2005) are assessed and compared to local IDF curves from 74 cities across South America. An extreme value distribution was fitted to the Eta precipitation data of different durations (< 1 day) in order to identify events of a defined probability of occurrence. It is evaluated the Eta simulations nested in 4 GCMs, so-called here as Eta-BESM, Eta-CanESM2, Eta-HadGEM2-ES, and Eta-MIROC5 runs and the MSWEP database.

Figure 11 shows a comparison between maximum precipitations of 2-year and 100-year return period and 3-hours duration from Eta model (Figure 11a) and from rain gauges based IDF curves (Figure 11b). The color legend range of the IDF curves is different from the one used for Eta because the formers are associated to specific gauge stations while the latter are composed by 400 km² gridded cells, thus it was chosen an appropriate map legend to facilitate visualization. Eta model results show three regions of high precipitation in South America, for both 2- and 100-year return periods. The first is the equatorial western Amazon region, where 2 year (100 year) maximum precipitation values reach 12 mm (22 mm). The second is Paraguay, Uruguay, Northern Argentina, and Southern Brazil, east of the Andes, between 20 and 40 S. The third is along the western slope of the Southern Andes, in Chile, from 25 S to about 50 S. All the three high precipitation regions in South America are common features of the Eta model, regardless of the driven GCM.

The IDF curves obtained from ground-based rain gauges (Figure 11b) on the other hand, reveal a less clear pattern of spatial variability. A clear pattern, however, can be seen

along the western slope of the Southern Andes, in Chile, from 25 S to about 50 S, where gauge based IDF curves show 2-year maximum precipitation values that are clearly lower than in most of the other locations in South America. Gauge based IDF curves also do not show the contrast between eastern and western equatorial zone, that is seen in Eta results. Gauge based IDF curves do also not show the high precipitation region over Paraguay, Uruguay, Northern Argentina, and Southern Brazil. Also, it was observed from the IDF curves relatively high precipitation intensities on the northeast Atlantic coast, while the Eta simulations indicated lower indices.

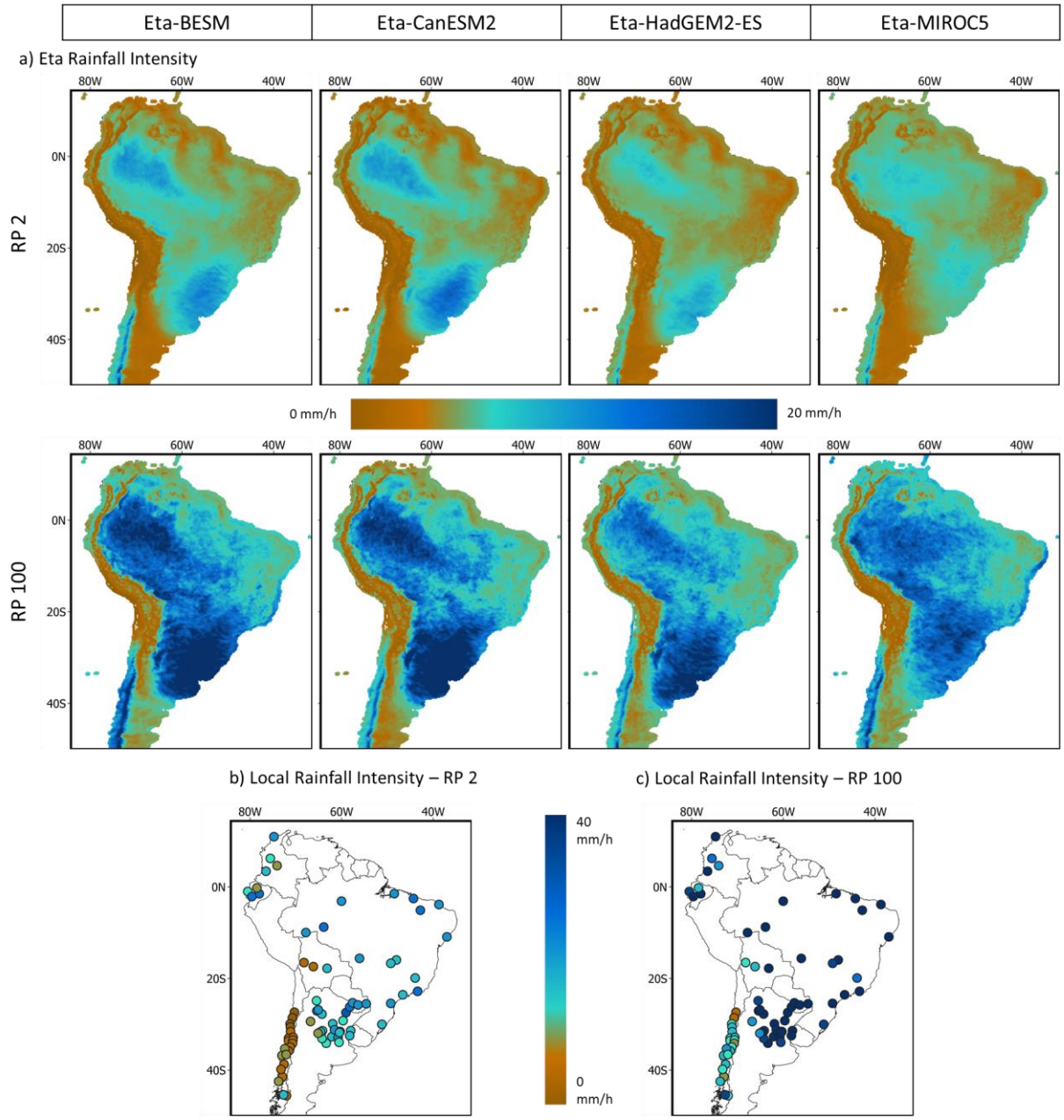

Figure 11. Rainfall intensity related to a 3-hour event. a) Eta cell average and return period of 2 (top) and 100 (bottom) years; b) local point IDFs and return period of 2 years; c) local point IDFs and return period of 100 years.

The spatial pattern of extreme daily precipitation intensities from Eta, displayed in Figure 12 , resembles to what is demonstrated in Figure 11 (3-hours duration). Except that the precipitation of 100-year return period on the western Amazon is average and the precipitation intensity along the Pacific coast of Chile, from 30S to 50S, became more pronounced. However, neither MSWEP nor the IDF curves presented such a high precipitation intensity on the Chilean coast compared to the rest of the continent. The Eta model overestimate the average summer (DJF) and winter (JJA) rainfall on this region (Chou et al., 2014b), which might have effects on the extreme precipitation indices. The MSWEP dataset has the same cell resolution as Eta and yielded considerably higher rainfall intensities, even in the northeastern Brazil (around 10S / 40W) and northern Andes Cordillera (above the Equator line).

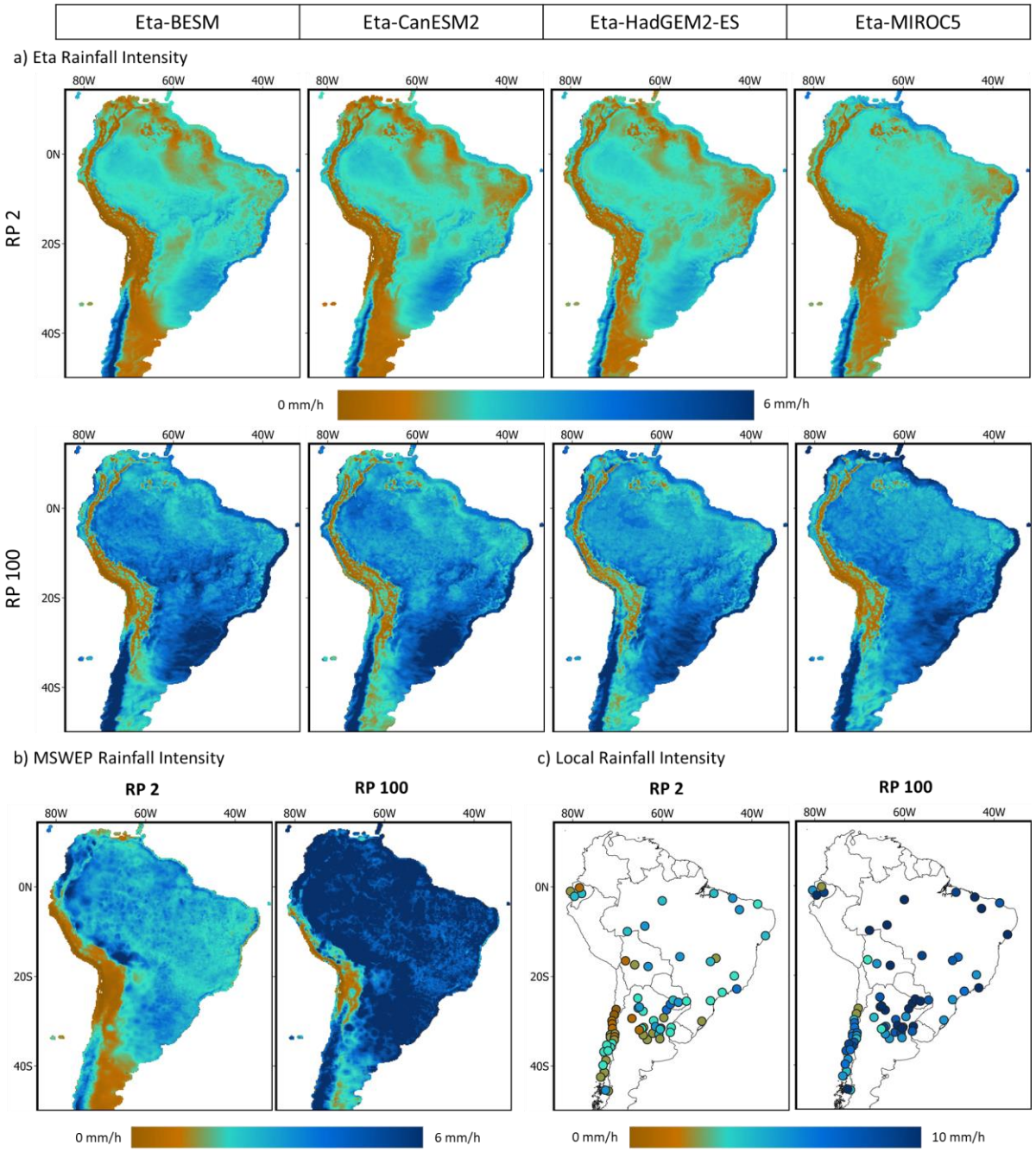

Figure 12. Rainfall intensity related to a 1-day event. a) Eta cell average and return period of 2 (top) and 100 (bottom) years; b) MSWEP cell average and return period of 2 (left) and 100 (right) years; c) local point IDFs and return period of 2 (left) and 100 (right) years.

The extreme precipitation of the Eta/ MSWEP cells were compared to the limits of the local IDF curves defined by the ARF coefficients (section 2.4, Figure 10). Overall, the Eta model underestimate short-scale extreme precipitation throughout the continent, except on the western Patagonia (Figure 13 and Figure 14). Extreme precipitations are normally related to subscale process, which is not adequately represented by current RCMs. Convective rainfall in models are produced through convective parametrization schemes which commonly underestimate sub-daily precipitation intensities (Fosser et al., 2014; Prein et al., 2013). The Eta model precipitation underestimate was already pointed out by Chou *et al.*

(2014b) and Dereczynski *et al.* (2020) as a possible source of error within the Eta model. In a larger temporal scale, RCMs tends to underestimate the average precipitation on South America and to overestimate rainfall induced by topography on the Andes Cordillera (Solman et al., 2013). Still, there is a reasonable agreement on the southeastern South America, especially for the Eta-CanESM2 model, while Eta-MIROC5 highly underestimate precipitation intensities in this region. On the other hand, the MSWEP database presented lower divergence but slightly overestimate precipitation intensity throughout SA compared to the punctual IDFs curves.

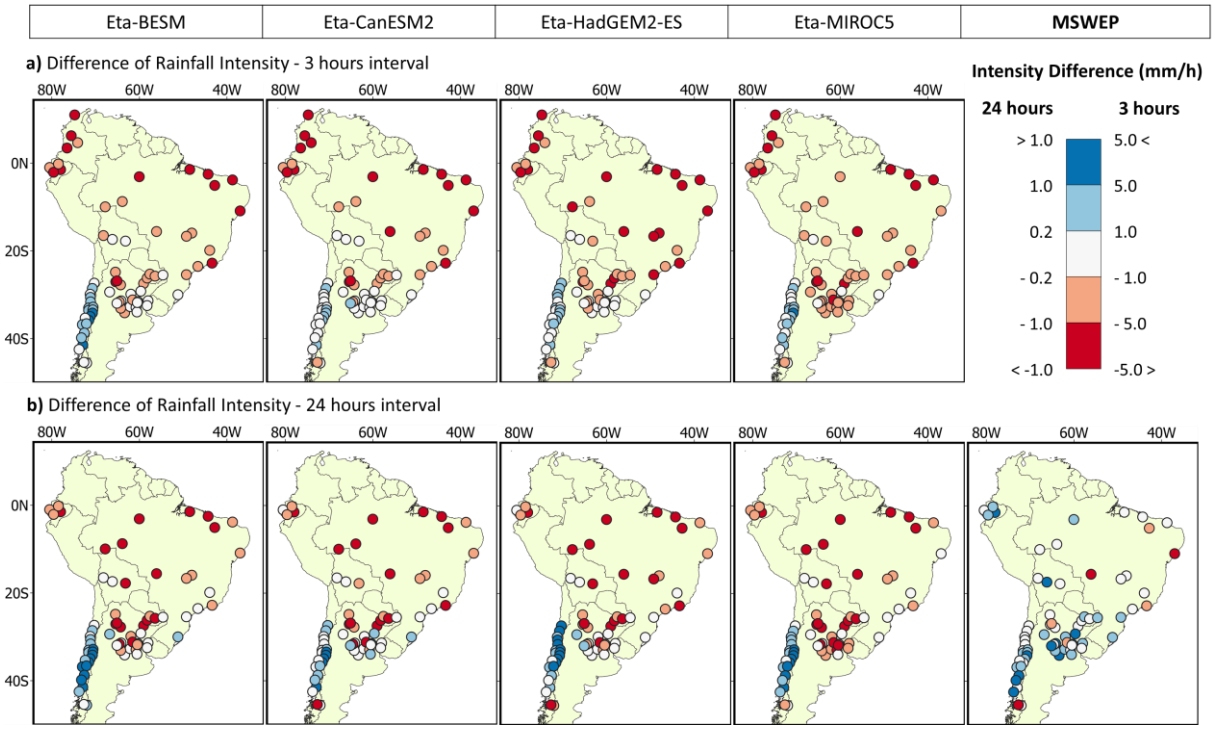

Figure 13. Difference in precipitation intensity of a 2-years return period event between local point IDFs and Eta cells nested in different GCMs: a) 3-hour interval; b) 24-hour interval.

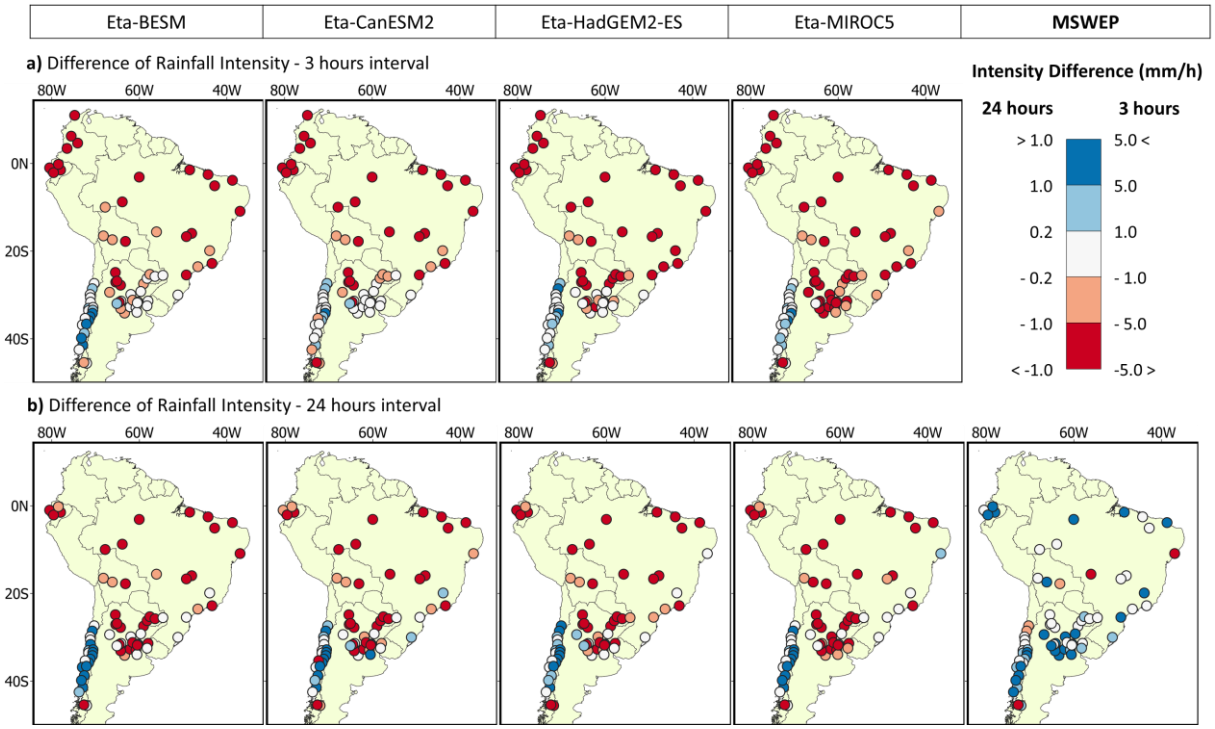

Figure 14. Difference in precipitation intensity of a 100-year return period event between local point IDFs and MSWEP/Eta cells nested in different GCMs: a) 3-hours interval; b) 24-hours interval.

3.2. Temporal and Spatial Scale Analysis

In this section, different temporal and spatial scales are tested to find out how errors in extreme precipitation change with scale. The Eta and MSWEP gridded cells are aggregated from 0.2-degree (R_0.2) up to 1.0-degree (R_1.0) and it is compared 1-day (1D) and 5-day (5D) precipitation intervals. It is also tested extreme precipitation rates for different return periods: 2 (RP2), 10 (RP10) and 100 (RP100) years. As IDF curves are not appropriated for large areas and precipitation durations, only MSWEP dataset was utilized for this assessment.

Figure 15 display the differences between Eta and MSWEP extreme precipitation in South America for different spatial and temporal scales. In general, the Eta model underestimates extreme precipitation of 1- and 5-days duration, as more than 75% of the differences are negative. It is understandable the existence of great differences between distinct datasets as a single expressive extreme event can considerably alter the Gumbel distribution fitted to the precipitation data. However, the Eta-MSWEP differences present identifiable spatial patterns and are inherent to all Eta simulations, which might indicate modelling systematic bias. All the Eta simulations (Eta-BESM, Eta-CanESM2, Eta-HadGEM2-ES and Eta-MIROC5) presented similar negative biases for extreme precipitation. However, there is no dominant bias for average annual precipitation (Figure 15c). These results agrees with Avila-Diaz *et al.* (2020) who observed negative bias of extreme precipitation of 1 and 5 days duration simulated by Eta in Brazil.

As expected, the differences in precipitation intensity increase with return period and decrease with increasing cell sizes and precipitation intervals (Figure 15). Moving from a cell area of 400 km² (0.2º resolution) to 10,000 km² (1.0º resolution), the relative Eta-MSWEP difference in extreme precipitation reduces in 3.7 percentage points on average. Changing the precipitation duration from 1 to 5 days, the relative difference reduces in 8.4 percentage points on average. For instance, the median relative difference of the RP100 / 1D / R_0.2 events is 45.4% while the median relative difference of the RP100 / 5D / R_1.0 events is 30.5%: a reduction of nearly 15% percentage points through temporal and spatial aggregation. For the former (latter) 3/4 of the cells present differences lower than 60% (46%). The biases are smaller for precipitation events of 2-year return period, as the precipitation volume difference are below 50% for at least 75% of the cells (third quartile). These results indicate that both spatial and temporal aggregation reduce the biases, but the temporal aggregation is more relevant.

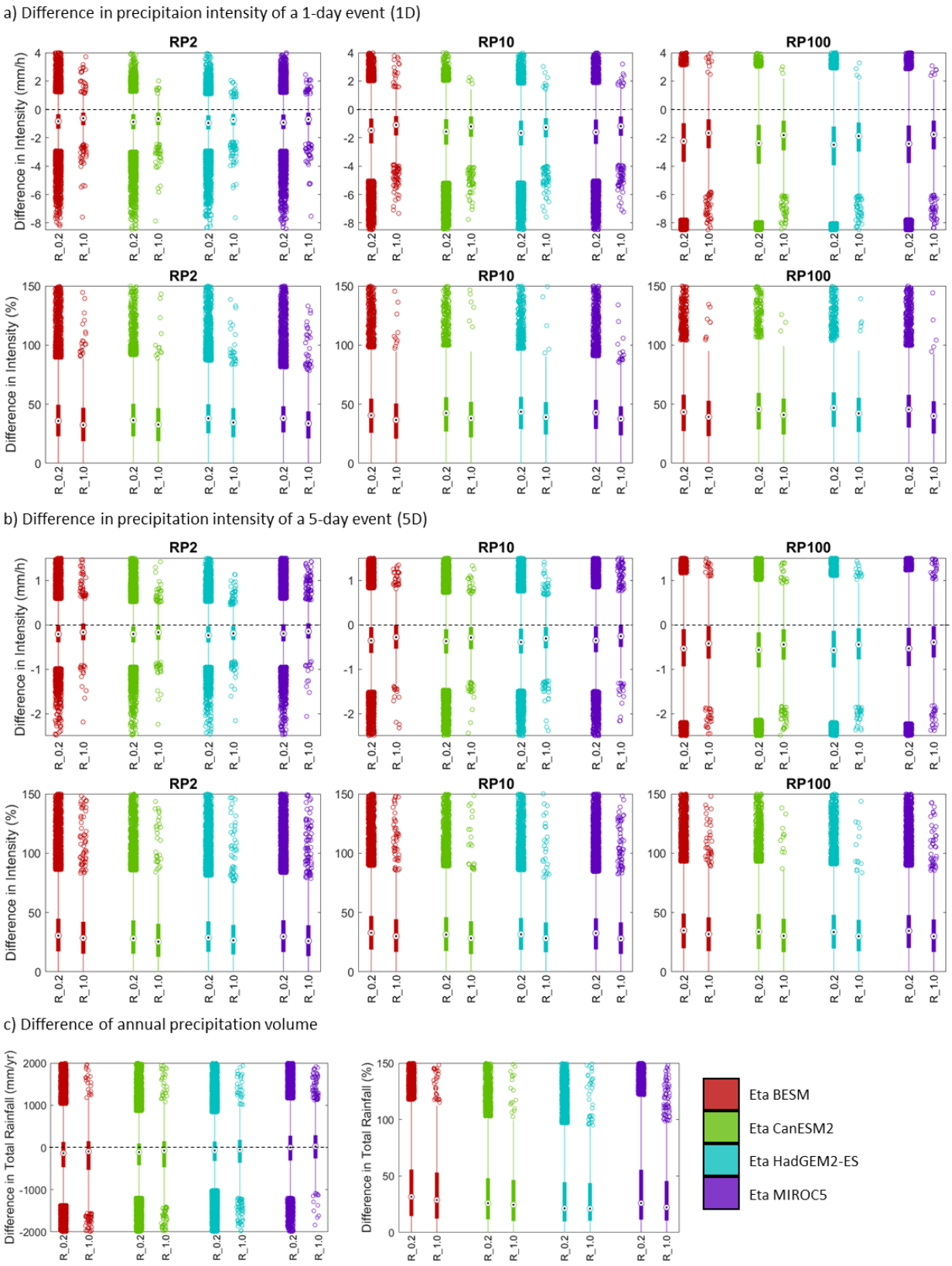

Figure 15. Boxplots of the differences between Eta and MSWEP cells in absolute and relative terms for different return periods. a) precipitation interval of 1 day; b) precipitation interval of 5 days; c) average annual precipitation

Figure 16 demonstrates how extreme precipitation intensity decreases with increasing cell size. An area Reduction Factor was obtained dividing the average extreme precipitation

of a specific cell size grid (>0.2º) by the average extreme precipitation of a 0.2º resolution grid. As expected, this Reduction Factor decreases with increasing area and return period, possibly because convective rainfalls (short-scale phenomena) have higher influence on extreme events (Breinl et al., 2020). For extreme precipitation of 1-day duration, the MSWEP Reduction Factor curve has larger slope, which means that the extreme precipitation events of the Eta model are probably more spatially dependent. This reinforces the fact that the Eta model underestimation of extreme events is smaller at coarser resolution grids. On the other hand, Eta and MSWEP Reduction Factor curves are quite similar for 5-day duration events, which means that the Eta model might have a more accurate spatial representation of extreme precipitation processes in such temporal scale.

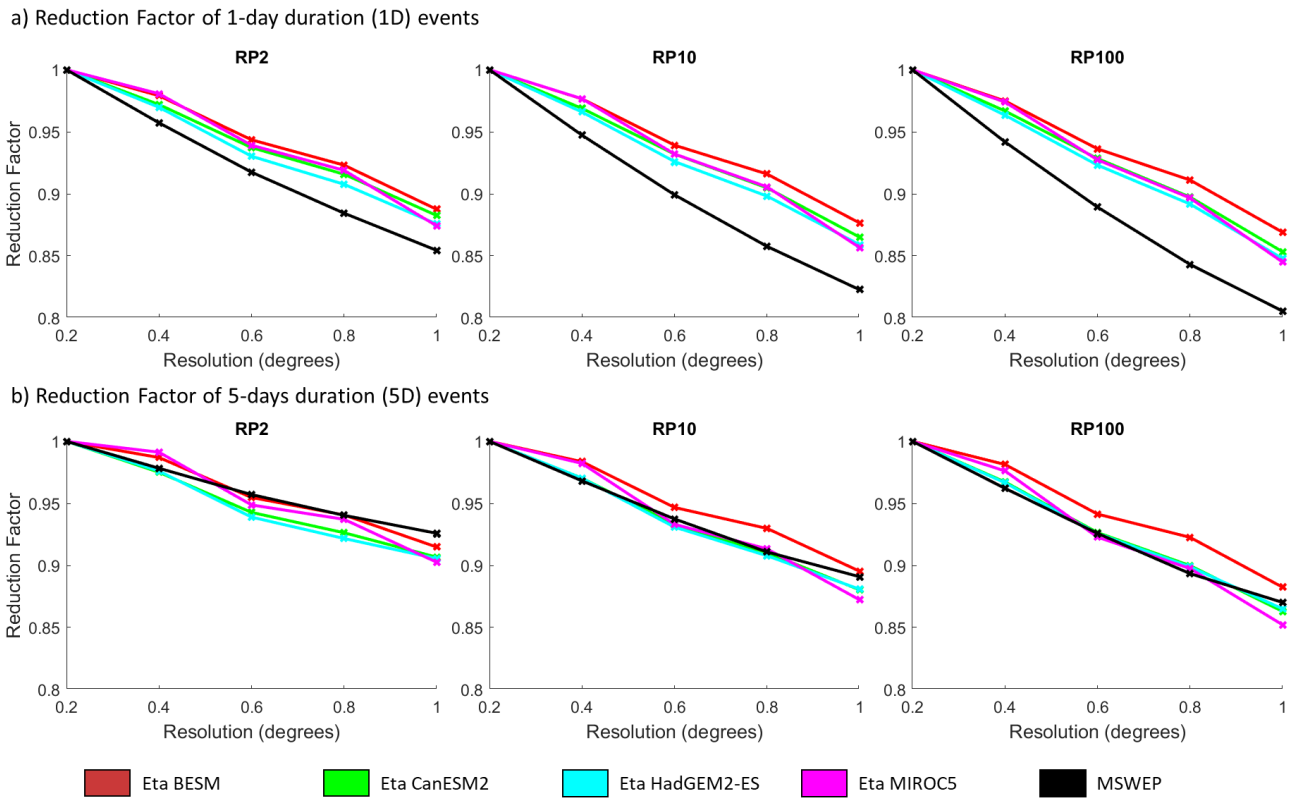

Figure 16. Average precipitation intensity reduction with the increase of cell size for events of different return periods (RP) in South America. a) 1-day duration events; b) 5-days duration events

In addition, it is assessed to what extent the MSWEP and Eta precipitation data are spatially correlated and how it changes with scale. In other words, it is evaluated in general how spatially accurate the Eta simulated rainfall is (right volume on the right spot). The Pearson correlation coefficients (ρ) between the Eta simulations and the MSWEP dataset are presented on Table 2. It can be seen a positive correlation between the datasets which is especially high for events of 2 return period (ρ around 0.5). Once again, it is shown that spatial and temporal aggregation approximates Eta simulations to the MSWEP dataset. The correlation of very extreme events (RP100) in a 5-day interval (average ρ of 0.41) is higher than events of 1-day duration (average ρ of 0.27). In general, the correlation increases by $\Delta\rho$=0.03 when aggregating the cell size from 0.2º to 1.0º resolution and it increases by

$\Delta\rho$=0.10 when considering a longer precipitation interval, from 1 to 5 days. For comparison purposes, the correlation coefficients between the Eta simulations themselves (Eta-BESM, Eta-CanESM2, Eta-HadGEM2-ES and Eta-MIROC5) are generally over 0.8 and it is close to one for events with higher probability of occurrence (RP2). In average precipitation, Eta can represent very well the spatial rainfall patterns in South America. The correlation of annual average precipitation between Eta and MSWEP approximates to the correlation between Eta simulations nested in different GCMs (ρ around 0.85), especially the Eta-HadGEM2. In summary, this correlation analyses indicate that capability of the Eta RCM model to represent spatial patterns of intense precipitation increases with the temporal scale but also with the spatial scale to smaller extent.

Table 2. Correlation coefficients between Eta and MSWEP for different return periods, rainfall duration and cell size.

Eta-BESM	1 DAY			5 DAYS			ANNUAL
	RP100	RP10	RP2	RP100	RP10	RP2	
R_0.2	**0.268**	**0.348**	**0.459**	**0.406**	**0.450**	**0.499**	**0.549**
R_0.4	**0.272**	**0.349**	**0.456**	**0.403**	**0.445**	**0.494**	**0.536**
R_1.0	**0.288**	**0.364**	**0.473**	**0.423**	**0.465**	**0.515**	**0.539**
Eta-CanESM2	1 DAY			5 DAYS			ANNUAL
	RP100	RP10	RP2	RP100	RP10	RP2	
R_0.2	**0.267**	**0.369**	**0.512**	**0.431**	**0.489**	**0.557**	**0.645**
R_0.4	**0.281**	**0.379**	**0.516**	**0.448**	**0.504**	**0.567**	**0.637**
R_1.0	**0.301**	**0.396**	**0.533**	**0.474**	**0.527**	**0.589**	**0.661**
Eta-HadGEM2-ES	1 DAY			5 DAYS			ANNUAL
	RP100	RP10	RP2	RP100	RP10	RP2	
R_0.2	**0.223**	**0.328**	**0.478**	**0.372**	**0.437**	**0.521**	**0.728**
R_0.4	**0.248**	**0.346**	**0.486**	**0.398**	**0.456**	**0.530**	**0.719**
R_1.0	**0.274**	**0.368**	**0.505**	**0.425**	**0.480**	**0.551**	**0.738**
Eta-MIROC5	1 DAY			5 DAYS			ANNUAL
	RP100	RP10	RP2	RP100	RP10	RP2	
R_0.2	**0.276**	**0.358**	**0.466**	**0.382**	**0.431**	**0.490**	**0.657**
R_0.4	**0.287**	**0.366**	**0.472**	**0.390**	**0.439**	**0.500**	**0.683**
R_1.0	**0.313**	**0.394**	**0.504**	**0.424**	**0.475**	**0.543**	**0.745**

3.3. Precipitation bias effects on Streamflow

Finally, it is evaluated how the precipitation uncertainties from Eta simulations affects simulations of flood discharges. The precipitation yielded by Eta and MSWEP are used as inputs to the MGB-SA which provide daily discharge time series for all South American basins over 1,000 km2 area and latitude lower than 50S. The hydrological model can connect the different grid cells within a drainage network and may accumulate or dissipate the precipitation uncertainties through the increasing basin areas. Discharges yielded by the MGB-SA forced with MSWEP precipitation data is used as reference.

.

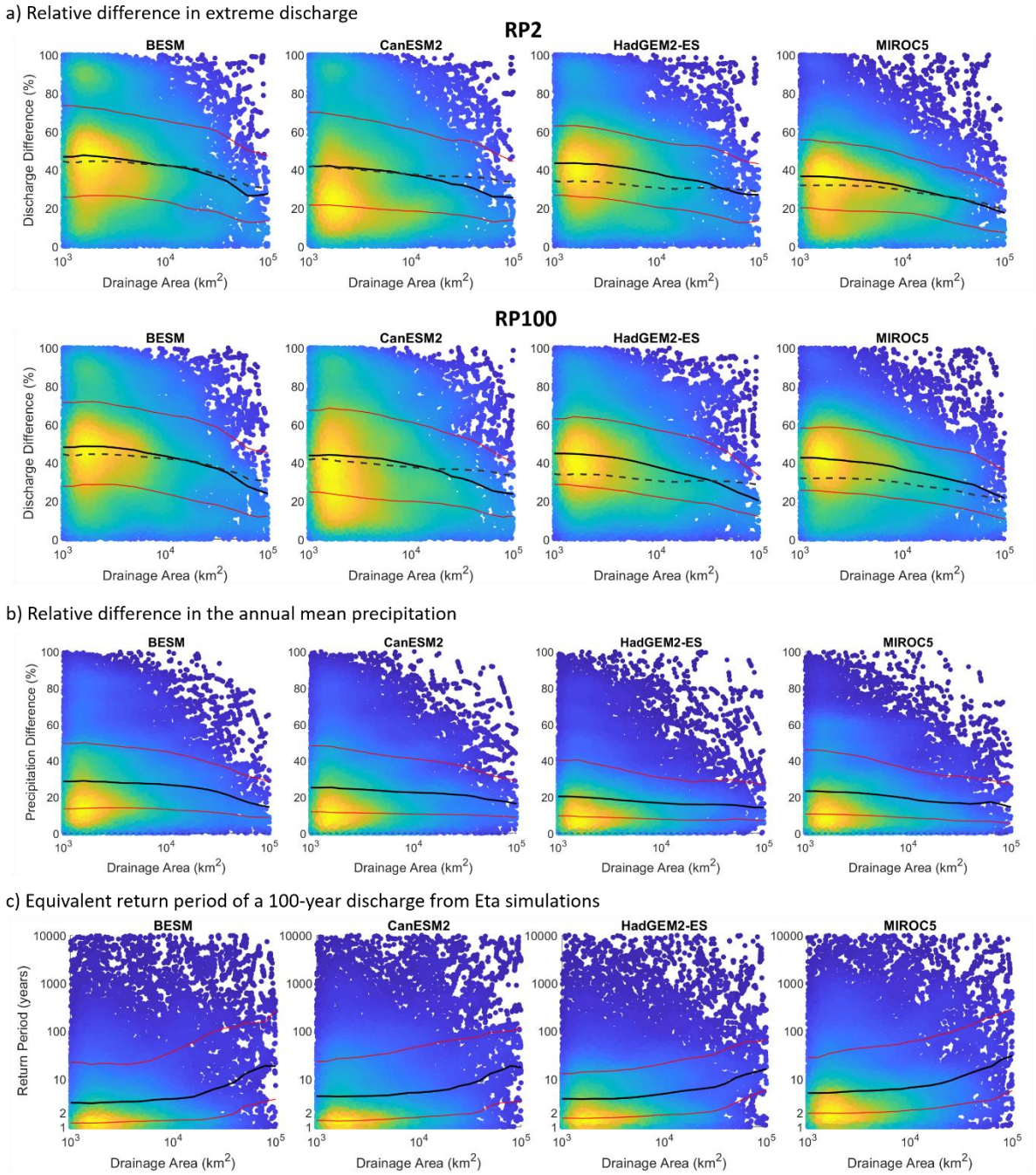

Figure 17. Relative differences of (a) extreme discharge and (b) mean precipitation between Eta and reference (MSWEP) simulations in a basin by its accumulated drainage area. (c) Equivalent return period of a 100-year discharge from Eta simulations related to the extreme discharges of the reference simulation. Blue dots represent individual basins; the yellowish intensity is related to the density of blue dots in the graph; the black and red lines show the median and quartiles (1st and 3rd) considering basins from a drainage area interval; and the dashed grey line on (a) represents the basins median of the long-term mean discharge.

In general, the MGB-Eta simulations underestimate extreme and mean discharge. As river streamflow is mainly governed by the accumulated rainfall upstream, the bias signal of discharge and precipitation are basically the same. Figure 17 display how the relative errors in absolute terms reduce with increasing drainage area. The relative differences in the long-

term mean discharge (dashed lines in Figure 17a), which is around 40%, is basically the double of the relative differences in mean precipitation (Figure 17b). These results indicate a precipitation elasticity of streamflow, $\delta Q/\delta P$ (Brêda et al., 2020; Chiew, 2006), around 1.7 for South America in average. Also, mean precipitation and mean discharge errors present moderate decrease with drainage area.

For extreme discharges, the Eta simulations (Eta-BESM, Eta-CanESM2, Eta-HadGEM2-ES and Eta-MIROC5) presented similar average biases which reduces with increasing drainage area. The average relative "bias" of extreme discharges for 1,000 km² basins is approximately 46% (Figure 17a). This bias decreases to 40% for 10,000 km² basins and to 25% for 100,000 km² basins. A greater negative slope in the drainage area vs discharge bias curve is observed between 10^4 and 10^5 km². The Eta biases reduction from small to large basins are explained by two main aspects: 1. the streamflow at the basin outlet is proportional to the accumulated rainfall upstream (spatial aggregation); 2. the time of response of larger basins (>100,000 km²) is in the order of week to months magnitudes and extreme discharge are related to precipitation of longer intervals (temporal aggregation). Thus, as the Eta extreme precipitation biases reduces with spatial and temporal aggregation (section 3.2), so do the discharge biases.

Errors of extreme discharge are more sensitive to the basin drainage area if compared to errors of mean discharge. The errors of extreme discharge (RP2 and RP100 – median of 46%) are higher than the errors of mean discharge (40%) for basins of 1,000 km² (Figure 17a). However, the relative errors of extreme discharge significantly reduce with increasing drainage area (accentuated negative slope). For basins size around 10,000 to 30,000 km², the relative errors of extreme and mean discharge are basically the same, as the dashed line intercepts the black line in Figure 17a; and for larger basins the errors of extreme discharge are even smaller. Thus, it might be an interesting indicator that extreme events are better represented for basins larger than 30,000 km².

Some might argue that the natural variability of extreme discharges is higher for smaller basins than for larger basins, which might explain this error reduction with the increasing drainage area. For example, a 20% error of discharge in a 1,000 km² basin (in the order of 100 m³/s) might be the difference between a 2-year and a 5-year return period event; however, for large basins, going from 10,000 m3/s to 12,000 m3/s may represent a more significant difference in frequency and impact. Thus, the analysis of relative errors presented in Figure 17(a) is not enough to evaluate if the errors related to the RCM biases are in fact reducing with drainage area or if it is only a matter of relative errors reduction due to the basin size. Therefore, we evaluated the errors in terms of equivalent frequency (Figure 17c). It was detected the return period from the extreme distribution of the reference simulation equivalent to the calculated 100-year discharges of the Eta simulations. In general, the 100-year discharges generated by Eta are equivalent to the 5-year discharges of the reference simulation for basins around 1,000 km², but these events approximate to a 20-year return period for basins around 100,000 km². The positive slope from the drainage area

x return period curve is mainly noticed for basins greater than 30,000 km² despite of the driven GCM, which agrees with the previous analysis about the relative errors. From these results, there is a high confidence that the flooding errors generated from the Eta RCM in fact reduce with the increasing drainage area.

The spatial distribution of the Eta-MSWEP differences related to extreme discharges is presented on Figure 18a. It was chosen events of 10-year return period (RP10) to be displayed on the map and a similar pattern was found for RP2 and RP100 events. Using Eta simulated precipitation as input clearly leads MGB to underestimate discharge on the north and central regions of the continent and overestimate it on the west coast of Chile (from 20S to 50S). Negative biases are found mainly on Paraguay, Orinoco, and Amazon (downstream the Negro confluence) rivers. On the northeast of Brazil, the bias signal is dependent on the driving GCM as the downscaling precipitation of MIROC5 and BESM yielded larger positive bias while HadGEM2-ES and CanESM2 mostly present a negative bias of discharge. Although Eta simulations underestimate extreme precipitation in most South America (see sections 3 and 3.2), the extreme discharge of some important large rivers are unbiased or present a smaller positive bias, such as in the upper Amazon (upstream the Negro confluence), Tocantins (except Eta-HadGEM2-ES), São Francisco, Magdalena and Colorado rivers. The spatial and temporal aggregation played an important role in reducing the negative biases downstream in the basins. For example, it can be seen on the Paraná, Magdalena, and São Francisco basins that Eta precipitation causes underestimation of extreme discharge over small rivers, but this effect is dissipated downstream with increasing drainage area. For larger basins, the spatial distribution of the differences in extreme discharge resemble to the annual precipitation biases (Figure 18b) and not the short-temporal scales differences that can be identified on Figure 12.

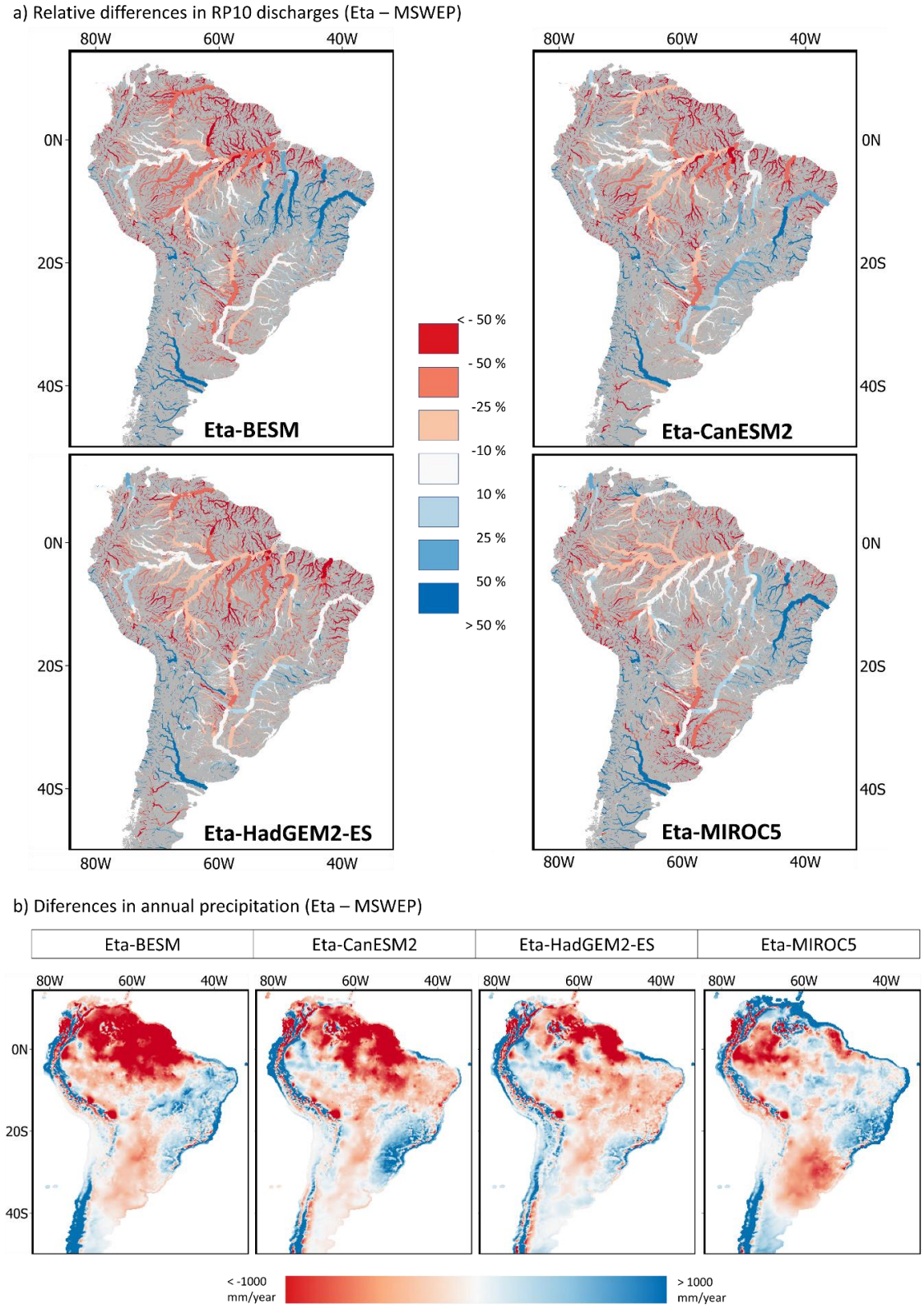

Figure 18. a) Relative differences between Eta and MSWEP in discharges that has a return period of 10 years simulated by the MGB-SA. The line thickness is proportional to the upstream drainage area. b) Absolute differences in annual precipitation between Eta and MSWEP.

4. CONCLUSION

Climate projections are occasionally used for hydrological impact studies in South America without a prior investigation on the climate model performances for different scales of application. Extreme precipitation is a critical feature in climate modeling since they are often associated with subscale processes and carries great uncertainties even on high resolution RCMs. Thus, this paper investigated how the Eta RCM nested in 4 GCMs performed in relation to short-scale (<1 day and 400 km² area) extreme precipitation and how these uncertainties change with different temporal and spatial scales. In addition, it was evaluated the effect of Eta precipitation biases on discharge estimates through hydrological simulations using the MGB-SA model. Local IDF curves and the MSWEP v2 precipitation database were used as reference for performance evaluation.

Eta underestimates short-scale extreme precipitation in most South America except on the west coast of Patagonia. These biases are independent to the driving GCMs which indicates that they are associated with Eta model systematic biases. The Eta underestimation for extreme daily precipitation was also pointed by Avila-Diaz *et al.* (2020) for Brazil. A poor performance for short-scale was expected since errors in sub-daily precipitation are common for non-convective-permitting models (Fowler et al., 2021a; Prein et al., 2015) as Eta. Thus, it might be more appropriate to reach for qualitative approaches for short-scale analysis, acknowledging theoretical studies about sub-daily extreme precipitation (e.g. Westra *et al.*, 2014; Barbero *et al.*, 2018; Fowler *et al.*, 2021b), while convective-permitting modelling is still under development.

However, the RCM errors over extreme precipitation tend to reduce with increasing area and duration. Extreme daily precipitation simulated by Eta presented a stronger spatial dependence compared with MSWEP (Figure 16), which reinforce that short-scale processes are still not well represented by Eta. However, the spatial dependence of simulated precipitation events of 5-days duration is similar to MSWEP. It is more evident the benefits of longer precipitation intervals (1 to 5 days) than larger spatial aggregation (0.2° to 1.0° resolution) to reduce extreme precipitation biases. Extreme events of 5-day duration present significantly lower biases (Figure 15) and higher spatial correlation (Table 2) compared to extreme events of 1-day duration.

The relative differences in mean discharge yielded with Eta and MSWEP data follow the same pattern of the relative differences in precipitation but with errors multiplied by a factor of 1.7 (rainfall elasticity of streamflow) in average. The relative differences of extreme discharge are high for small basins (median is around 40%). However, these “errors” reduce with increasing drainage area, especially for basins larger than 30,000 km². For basins of such size, relative errors of extreme and mean discharge are basically the same. In terms of frequency, the 100-year discharges of Eta simulations are equivalent to a 5-year discharge of the reference simulation (MSWEP) for basins around 1,000 km², and to a 20-year discharge for basins of 100,000 km². It can be observed that the errors in frequency of extreme events

from Eta simulations significantly reduces for basins larger than 30,000 km². Lower errors of extreme discharge in large basins may be related to: the averaging precipitation over the basin (spatial aggregation) and the extreme precipitation event of longer interval (temporal aggregation). At basins greater than 300,000 km², the extreme discharge biases are highly correlated and probably largely influenced by the upstream annual mean precipitation and not specific precipitation events.

Although it is observed important biases for short-scale extreme events, those are somehow reduced in a regional to continental perspective. The results did not depend on the driven GCM, which mean that they are mostly related to the Eta RCM intrinsic biases. Also, we observed that the bias of extreme discharge reduces with drainage area especially for basins larger than 30,000 km², which might indicate an area threshold for environmental investigations using the Eta RCM. It is important that hydrological researchers adhere to an uncertainty approach by matching the scale of the hydrological assessment to previous climatological evaluations, incorporating their uncertainties. RCMs provide several output features but not all of them are meant to be used for impact assessments without an adequate data treatment. Although this paper only explored the overall biases of the Eta model, it has proposed a framework for hydrological assessment of RCMs and some results discussed here could be generalized.

5. REFERENCES

Adam K, Fan F, Pontes P, Bravo J, Collischonn W. 2015. Mudanças climáticas e vazões extremas na Bacia do Rio Paraná / Climate Change and Extreme Streamflows in Paraná River Basin. *Revista Brasileira de Recursos Hídricos*, 20(4): 999–1007. https://doi.org/10.21168/rbrh.v20n4.p999-1007.

Allen RJ, DeGaetano AT. 2005. Areal Reduction Factors for Two Eastern United States Regions with High Rain-Gauge Density. *Journal of Hydrologic Engineering*, 10(4): 327–335. https://doi.org/10.1061/(ASCE)1084-0699(2005)10:4(327).

Almagro A, Oliveira PTS, Rosolem R, Hagemann S, Nobre CA. 2020. Performance evaluation of Eta/HadGEM2-ES and Eta/MIROC5 precipitation simulations over Brazil. *Atmospheric Research*. Elsevier B.V, 244: 105053. https://doi.org/10.1016/j.atmosres.2020.105053.

Alvarenga LA, Mello CR de, Colombo A, Cuartas LA, Chou SC. 2016. Hydrological responses to climate changes in a headwater watershed. *Ciência e Agrotecnologia*, 40(6): 647–657. https://doi.org/10.1590/1413-70542016406027716.

Andrade CWL, Montenegro SMGL, Montenegro AAA, Lima JR d. S, Srinivasan R, Jones CA. 2020. Climate change impact assessment on water resources under RCP scenarios: A case study in Mundaú River Basin, Northeastern Brazil. *International Journal of Climatology*, (October 2018): 1–17. https://doi.org/10.1002/joc.6751.

Antico PL, Chou SC, Brunini CA. 2020. The foehn wind east of the Andes in a 20-year climate simulation. *Meteorology and Atmospheric Physics*. Springer Vienna, (1988). https://doi.org/10.1007/s00703-020-00752-3.

Arakawa A. 2004. The cumulus parameterization problem: Past, present, and future. *Journal of Climate*, 17(13): 2493–2525. https://doi.org/10.1175/1520-0442(2004)017<2493:RATCPP>2.0.CO;2.

Avila-Diaz A, Abrahão G, Justino F, Torres R, Wilson A. 2020. Extreme climate indices in Brazil: evaluation of downscaled earth system models at high horizontal resolution. *Climate Dynamics*. Springer Berlin Heidelberg, 54(11–12): 5065–5088. https://doi.org/10.1007/s00382-020-05272-9.

Ávila A, Justino F, Wilson A, Bromwich D, Amorim M. 2016. Recent precipitation trends, flash floods and landslides in southern Brazil. *Environmental Research Letters*. IOP Publishing, 11(11). https://doi.org/10.1088/1748-9326/11/11/114029.

Bador M, Boé J, Terray L, Alexander L V., Baker A, Bellucci A, Haarsma R, Koenigk T, Moine MP, Lohmann K, Putrasahan DA, Roberts C, Roberts M, Scoccimarro E, Schiemann R, Seddon J, Senan R, Valcke S, Vanniere B. 2020. Impact of Higher Spatial Atmospheric Resolution on Precipitation Extremes Over Land in Global Climate Models. *Journal of Geophysical Research: Atmospheres*, 125(13): 1–23. https://doi.org/10.1029/2019JD032184.

Barbero R, Westra S, Lenderink G, Fowler HJ. 2018. Temperature-extreme precipitation scaling: a two-way causality? *International Journal of Climatology*, 38: e1274–e1279. https://doi.org/10.1002/joc.5370.

Beck HE, Wood EF, Pan M, Fisher CK, Miralles DG, Van Dijk AIJM, McVicar TR, Adler RF. 2019. MSWep v2 Global 3-hourly 0.1° precipitation: Methodology and quantitative assessment. *Bulletin of the American Meteorological Society*, 100(3): 473–500. https://doi.org/10.1175/BAMS-D-17-0138.1.

Bertoni JC, Tucci CEM. 1993. Precipitação. In: UFRGS E da (ed) *Hidrologia. Ciências e Aplicação*. ABRH: Porto Alegre, 943.

Biemans H, Hutjes RWA, Kabat P, Strengers BJ, Gerten D, Rost S. 2009. Effects of precipitation uncertainty on discharge calculations for main river basins. *Journal of Hydrometeorology*, 10(4): 1011–1025. https://doi.org/10.1175/2008JHM1067.1.

Borges de Amorim P, Chaffe PB. 2019. Towards a comprehensive characterization of evidence in synthesis assessments: the climate change impacts on the Brazilian water resources. *Climatic Change*. Climatic Change, 155(1): 37–57. https://doi.org/10.1007/s10584-019-02430-9.

Bravo JM, Collischonn W, da Paz AR, Allasia D, Domecq F. 2014. Impact of projected climate change on hydrologic regime of the Upper Paraguay River basin. *Climatic Change*, 127(1): 27–41. https://doi.org/10.1007/s10584-013-0816-2.

Brêda JPLF, de Paiva RCD, Collischon W, Bravo JM, Siqueira VA, Steinke EB. 2020. Climate change impacts on South American water balance from a continental-scale hydrological model driven by CMIP5 projections. *Climatic Change*. Climatic Change, 159(4): 503–522. https://doi.org/10.1007/s10584-020-02667-9.

Breinl K, Müller-Thomy H, Blöschl G. 2020. Space–Time Characteristics of Areal Reduction Factors and Rainfall Processes. *Journal of Hydrometeorology*, 21(4): 671–689. https://doi.org/10.1175/jhm-d-19-0228.1.

Castro ALP de, Silva CNP, Silveira A. 2011. Curvas Intensidade-Duração-Frequência das precipitações extremas para o município de Cuiabá (MT) / Intensity-Duration-Frequency Curves of extreme precipitation for the city of Cuiabá (MT). *Revista Ambiência*, 7(2): 305–315. https://doi.org/10.5777/ambiencia.2011.02.08.

Catalini CG. 2018. Predicción de Lluvias Máximas en Argentina Desarrollos y Nuevas Aplicaciones. Universidad Nacional de Córdoba. Facultad de Ciencias Exactas, Físicas y ….

Chiew FHS. 2006. Estimation of rainfall elasticity of streamflow in Australia. *Hydrological Sciences Journal*, 51(4): 613–625. https://doi.org/10.1623/hysj.51.4.613.

Chou SC, Lyra A, Mourão C, Dereczynski C, Pilotto I, Gomes J, Bustamante J, Tavares P, Silva A, Rodrigues D, Campos D, Chagas D, Sueiro G, Siqueira G, Marengo J. 2014a. Assessment of Climate Change over South America under RCP 4.5 and 8.5 Downscaling Scenarios. *American Journal of Climate Change*, 03(05): 512–527. https://doi.org/10.4236/ajcc.2014.35043.

Chou SC, Lyra A, Mourão C, Dereczynski C, Pilotto I, Gomes J, Bustamante J, Tavares P, Silva A, Rodrigues D, Campos D, Chagas D, Sueiro G, Siqueira G, Nobre P, Marengo J. 2014b. Evaluation of the Eta Simulations Nested in Three Global Climate Models. *American Journal of Climate Change*, 03(05): 438–454. https://doi.org/10.4236/ajcc.2014.35039.

Chou SC, Marengo JA, Lyra AA, Sueiro G, Pesquero JF, Alves LM, Kay G, Betts R, Chagas DJ, Gomes JL, Bustamante JF, Tavares P. 2012. Downscaling of South America present climate driven by 4-member HadCM3 runs. *Climate Dynamics*, 38(3–4): 635–653. https://doi.org/10.1007/s00382-011-1002-8.

Chou SC, Nunes AMB, Cavalcanti IFA. 2000. Extended range forecasts over South America using the regional eta model. *Journal of Geophysical Research: Atmospheres*, 105(D8): 10147–10160. https://doi.org/10.1029/1999JD901137.

Chylek P, Li J, Dubey MK, Wang M, Lesins G. 2011. Observed and model simulated 20th century Arctic temperature variability: Canadian Earth System Model CanESM2. *Atmospheric Chemistry and Physics Discussions*, 11(8): 22893–22907. https://doi.org/10.5194/acpd-11-22893-2011.

Collins WJ, Bellouin N, Gedney N, Halloran P, Hinton T, Hughes J, Jones CD. 2011. Model Development Development and evaluation of an Earth-System model – HadGEM2. , 1051–1075. https://doi.org/10.5194/gmd-4-1051-2011.

Cuevas L, Rolón A. 2010. Actualización de las curvas intensidad-duración-frecuencia de precipitación en el Paraguay. Universidad Nacional de Asunción.

de Oliveira VA, de Mello CR, Beskow S, Viola MR, Srinivasan R. 2019. Modeling the effects of climate change on hydrology and sediment load in a headwater basin in the Brazilian Cerrado biome. *Ecological Engineering*. Elsevier, 133(October 2018): 20–31. https://doi.org/10.1016/j.ecoleng.2019.04.021.

de Oliveira VA, de Mello CR, Viola MR, Srinivasan R. 2017. Assessment of climate change impacts on streamflow and hydropower potential in the headwater region of the Grande river basin, Southeastern Brazil. *International Journal of Climatology*, 37(15): 5005–5023. https://doi.org/10.1002/joc.5138.

Debortoli NS, Camarinha PIM, Marengo JA, Rodrigues RR. 2017. An index of Brazil's vulnerability to expected increases in natural flash flooding and landslide disasters in the context of climate change. *Natural Hazards*, 86(2): 557–582. https://doi.org/10.1007/s11069-016-2705-2.

Dereczynski C, Chan Chou S, Lyra A, Sondermann M, Regoto P, Tavares P, Chagas D, Gomes JL, Rodrigues DC, Skansi M de los M. 2020. Downscaling of climate extremes over South America – Part I: Model evaluation in the reference climate. *Weather and Climate Extremes*, 29(March). https://doi.org/10.1016/j.wace.2020.100273.

Distrito Federal. 2009. *Plano Diretor de Drenagem Urbana do Distrito Federal: Relatório de Produto 4*. Brasília.

Fagundes HO, Fan FM, Paiva RCD, Siqueira VA, Buarque DC, Kornowski LW, Laipelt L, Collischonn W. 2020. Sediment flows in South America supported by daily hydrologic-hydrodynamic modeling. *Water Resources Research*. https://doi.org/10.1029/2020WR027884.

Falco M, Carril AF, Menéndez CG, Zaninelli PG, Li LZX. 2019. Assessment of CORDEX simulations over South America: added value on seasonal climatology and resolution considerations. *Climate*

Dynamics. Springer Berlin Heidelberg, 52(7–8): 4771–4786. https://doi.org/10.1007/s00382-018-4412-z.

Fendrich R. 1998. *Chuvas intensas para obras de drenagem (no estado do Paraná)*. Champagnat.

Fernández PC, Fattorelli S, Rodríguez S, Fornero L. 1999. Regional Analysis of Convective Storms. *Journal of Hydrologic Engineering*, 4(4): 317–325. https://doi.org/10.1061/(ASCE)1084-0699(1999)4:4(317).

Feser F, Rrockel B, Storch H, Winterfeldt J, Zahn M. 2011. Regional climate models add value to global model data a review and selected examples. *Bulletin of the American Meteorological Society*, 92(9): 1181–1192. https://doi.org/10.1175/2011BAMS3061.1.

Fischer EM, Knutti R. 2016. Observed heavy precipitation increase confirms theory and early models. *Nature Climate Change*. Nature Publishing Group, 6(11): 986–991. https://doi.org/10.1038/nclimate3110.

Flato G, Marotzke J, Abiodun B, Braconnot P, Chou SC, Collins W, Cox P, Driouech F, Emori S, Eyring V, Forest C, Gleckler P, Guilyardi E, Jakob C, Kattsov V, Reason C, Rummukainen M. 2013. Evaluation of Climate Models. *Climate Change 2013: The Physical Science Basis. Contribution of Working Group I to the Fifth Assessment Report of the Intergovernmental Panel on Climate Change*, 741–866. https://doi.org/10.1017/CBO9781107415324.

Fontolan M, Xavier ACF, Pereira HR, Blain GC. 2019. Using climate change models to assess the probability of weather extremes events: A local scale study based on the generalized extreme value distribution. *Bragantia*, 78(1): 146–157. https://doi.org/10.1590/1678-4499.2018144.

Fosser G, Khodayar S, Berg P. 2014. Benefit of convection permitting climate model simulations in the representation of convective precipitation. *Climate Dynamics*, 44(1–2): 45–60. https://doi.org/10.1007/s00382-014-2242-1.

Fowler HJ, Ali H, Allan RP, Ban N, Barbero R, Berg P, Blenkinsop S, Cabi NS, Chan S, Dale M, Dunn RJH, Ekström M, Evans JP, Fosser G, Golding B, Guerreiro SB, Hegerl GC, Kahraman A, Kendon EJ, Lenderink G, Lewis E, Li X, O'Gorman PA, Orr HG, Peat KL, Prein AF, Pritchard D, Schär C, Sharma A, Stott PA, Villalobos-Herrera R, Villarini G, Wasko C, Wehner MF, Westra S, Whitford A. 2021a. Towards advancing scientific knowledge of climate change impacts on short-duration rainfall extremes. *Philosophical Transactions of the Royal Society A: Mathematical, Physical and Engineering Sciences*, 379(2195). https://doi.org/10.1098/rsta.2019.0542.

Fowler HJ, Wasko C, Prein AF. 2021b. Intensification of short-duration rainfall extremes and implications for flood risk: Current state of the art and future directions. *Philosophical Transactions of the Royal Society A: Mathematical, Physical and Engineering Sciences*, 379(2195). https://doi.org/10.1098/rsta.2019.0541.

Fragoso Jr CR. 2004. Regionalização de vazão máxima instantânea com base na precipitação de projeto. *Revista Eletrônica de Recursos Hídricos*, 1(1).

Gervais M, Gyakum JR, Atallah E, Tremblay LB, Neale RB. 2014. How well are the distribution and extreme values of daily precipitation over North America represented in the community climate system model? A comparison to reanalysis, satellite, and gridded station data. *Journal of Climate*, 27(14): 5219–5239. https://doi.org/10.1175/JCLI-D-13-00320.1.

Giorgi F. 2019. Thirty Years of Regional Climate Modeling: Where Are We and Where Are We Going next? *Journal of Geophysical Research: Atmospheres*, 124(11): 5696–5723. https://doi.org/10.1029/2018JD030094.

Giorgi F, Jones C, Asrar G. 2009. Addressing climate information needs at the regional level: the

CORDEX framework. … *Organization (WMO) Bulletin*, 58(July): 175–183.

Gulizia C, Camilloni I. 2015. Comparative analysis of the ability of a set of CMIP3 and CMIP5 global climate models to represent precipitation in South America. *International Journal of Climatology*, 35(4): 583–595. https://doi.org/10.1002/joc.4005.

Haarsma RJ, Roberts MJ, Vidale PL, Catherine A, Bellucci A, Bao Q, Chang P, Corti S, Fučkar NS, Guemas V, Von Hardenberg J, Hazeleger W, Kodama C, Koenigk T, Leung LR, Lu J, Luo JJ, Mao J, Mizielinski MS, Mizuta R, Nobre P, Satoh M, Scoccimarro E, Semmler T, Small J, Von Storch JS. 2016. High Resolution Model Intercomparison Project (HighResMIP v1.0) for CMIP6. *Geoscientific Model Development*, 9(11): 4185–4208. https://doi.org/10.5194/gmd-9-4185-2016.

Hirabayashi Y, Mahendran R, Koirala S, Konoshima L, Yamazaki D, Watanabe S, Kim H, Kanae S. 2013. Global flood risk under climate change. *Nature Climate Change*. Nature Publishing Group, 3(9): 816–821. https://doi.org/10.1038/nclimate1911.

Hirabayashi Y, Tanoue M, Sasaki O, Zhou X, Yamazaki D. 2021. Global exposure to flooding from the new CMIP6 climate model projections. *Scientific Reports*. Nature Publishing Group UK, 11(1): 1–7. https://doi.org/10.1038/s41598-021-83279-w.

IDEAM. 2017. *CURVAS INTENSIDAD DURACION FRECUENCIA - IDF*. Bogotá.

Iglesias A, Garrote L. 2015. Adaptation strategies for agricultural water management under climate change in Europe. *Agricultural Water Management*. Elsevier B.V., 155: 113–124. https://doi.org/10.1016/j.agwat.2015.03.014.

INAMHI. 2019. Determinación de ecuaciones para el cálculo de intensidades máximas de precipitación. *Instituto Nacional de Meteorología e Hidrología*, (2): 282.

Jati DA, Cristiane N, Pinheiro P. 2020. Revista Brasileira de Geografia Física and mean air temperature. , 01: 211–228.

Kim J, Lee J, Kim D, Kang B. 2019. The role of rainfall spatial variability in estimating areal reduction factors. *Journal of Hydrology*. Elsevier, 568(November): 416–426. https://doi.org/10.1016/j.jhydrol.2018.11.014.

Knist S, Goergen K, Simmer C. 2020. Evaluation and projected changes of precipitation statistics in convection-permitting WRF climate simulations over Central Europe. *Climate Dynamics*. Springer Berlin Heidelberg, 55(1–2): 325–341. https://doi.org/10.1007/s00382-018-4147-x.

Knutti R, Sedláček J. 2013. Robustness and uncertainties in the new CMIP5 climate model projections. *Nature Climate Change*. Nature Publishing Group, 3(4): 369–373. https://doi.org/10.1038/nclimate1716.

Kooperman GJ, Pritchard MS, Burt MA, Branson MD, Randall DA. 2016. Robust effects of cloud superparameterization on simulated daily rainfall intensity statistics across multiple versions of the <scp>C</scp> ommunity <scp>E</scp> arth <scp>S</scp> ystem <scp>M</scp> odel. *Journal of Advances in Modeling Earth Systems*, 8(1): 140–165. https://doi.org/10.1002/2015MS000574.

Lebel T, Laborde JP. 1988. A geostatistical approach for areal rainfall statistics assessment. *Stochastic Hydrology and Hydraulics*, 2(4): 245–261. https://doi.org/10.1007/BF01544039.

Lee MH, Im ES, Bae DH. 2019. Impact of the spatial variability of daily precipitation on hydrological projections: A comparison of GCM- and RCM-driven cases in the Han River basin, Korea. *Hydrological Processes*, (December 2018): 2240–2257. https://doi.org/10.1002/hyp.13469.

Lehner B, Döll P, Alcamo J, Henrichs T, Kaspar F. 2006. Estimating the impact of global change on flood and drought risks in Europe: A continental, integrated analysis. *Climatic Change*, 75(3): 273–

299. https://doi.org/10.1007/s10584-006-6338-4.

Lenderink G, Fowler HJ. 2017. Hydroclimate: Understanding rainfall extremes. *Nature Climate Change*. Nature Publishing Group, 7(6): 391–393. https://doi.org/10.1038/nclimate3305.

Llopart M, Simões Reboita M, Porfírio da Rocha R. 2020. Assessment of multi-model climate projections of water resources over South America CORDEX domain. *Climate Dynamics*. Springer Berlin Heidelberg, 54(1–2): 99–116. https://doi.org/10.1007/s00382-019-04990-z.

Lyra A, Tavares P, Chou SC, Sueiro G, Dereczynski C, Sondermann M, Silva A, Marengo J, Giarolla A. 2018. Climate change projections over three metropolitan regions in Southeast Brazil using the non-hydrostatic Eta regional climate model at 5-km resolution. *Theoretical and Applied Climatology*. Theoretical and Applied Climatology, 132(1–2): 663–682. https://doi.org/10.1007/s00704-017-2067-z.

Marengo JA, Chou SC, Kay G, Alves LM, Pesquero JF, Soares WR, Santos DC, Lyra AA, Sueiro G, Betts R, Chagas DJ, Gomes JL, Bustamante JF, Tavares P. 2012. Development of regional future climate change scenarios in South America using the Eta CPTEC/HadCM3 climate change projections: Climatology and regional analyses for the Amazon, São Francisco and the Paraná River basins. *Climate Dynamics*, 38(9–10): 1829–1848. https://doi.org/10.1007/s00382-011-1155-5.

Marengo JA, Rusticucci M, Penalba O, Renom M. 2010. An intercomparison of observed and simulated extreme rainfall and temperature events during the last half of the twentieth century: Part 2: Historical trends. *Climatic Change*, 98(3): 509–529. https://doi.org/10.1007/s10584-009-9743-7.

Martinez RGA, Condori ML, Salazar MES. 2009. Curvas IDF para diferentes categorías de análisis de eventos extremos de las ciudades del eje central de Bolivia (La Paz, El Alto, Cochabamba y Santa Cruz). Universidad Mayor de San Andres.

Meresa HK, Romanowicz RJ. 2017. The critical role of uncertainty in projections of hydrological extremes. *Hydrology and Earth System Sciences*, 21(8): 4245–4258. https://doi.org/10.5194/hess-21-4245-2017.

Mesinger F. 1984. A blocking technique for representation of mountains in atmospheric models. *Riv. Meteor. Aeronaut.*, 44: 195–202.

Mesinger F, Chou SC, Gomes JL, Jovic D, Bastos P, Bustamante JF, Lazic L, Lyra AA, Morelli S, Ristic I, Veljovic K. 2012. An upgraded version of the Eta model. *Meteorology and Atmospheric Physics*, 116(3–4): 63–79. https://doi.org/10.1007/s00703-012-0182-z.

Milly PCD, Betancourt J, Falkenmark M, Hirsch RM, Kundzewicz ZW, Lettenmaier DP, Stouffer RJ. 2008. Climate change: Stationarity is dead: Whither water management? *Science*, 319(5863): 573–574. https://doi.org/10.1126/science.1151915.

Milly PCD, Dunne KA, Vecchia A V. 2005. Global pattern of trends in streamflow and water availability in a changing climate. *Nature*, 438(7066): 347–350. https://doi.org/10.1038/nature04312.

Ministerio de Vivienda y Urbanismo. 1996. Marco Geográfico. *Técnicas Alternativas para Soluciones de Aguas Lluvias en Sectores Urbanos.* Santiago, 663.

Mortazavi-Naeini M, Kuczera G, Kiem AS, Cui L, Henley B, Berghout B, Turner E. 2015. Robust optimization to secure urban bulk water supply against extreme drought and uncertain climate change. *Environmental Modelling and Software*. Elsevier Ltd, 69: 437–451. https://doi.org/10.1016/j.envsoft.2015.02.021.

Naghettini M. 2017. *Fundamentals of statistical hydrology*. Springer.

Neumann JE, Price J, Chinowsky P, Wright L, Ludwig L, Streeter R, Jones R, Smith JB, Perkins W,

Jantarasami L, Martinich J. 2015. Climate change risks to US infrastructure: impacts on roads, bridges, coastal development, and urban drainage. *Climatic Change*, 131(1): 97–109. https://doi.org/10.1007/s10584-013-1037-4.

New M, Lister D, Hulme M, Makin I. 2002. A high-resolution data set of surface climate over global land areas. *Climate Research*, 21(1): 1–25. https://doi.org/10.3354/cr021001.

Nobre P, Siqueira LSP, De Almeida RAF, Malagutti M, Giarolla E, Castelã O GP, Bottino MJ, Kubota P, Figueroa SN, Costa MC, Baptista M, Irber L, Marcondes GG. 2013. Climate simulation and change in the brazilian climate model. *Journal of Climate*, 26(17): 6716–6732. https://doi.org/10.1175/JCLI-D-12-00580.1.

Oliveira GG, Pedrollo OC, Castro NMR. 2015. Stochastic approach to analyzing the uncertainties and possible changes in the availability of water in the future based on scenarios of climate change. *Hydrology and Earth System Sciences*, 19(8): 3585–3604. https://doi.org/10.5194/hess-19-3585-2015.

Oliveira LFC, Cortês FC, Wehr TR, Borges LB, Sarmento PHL, Griebeler NP. 2005. Intensidade-Duração-Frequência De Chuvas Intensas Para Localidades No Estado De Goiás E Distrito Federal. *Pesquisa Agropecuária Tropical*, 35(1): 13–18.

Papalexiou SM, Montanari A. 2019. Global and Regional Increase of Precipitation Extremes Under Global Warming. *Water Resources Research*, 55(6): 4901–4914. https://doi.org/10.1029/2018WR024067.

Pesquero JF, Chou SC, Nobre CA, Marengo JA. 2010. Climate downscaling over South America for 1961–1970 using the Eta Model. *Theoretical and Applied Climatology*, 99(1–2): 75–93. https://doi.org/10.1007/s00704-009-0123-z.

Pontes PRM, Fan FM, Fleischmann AS, de Paiva RCD, Buarque DC, Siqueira VA, Jardim PF, Sorribas MV, Collischonn W. 2017. MGB-IPH model for hydrological and hydraulic simulation of large floodplain river systems coupled with open source GIS. *Environmental Modelling and Software*, 94: 1–20. https://doi.org/10.1016/j.envsoft.2017.03.029.

Prein AF, Gobiet A, Suklitsch M, Truhetz H, Awan NK, Keuler K, Georgievski G. 2013. Added value of convection permitting seasonal simulations. *Climate Dynamics*, 41(9–10): 2655–2677. https://doi.org/10.1007/s00382-013-1744-6.

Prein AF, Langhans W, Fosser G, Ferrone A, Ban N, Goergen K, Keller M, Tölle M, Gutjahr O, Feser F, Brisson E, Kollet S, Schmidli J, Van Lipzig NPM, Leung R. 2015. A review on regional convection-permitting climate modeling: Demonstrations, prospects, and challenges. *Reviews of Geophysics*, 53(2): 323–361. https://doi.org/10.1002/2014RG000475.

Ribeiro Neto A, da Paz AR, Marengo JA, Chou SC. 2016. Hydrological Processes and Climate Change in Hydrographic Regions of Brazil. *Journal of Water Resource and Protection*, 08(12): 1103–1127. https://doi.org/10.4236/jwarp.2016.812087.

Santos CAS, Rocha FA, Ramos TB, Alves LM, Mateus M, de Oliveira RP, Neves R. 2019. Using a hydrologic model to assess the performance of regional climate models in a semi-arid Watershed in Brazil. *Water (Switzerland)*, 11(1): 1–17. https://doi.org/10.3390/w11010170.

Santos ECX, Naghettini M. 2003. Agregação do coeficiente de abatimento espacial à região metropolitana de Belo Horizonte. *Revista Brasileira de Recursos Hídricos*, 8(1): 189–199.

Sherwood SC, Bony S, Dufresne JL. 2014. Spread in model climate sensitivity traced to atmospheric convective mixing. *Nature*, 505(7481): 37–42. https://doi.org/10.1038/nature12829.

Silva FOE da, Palácio FFR, Campos JNB. 2013. Equação de chuvas para Fortaleza-CE com dados do pluviógrafo da UFC. *Revista DAE*. Revista DAE, 61(192): 48–59. https://doi.org/10.4322/dae.2014.106.

Silveira A. 2001. Abatimento espacial da chuva em Porto Alegre. *Revista Brasileira de Recursos Hídricos*, 6(2): 5–13. https://doi.org/10.21168/rbrh.v6n2.p5-13.

Silveira A, Bemfica D, Goldenfum J. 2000. Análise da Aplicabilidade de Padrões de Chuva de Projeto a Porto Alegre. *Revista Brasileira de Recursos Hídricos*, 5(4): 5–16. https://doi.org/10.21168/rbrh.v5n4.p5-16.

Siqueira VA, Fan FM, Paiva RCD de, Ramos M-H, Collischonn W. 2020. Potential skill of continental-scale, medium-range ensemble streamflow forecasts for flood prediction in South America. *Journal of Hydrology*, 590: 125430. https://doi.org/10.1016/j.jhydrol.2020.125430.

Sivapalan M, Blöschl G. 1998. Transformation of point rainfall to areal rainfall: Intensity-duration-frequency curves. *Journal of Hydrology*, 204(1–4): 150–167. https://doi.org/10.1016/S0022-1694(97)00117-0.

Skansi M de los M, Brunet M, Sigró J, Aguilar E, Arevalo Groening JA, Bentancur OJ, Castellón Geier YR, Correa Amaya RL, Jácome H, Malheiros Ramos A, Oria Rojas C, Pasten AM, Sallons Mitro S, Villaroel Jiménez C, Martínez R, Alexander L V., Jones PD. 2013. Warming and wetting signals emerging from analysis of changes in climate extreme indices over South America. *Global and Planetary Change*. Elsevier B.V., 100: 295–307. https://doi.org/10.1016/j.gloplacha.2012.11.004.

Skaugen T. 1997. Classification of rainfall into small- and large-scale events by statistical pattern recognition. *Journal of Hydrology*, 200(1–4): 40–57. https://doi.org/10.1016/S0022-1694(97)00003-6.

Solman SA, Sanchez E, Samuelsson P, da Rocha RP, Li L, Marengo J, Pessacg NL, Remedio ARC, Chou SC, Berbery H, Le Treut H, de Castro M, Jacob D. 2013. Evaluation of an ensemble of regional climate model simulations over South America driven by the ERA-Interim reanalysis: Model performance and uncertainties. *Climate Dynamics*, 41(5–6): 1139–1157. https://doi.org/10.1007/s00382-013-1667-2.

Sorribas MV, Paiva RCD, Melack JM, Bravo JM, Jones C, Carvalho L, Beighley E, Forsberg B, Costa MH. 2016. Projections of climate change effects on discharge and inundation in the Amazon basin. *Climatic Change*, 136(3–4): 555–570. https://doi.org/10.1007/s10584-016-1640-2.

Stocker TF, Qin D, Plattner G-K, Tignor M, Allen SK, Boschung J, Nauels A, Xia Y, Bex V, Midgley PM. 2013. Climate change 2013: The physical science basis. Cambridge University Press Cambridge.

Sun Q, Miao C, Duan Q, Ashouri H, Sorooshian S, Hsu KL. 2018. A Review of Global Precipitation Data Sets: Data Sources, Estimation, and Intercomparisons. *Reviews of Geophysics*, 56(1): 79–107. https://doi.org/10.1002/2017RG000574.

Sun Q, Zhang X, Zwiers F, Westra S, Alexander L V. 2021. A global, continental, and regional analysis of changes in extreme precipitation. *Journal of Climate*, 34(1): 243–258. https://doi.org/10.1175/JCLI-D-19-0892.1.

Svensson C, Jones DA. 2010. Review of methods for deriving areal reduction factors. *Journal of Flood Risk Management*, 3(3): 232–245. https://doi.org/10.1111/j.1753-318X.2010.01075.x.

Teutschbein C, Seibert J. 2010. Regional climate models for hydrological impact studies at the catchment scale: A review of recent modeling strategies. *Geography Compass*, 4(7): 834–860. https://doi.org/10.1111/j.1749-8198.2010.00357.x.

Valverde MC, Marengo JA. 2014. Extreme Rainfall Indices in the Hydrographic Basins of Brazil. *Open Journal of Modern Hydrology*, 04(01): 10–26. https://doi.org/10.4236/ojmh.2014.41002.

Vergasta LA, Correia FWS, Chou SC, Nobre P, Lyra A de A, Gomes W de B, Capistrano V, Veiga JAP. 2021. Avaliação do Balanço de água na Bacia do Rio Madeira Simulado Pelo Modelo Regional Climático Eta e o Modelo Hidrológico de Grandes Bacias MGB. *Revista Brasileira de Meteorologia*. https://doi.org/10.1590/0102-77863610005.

Vetter T, Reinhardt J, Flörke M, van Griensven A, Hattermann F, Huang S, Koch H, Pechlivanidis IG, Plötner S, Seidou O, Su B, Vervoort RW, Krysanova V. 2017. Evaluation of sources of uncertainty in projected hydrological changes under climate change in 12 large-scale river basins. *Climatic Change*. Climatic Change, 141(3): 419–433. https://doi.org/10.1007/s10584-016-1794-y.

Watanabe M, Suzuki T, O'Ishi R, Komuro Y, Watanabe S, Emori S, Takemura T, Chikira M, Ogura T, Sekiguchi M, Takata K, Yamazaki D, Yokohata T, Nozawa T, Hasumi H, Tatebe H, Kimoto M. 2010. Improved climate simulation by MIROC5: Mean states, variability, and climate sensitivity. *Journal of Climate*, 23(23): 6312–6335. https://doi.org/10.1175/2010JCLI3679.1.

Weather Bureau. 1958. Technical Paper No. 29 (Rainfall Intensity-Frequency Regime Part 4-Northeastern United States). *Superintendent of Documents, US Government Printing Office*, (May 1959).

Weiss LL. 1964. Ratio of true to fixed-interval maximum rainfall. *Journal of the Hydraulics Division*. ASCE, 90(1): 77–82.

Westra S, Fowler HJ, Evans JP, Alexander L V., Berg P, Johnson F, Kendon EJ, Lenderink G, Roberts NM. 2014. Future changes to the intensity and frequency of short-duration extreme rainfall. *Reviews of Geophysics*, 522–555.

Wright DB, Smith JA, Baeck ML. 2014. Critical examination of area reduction factors. *Journal of Hydrologic Engineering*, 19(4): 769–776. https://doi.org/10.1061/(ASCE)HE.1943-5584.0000855.

Xavier AC, King CW, Scanlon BR. 2016. Daily gridded meteorological variables in Brazil (1980–2013). *International Journal of Climatology*, 36(6): 2644–2659. https://doi.org/10.1002/joc.4518.

Yoo C, Jun C, Park C. 2015. Effect of Rainfall Temporal Distribution on the Conversion Factor to Convert the Fixed-Interval into True-Interval Rainfall. *Journal of Hydrologic Engineering*, 20(10): 04015018. https://doi.org/10.1061/(ASCE)HE.1943-5584.0001178.

Zahed FK, Marcellini SS. 1995. Precipitações Máximas. In: Editora da UFRGS. ABRH (ed) *Drenagem Urbana*. Porto Alegre.

ARTIGO 3

Assessing the Climate Change impacts on flood discharge in South America and the influence of its main drivers

Authors:

João Paulo Lyra Fialho Brêda
Rodrigo Cauduro Dias de Paiva
Walter Collischon
Vinicius Alencar Siqueira

Abstract

A warmer atmosphere is able to hold more water which consequently intensifies the hydrological cycle. The projected increase in extreme precipitation has been associated with greater floods; however, most recent studies have argued that the reduced soil moisture could be causing the opposite effect. We aim to understand how the hydrometeorological variables affect flood discharge and what the projections are for South America, a vulnerable continent that has been barely studied regarding flood trends. It was used climate data from Eta simulations nested in 4 global climate models (BESM, CanESM2, HadGEM2-ES, MIROC5) as input for the MGB-SA hydrological model to yield flood discharge estimates. Then we were able to project the climate impacts on extreme precipitation, antecedent soil moisture, and flood discharge for large rivers (> 1,000 km²) and understand how these variables are related. Our results showed a strong sign that antecedent soil moisture is expected to be reduced in most of the continent except in Southeastern South America (SESA). On the other hand, there are mixed signs for rarer precipitation but a clear spatial pattern for 2-year precipitations (RP2), which is expected to increase on the SESA and west Amazon and decrease on Central South America (CSA). For basins larger than 100,000 km², results indicate a negative change sign, especially for 2-year precipitations, meaning that rainfall events that generate ordinary floods in large South American rivers are expected to decrease in the XXI century due to climate change. The change signs for flood discharge are spatially similar to extreme precipitation; however, many rivers are expected to reduce floods in the future while presenting a positive change sign for extreme precipitation. While only half of the South American basins are expected to present reduced 2-year precipitations, nearly 70% of the rivers present a negative sign for 2-year floods, which can be attributed to the reduced antecedent soil moisture.

1. INTRODUCTION

The frequency and intensity of extreme rainfall events are expected to increase due to global warming (Lenderink and Fowler, 2017; O'Gorman, 2015). The Clausius-Clapeyron relation indicates that a warmer atmosphere is able to hold more water vapor at a rate of 6-7% per degree Celsius. With more water in the atmosphere, rarer storms are predicted to increase in magnitude, raising its potential damage (Fischer and Knutti, 2016; Myhre et al., 2019; Risser and Wehner, 2017). This effect is expected to be even more pronounced for sub-daily and local precipitation events (Fowler et al., 2021b; Lenderink and Van Meijgaard, 2008; Prein et al., 2017), which poses a great threat to vulnerable people living on urban impervious areas and hillslopes.

On the other hand, droughts are predicted to be more recurrent and intense as well (Cook et al., 2014; Dai, 2013). The relative humidity is expected to decrease with temperature increases over land, especially in regions with limited moisture availability (Byrne and O'Gorman, 2018, 2016). Reduced relative humidity inhibits convective formations (Yin et al., 2018), affecting the precipitation volume over land and reinforcing the "drier in dry, and wetter in wet" paradigm (Feng and Zhang, 2015). In addition, the rise of temperature strengthens evapotranspiration; in consequence, it will reduce soil moisture and expand aridity (Asadi Zarch et al., 2017; Samaniego et al., 2018), which directly affects agriculture and water supply worldwide (Liu et al., 2021; Meza et al., 2020).

These climatic alterations also have an immediate impact on flooding. At first, it was expected that global warming would increase the flood frequency (Alfieri et al., 2017; Milly et al., 2002) following the observed increases in extreme precipitation (Papalexiou and Montanari, 2019; Sun et al., 2021). However, some recent results showed that increases in precipitation do not necessarily translate to increases in flood magnitude, and an interesting debate has risen about this claim (see (Do et al., 2020; Wasko et al., 2019; Wasko and Sharma, 2017; Yin et al., 2019, 2018)). (Sharma et al., 2018) presented other flood drivers affected by global warming in addition to extreme precipitation, such as reduced soil moisture, earlier snowmelt, and increased canopy storage capacity (Yu et al., 2020). In particular, flood intensity is highly sensitive to antecedent soil moisture (Blöschl et al., 2015; Ivancic and Shaw, 2015; Wasko et al., 2020; Wasko and Nathan, 2019), which is expected to decrease with climate change. A drier soil can hold more water from rainfall, thus reducing runoff and flood magnitude. Therefore, projections of flood discharge will not necessarily present the same trend as extreme precipitation since there are other important flood drivers also affected by climate change. In addition, there is more confidence in the projected increase of fluvial flooding related to anticipated spring snowmelt than extreme precipitation (Blöschl et al., 2015; Kundzewicz et al., 2014).

Nevertheless, more investigation is necessary to understand how climate change may impact flooding, as every region has its particularities. Even the projected changes in intense precipitation are not always positive. Precipitation intensity seems to decrease with

temperature in tropical areas, while high latitude regions present storms intensification above the Clausius–Clapeyron relation (Utsumi et al., 2011; Westra et al., 2014; Yin et al., 2018). Global-scale investigations have also detected mixed and spatially complex flooding trends, with different levels of grouping categories such as continents (Berghuijs et al., 2017; Do et al., 2017), regions (Gudmundsson et al., 2021), and climates zones (Do et al., 2017; Slater et al., 2021). Studies have found different trend signs for streamflow extremes using distinct statistical approaches and databases. For instance, (Do et al., 2017) observed a negative trend in the USA, while (Berghuijs et al., 2017) observed a positive one. In Europe, studies (Blöschl et al., 2019; Gudmundsson et al., 2021) currently converge to a tendency of more flooding in the North (e.g. U.K., Germany, Netherlands) and less flooding in the South (e.g. Greece, Italy, Portugal). However, some continents as South America have not been fully assessed on global studies due to the limited data record, either for precipitation (Sun et al., 2021; Yin et al., 2018) or floods (Do et al., 2017).

South America possesses large rivers systems for which it has been called the “fluvial continent” (Fleischmann et al., 2021; Kandus et al., 2018). It contains great wetlands such as the Pantanal, and river inundations provide important ecosystem services in those places, regulating biogeochemical processes (Junk et al., 2013). In addition, there are highly anthropized basins with large dams for hydropower generation, such as the Magdalena and La Plata Basins, and climate change threatens the dams' safety and the energy supply (da Silva et al., 2020; Fluixá-Sanmartín et al., 2018). Finally, but not less important, floods are one of the greatest natural hazards due to human settlements on floodplains. People in South America have recently felt the impacts of extreme events (Cunha et al., 2019; de Abreu et al., 2019; Netto et al., 2013; Nobre et al., 2016), and it is essential to investigate climate projections in such a vulnerable continent (Debortoli et al., 2017; Monte et al., 2021; Vörösmarty et al., 2013) to avoid further disasters.

Global Climate Models (GCMs) are widely used tools to evaluate potential impacts of climate change (Donat et al., 2016; Fischer and Knutti, 2016). In particular, assessing future alterations in the frequency of extreme events can benefit from downscaled simulations provided by Regional Climate Models (RCMs), as they have finer resolution than global ones and improved characterization of local features (Giorgi, 2019; Llopart et al., 2020). Regarding the South American domain, the Eta model (Mesinger et al., 2012) is one of the most popular RCMs for hydrological assessments, especially in Brazil (Borges de Amorim and Chaffe, 2019). Extreme precipitation indices (e.g. PRECPTOT, R99p, R95p, RX1day, RX5day, and CWD) from Eta have already been examined (Avila-Diaz et al., 2020; Chou et al., 2014b; Dereczynski et al., 2020). However, these studies have barely covered the climate change impacts regarding hydrological extremes in South America. In order to fill this gap, this study provides a single integrated and standardized approach for hydrological assessment over the continent, which is important for building comparisons between regions and understanding average changes and drivers of extreme flood events.

Using a hydrological model forced with climate projections, we can evaluate expected changes in flood discharge with a reasonable physical representation. A previous assessment of streamflow extremes on a continental scale was conducted by (Ribeiro Neto et al., 2016) for Brazilian basins, but their hydrological model lacked a proper flood routing scheme, which is crucial in large river basins in South America (Paiva et al., 2013). In this paper, we use a hydrodynamic-hydrological model for South America forced with projections from Eta for the RCP 4.5 and 8.5 scenarios from CMIP5. In this context, the objective of this study is twofold. First, we investigate climate change impacts on extreme events in South America in terms of antecedent soil moisture, precipitation, and flood discharge at different spatial scales. Second, we assess how projections of flood discharge are related to projected changes in its main drivers.

2. METHODOLOGY

We assess climate change impacts on three hydrological variables: flood discharge, extreme precipitation, and antecedent soil moisture. Biased-corrected (Section 2.4) precipitation data were obtained from Eta simulations (Section 2.3) nested in 4 Global Climate Models (GCM), while flood discharge and soil moisture were simulated by the MGB-SA hydrological model (Section 2.2). Then, we selected the maximum flood discharge and precipitation of each hydrological year for each river reach in the model. Finally, a characteristic time was estimated based on flow propagation to identify the soil moisture prior to a flood event and to define the duration of extreme precipitation events (Section 2.5).

The analysis was built on comparing the historical (1961-2005) and future (2021-2065) estimates of the highest, second-highest, and median values of the annual maximum precipitation and discharge. These estimates correspond to the 44- (RP44), 22- (RP22), and 2-years (RP2) return period events, respectively, according to the Weibull plotting position formula (Weibull, 1939). The relative differences and the change sign (increasing/positive and decreasing/negative) between historical and future periods were accessed for every downscaled climate model and all river reaches/catchments from the hydrological model. This assessment was made for each hydrological variable individually: extreme precipitation (section 3.1), antecedent soil moisture (Section 3.2), and flood discharge (Section 3.3). Finally, we investigate how the projected changes on these variables are related (Section 3.4).

2.1. The Hydrology of South America

South America occupies only 12% of the Earth's land surface but is responsible for 30% of the water flowing to the oceans (Clark et al., 2015b). It contains the 1st and 5th largest basins in the world, Amazon and La Plata (mainly formed by the Uruguay and Paraná River Basins, Figure 19.a), and the 1st and 4th largest rivers by discharge, Amazon and Orinoco, respectively. As nearly 80% of the continent lies within the tropics, most of the basins are dominated by a hot and humid climate that drives highly frequent convective rainfalls,

especially around the equator. Nevertheless, South America presents some climate diversity such as the semi-arid in Eastern South America (ESA), a large area with less than 1000 mm of rainfall per year (Figure 19.b) which depends on the São Francisco River for water supply; a polar climate in parts over the Andes Cordillera, especially in the higher altitudes; and an extremely dry climate, at the Peruvian and Atacama Deserts, located mostly on northern Chile (Veblen et al., 2007).

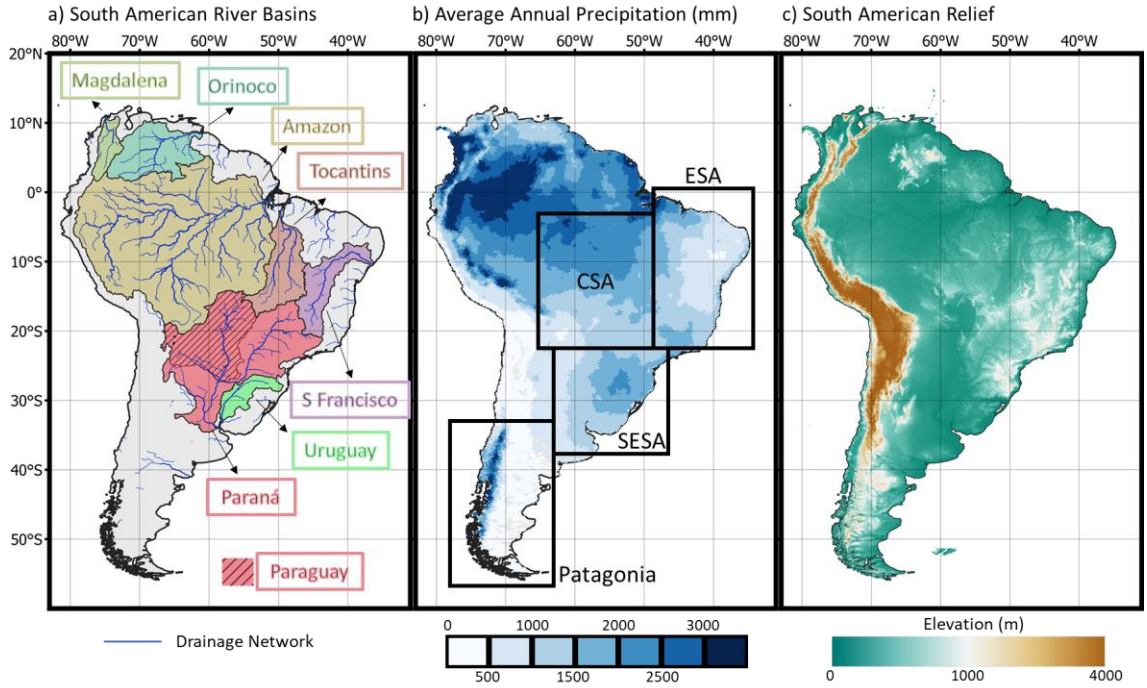

Figure 19. Hydrographic characteristics of South America: a) Largest River basins and the drainage network; b) average annual precipitation regime from the MSWEP database and some regions identification as the Eastern (ESA), Central (CSA) and Southeastern (SESA) South America; c) South American relief highlighting the Andean Cordillera on the west.

The Andes Cordillera is an important topographic barrier on the west part of the continent, which extends between the northern and southern tips (10ºN–55ºS) with altitudes above 4 km in some areas (Garreaud et al., 2009) (Figure 19.c). It has a direct effect on the air circulation, causing considerable high orographic rainfalls especially on the western Amazon and conducting moisture from the Amazon to the Southeastern South America - SESA (Alejandro Martinez and Dominguez, 2014; Espinoza et al., 2020). Concomitantly, the Andes Cordillera blocks the atmospheric moisture flow creating a rain-shadow effect and establishing dry climates over the Peruvian and Atacama Deserts and eastern Patagonia. As Patagonia exhibits a negative rainfall gradient from the Andes towards the east, the discharge regime of most Patagonian rivers is dominated by snowmelt from the headwater streams (Pasquini and Depetris, 2007). However, this article does not discuss results from these regions due to hydrological modeling limitations.

2.2. The MGB-SA Hydrological Model

MGB–SA is a continental-scale, semi-distributed hydrological-hydrodynamic model developed for integrated simulation of large South American basins (Vinicius A. Siqueira et al., 2018). The model is discretized in unit-catchments, each one divided into hydrological response units (HRU) with similar characteristics of soil and vegetation. The water balance is calculated over a single soil layer (i.e., a bucket model) for every unit-catchment and HRU, at a daily time step. Evapotranspiration is based on the Penman-Monteith equation. Surface, subsurface, and groundwater runoffs are sent to linear reservoirs to simulate catchment delay before flowing to the main river. Flow routing in the main channel is computed using a 1D local inertia hydrodynamic model, which also accounts for infiltration from flooded areas into the unsaturated soil column in floodplains. Until now, there is no simulation of snow melting processes in the MGB–SA, which does not compromise the results since runoff generation is governed by rainfall in most regions of South America (see the previous section).

Regarding the model setup, the drainage network is discretized in 15 km long river reaches, which produces over 30,000 unit-catchments for the whole continent with upstream areas > 1000 km². The MGB-SA was calibrated using as input the daily precipitation data from the MSWEP v1 database (Beck et al., 2017) and climatological data from the Climate Research Unity (CRU) Global Climate v.2. (New et al., 2002). The climate variables from CRU database used as input for MGB–SA simulations were temperature, wind speed, air relative humidity, atmospheric pressure, and shortwave radiation, which are used internally to calculate evapotranspiration. The MGB-SA discharge outputs were validated with hundred gauge stations and presented Nash-Sutcliffe efficiency >0.6 for over 55% of the gauges, outperforming global hydrological models. It has also performed satisfactorily for other hydrological variables, such as evapotranspiration and terrestrial water storage, which were compared to remote sensing data and reanalysis products (Vinicius A. Siqueira et al., 2018). Therefore, this model becomes suitable to represent different climate scenarios as addressed in this paper (Krysanova et al., 2018).

2.3. The Eta Regional Climate Model

Eta is an atmospheric model (Mesinger, 1984) with a long history of applications and developments by the Brazilian National Institute for Spatial Research (INPE) for Central and South America. Despite being initially built for numerical weather predictions (Chou et al., 2000), it has been recently adapted for regional climate studies (Marengo et al., 2012). Its name (Eta) relates to the vertical coordinate η, which creates a quasi-horizontal surface and prevents pressure-gradient forces errors that can be significant on steep regions such as the Andes Cordillera (Mesinger et al., 2012).

The Eta model covers the Central and South American continents from latitude 50ºS to 14.4ºN and longitude 84.2ºW to 31.6ºW. It has a horizontal resolution of 20 km and 38 vertical levels. We use the Eta model nested in 4 GCMs: BESM (Nobre et al., 2013b),

CanESM2 (Chylek et al., 2011), HadGEM2-ES (Collins et al., 2011), and MIROC5 (Watanabe et al., 2010). The GCMs provide sea surface temperature estimates, lateral boundary conditions of the state variables and initial conditions of soil moisture and temperature (Chou et al., 2014b).

We evaluated 2 representative concentration pathways (RCP) from CMIP5 (Taylor et al., 2012): RCP4.5 (Thomson et al., 2011) and RCP8.5 (Riahi et al., 2011), which correspond to a reasonable controlled and a high emission scenario, respectively. The scenarios are named after the expected increase in the radiative forcing for the end of the XXI century due to greenhouse gases (GHG) emissions, 4.5 and 8.5 W/m², respectively. The Eta output data from the historical (1961-2005) and future (2021-2065) periods were bias-corrected and used as inputs to the hydrological model.

2.4. Bias Correction

Bias correction is a post-processing step to approximate the simulated data to reality, as models have inherent and systematic errors. However, bias correction methods often introduce inconsistencies, as they modify the spatiotemporal covariance structure of the climate models and ignore the feedbacks among variables (Ehret et al., 2012; Maraun, 2016). The choice of a method for bias correction is one of the greatest sources of uncertainty, especially for extreme precipitation (Iizumi et al., 2017), and in some cases, the impact of bias correction uncertainty is higher than the climate signal itself (Hagemann et al., 2011). Nevertheless, streamflow is extremely sensitive to precipitation and systematic errors on such input variable can drastically impact hydrological simulations (Kavetski et al., 2006; Sperna Weiland et al., 2015). Thus, using a bias correction method becomes strictly necessary in order to reproduce realistic hydrographs (Muerth et al., 2013; Teutschbein and Seibert, 2012).

Several bias correction methods have been described and tested in the literature (Maraun, 2016; Teutschbein and Seibert, 2012). Among those, quantile mapping is one of the most adopted approaches for precipitation bias correction of hydrological impact assessments (Hempel et al., 2013; Pandey et al., 2019; Zheng et al., 2018). The quantile mapping method consists of calculating the probability of a simulated event through the modeled cumulative distribution function (CDF) and then estimate the equivalent (same probability) event using the observed CDF, which can be symbolized by the following equation:

$$P_{sim}^{*} = F_{obs}^{-1}\left(F_{sim}(P_{sim})\right)$$

Where F_{sim} is the CDF of the simulated data from the historical period; F_{obs}^{-1} refers to the inverse CDF of the observed data from the same historical period; P_{sim} is the simulated variable; and P_{sim}^{*} is the bias-corrected variable.

We have used an empirical quantile mapping method with limited linear extrapolation (restriction: $F_{sim}(P) \leq 1$) for removing bias of precipitation. For the remaining climate variables used as input to the hydrological model (e.g. temperature, wind speed), we adopted a linear scaling approach (Teutschbein and Seibert, 2012). We used the MSWEP v2.2 product (Beck et al., 2019) as our reference precipitation and the CRU database as the reference for other atmospheric variables.

2.5. Characteristic Time (Flood Wave Travel Time)

In order to adequately relate flood discharge and its respective drivers (antecedent soil moisture and precipitation), it is necessary to match the time scale of the hydrometeorological events that lead to floods. For example, the duration of a precipitation event must be compatible with the catchment size and its response time. Daily precipitation can be adequate for catchments up to 1,000 or even 10,000 km², but for larger catchments, floods are usually caused by rainfall events of longer duration. Thus, we propose adopting a characteristic time (T_c) to allow comparisons between flood discharge, extreme precipitation, and antecedent soil moisture.

We obtained T_c by calculating the flood wave travel time through the catchment mainstream. The drainage network of the MGB-SA model is discretized in equal reaches of 15 km length (Section 2.2). We estimated the flood wave travel time for every river reach considering the reach's length and the speed of a kinematic wave ($c = dQ/dA \approx \Delta Q/(\Delta V/\Delta x)$, where Q is the discharge, A is the wetted area and V is the stored volume over a river reach of Δx length). The kinematic wave celerity depends on the magnitude of the flood, so we estimated T_c by considering a reference discharge with a 2 year return period using the MGB-SA simulated time series of Q and V. Then, we divided the reaches lengths (≈ 15 km) by the calculated wave celerity (c) to obtain a traveling time per river reach. Finally, to estimate the catchment T_c we propagated the flood wave from upstream to downstream, adding traveling time increments from river reaches and keeping the value from the larger river at confluences.

Figure 20 demonstrates the estimated T_c for the modeled river reaches in South America. For example, the flood wave travel time for the Amazon River is about 56 days, and for the Paraná River, 35 days. Because MGB–SA's drainage network includes water bodies where intermittent rivers — or potentially no river — exist, especially in arid regions, we filtered out river reaches that the mean annual precipitation upstream is below 600 mm yr^{-1}.

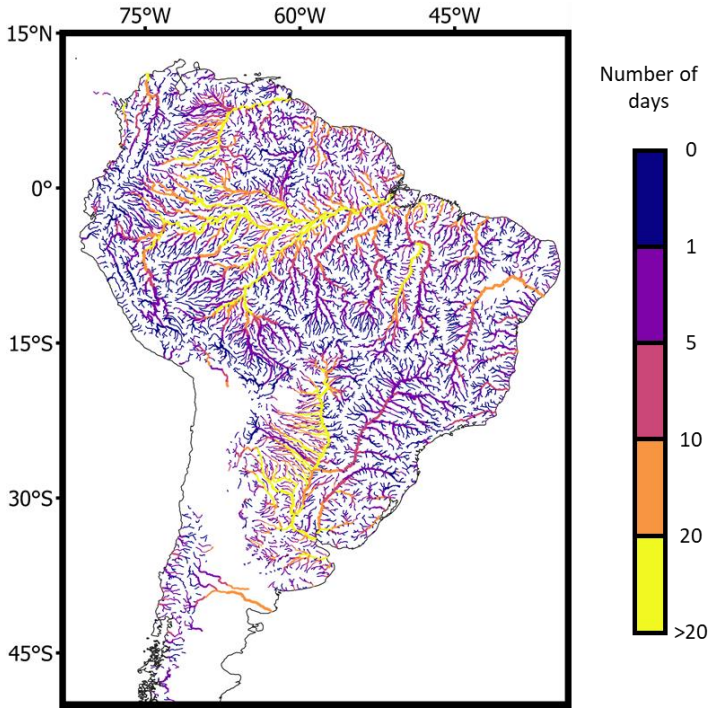

Figure 20. Characteristic Time (T_c) of a catchment given by the traveling period of a flood wave (days).

To ensure spatial and temporal consistency in the assessment, we developed a procedure to calculate both antecedent soil moisture and extreme precipitation at the level of river reaches based on T_c. First, we calculated the average precipitation upstream of a river reach with a duration of T_c days and then computed the maximum value for each year. Further, the values of antecedent soil moisture were estimated by the average upstream soil moisture exactly T_c days before the maximum simulated discharge of a given year. Thus, extreme precipitation and antecedent soil moisture were computed for every river reach and each year within the historical and future periods. This approach enabled us to perform direct comparisons by evaluating changes in signal between extreme discharges, precipitation, and antecedent soil moisture.

3. RESULTS AND DISCUSSION

3.1. Precipitation

The analysis for extreme precipitation is associated with the river discharge and the accumulated rainfall over a catchment (see section 2.5). Figure 21 demonstrates the spatial arrangement of the extreme precipitation change sign through the drainage network. It is important to remark that the colors are related to the change sign of extreme precipitation for the whole river basin upstream to the river reaches. It is presented the relative differences between the future and historical period for the RCP4.5 scenario, more specifically the upper (left column) and lower (center column) limits of the models' ensemble, and the agreement between the 4 downscaled climate models (BESM, CanESM2, HadGEM2-ES, MIROC5) regarding the change sign (right column). This evaluation is made for the 2- and 22-year return period events.

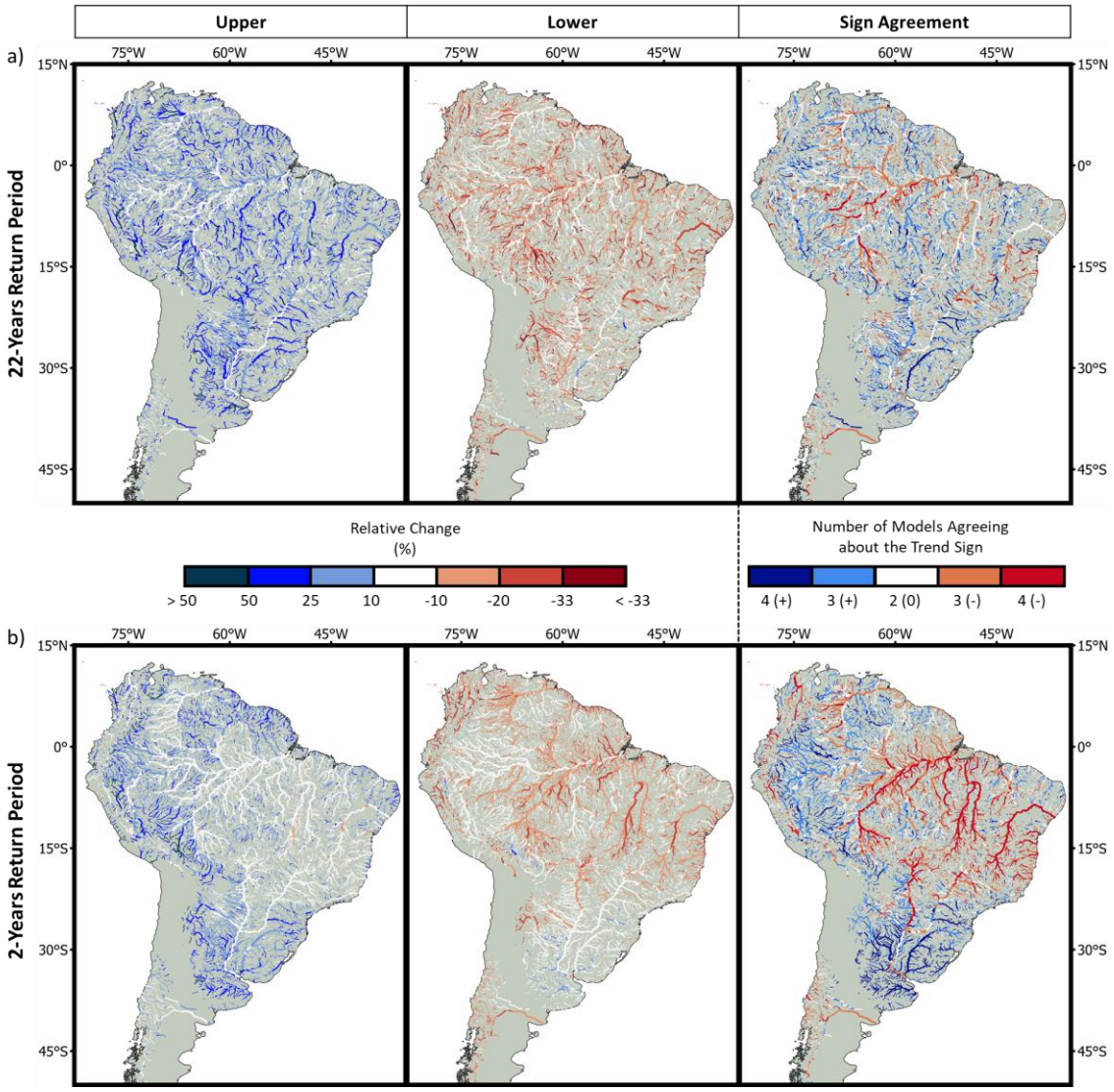

Figure 21. Relative change of extreme precipitation projections for the RCP4.5 scenario (2021-2065) compared to the historical period (1961-2005). Left and center panels show the upper (left) and lower (center) limits related to the ensemble of 4 downscaled climate models (BESM, CanESM2, HadGEM2-ES, MIROC5), respectively, while the right panel indicates the agreement between these models regarding the change sign. Relative differences are shown for the second-highest (a) and median (b) extreme precipitation from the future and historical periods.

Firstly, one can observe a considerable difference in spatial consistency between the 22-year (RP22) and 2-year (RP2) precipitation. The spatial arrangement of RP2 is clearer and more delineated. This can be explained by two main reasons: i) large uncertainty for the RP22 due to a relatively small sample size (44 years); ii) uncertainties related to the bias-correction method since the largest precipitation values are on the upper tail of the CDF curve.

Results from the 4 downscaled climate models indicate future increases of extreme precipitation for the Uruguay Basin, located in southeastern South America. For other rivers such as Tocantins, São Francisco, Magdalena, and Paraguay (right-branch river of the Paraná Basin), the simulations indicate a projected reduction for the RP2, but there is no clear sign for RP22. In other words, very extreme precipitation might increase in those

basins, but the magnitude of recurrent annual extreme precipitation is expected to decrease. In addition, a positive change can also be noted in the western Amazon. The results presented for extreme precipitation of high frequency (RP2) is similar to what was found for long-term mean precipitation in other studies (e.g. Brêda et al., 2020; Ribeiro Neto et al., 2016; Sorribas et al., 2016).

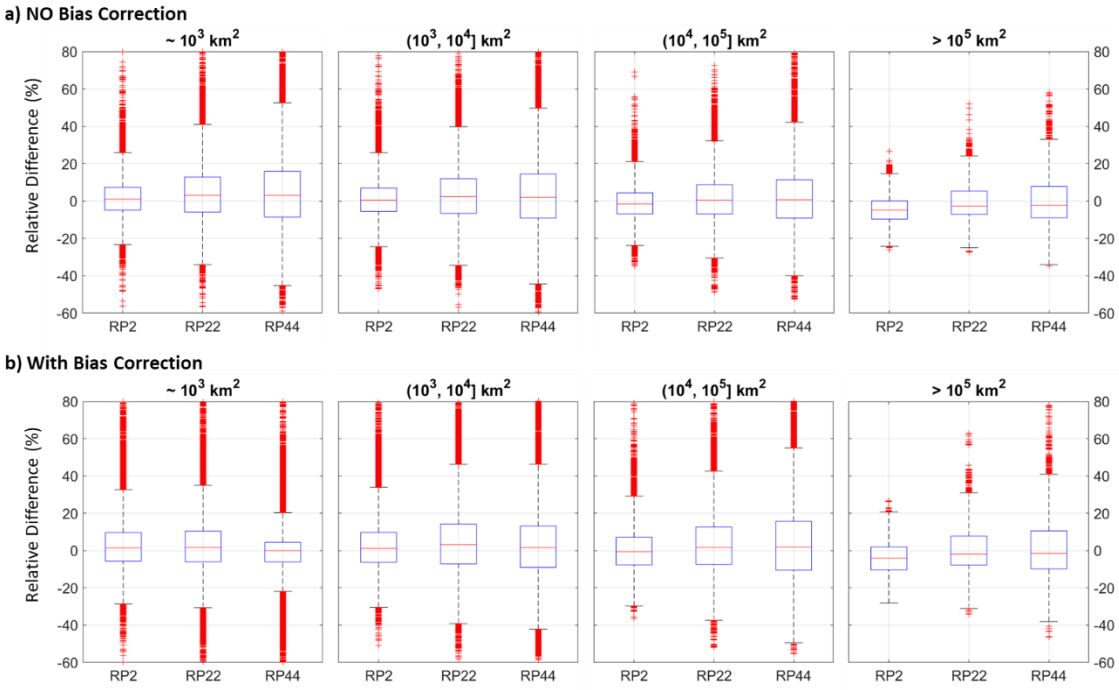

Figure 22. Relative differences of extreme precipitation simulated by Eta between the historical and future periods, on the RCP4.5 scenario. Results are shown for raw (a) and bias-corrected precipitation (b), considering different catchment sizes and return periods (2, 22, and 44 years).

To provide insights on how changes in extreme precipitation are linked to the analyzed spatial scale, Figure 22 shows boxplots of relative differences between the historical and future (RCP4.5 scenario) periods according to the catchment size.

Particularly, extreme precipitation is one of the most problematic variables to be evaluated in climate impact assessments due to extrapolations of the CDF curve (Cannon et al., 2015). Some authors have proposed alternative methods of bias correction focused on precipitation extremes (Maity et al., 2019; Mamalakis et al., 2017), which are slightly more effective but also more complex. We reckon the quantile mapping limitations; however, we have the caution to present results that have not been bias-corrected (Figure 22a) in order to understand the impact of this procedure.

In general, bias correction did not compromise the sign and range of the boxplots, except for the 44-year return period precipitation (RP44) on relatively small basins (≈ 1,000 km²). In this case, the bias correction method has reduced the boxplot interquartile range limiting precipitation differences and hiding the positive sign of RP44. Despite that, we can see that the sample medians are always close to 0%, but for the rarer events (RP22 and RP44) the medians are slightly positive for basins smaller than 100,000 km². For basins

larger than 100,000 km², results indicate a negative change sign, especially for RP2, meaning that rainfall events that generate ordinary floods in large South American rivers are expected to decrease in the XXI century due to climate change.

In conclusion, we can see that extreme precipitation will respond differently to global warming depending on its geographical location, its intensity, and the respective catchment size. RP2 is expected to decrease on central and eastern South America, but there is no clear sign for the rarer precipitations (RP22 and RP44). This means that, in some places, average annual extreme precipitation (RP2) might be reduced, but rarer precipitations might be more intense. This statement can be endorsed by Figure 22, as the sample median of RP22 and RP44 is often greater than the sample median of RP2. In addition, there is a clear difference in the sign of extreme precipitation between medium to large catchments (1,000 to 100,000 km²) and very large catchments (> 100,000 km²). This can be explained by the assumptions made for extreme precipitation, as the duration of such events was given by a characteristic time (i.e. flood wave travel time). For very large catchments, extreme precipitation lasts from days to weeks and is averaged over a considerably large area, representing a completely different process than short and local precipitations. The negative sign on very large catchments agrees with other studies that have concluded that convective rainfall is supposed to become more intense with global warming; however, they will present higher increases for shorter durations (Lenderink and Van Meijgaard, 2008; Wasko and Sharma, 2015) and lower spatial extent (Wasko et al., 2016).

3.2. Soil Moisture

Flood events depend not only on intense rainfalls but also on the initial conditions of the soil. In this article, the antecedent soil moisture refers to the catchment average soil saturation degree prior to an annual maximum discharge (see Section 2.5). Figure 23 shows change signs from four MGB–SA simulations, each one forced with Eta outputs nested in a different GCM (BESM, CanESM2, HadGEM2-ES, MIROC5).

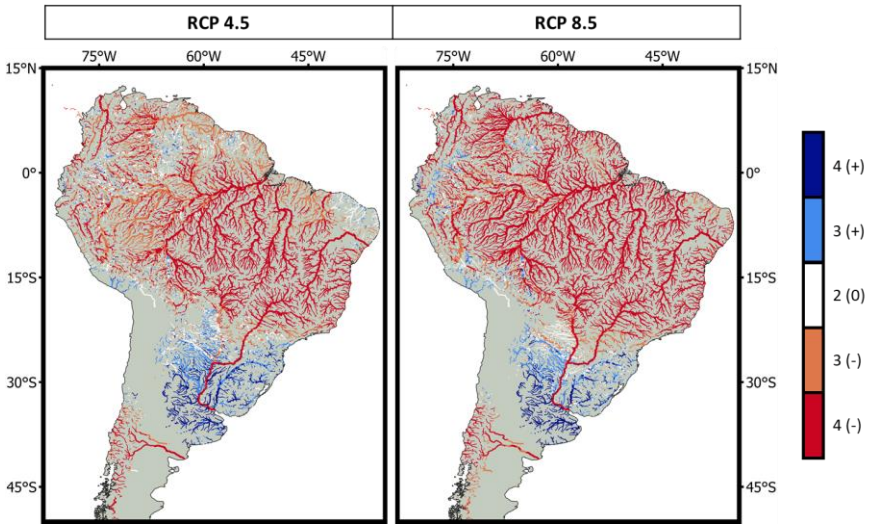

Figure 23. Number of downscaled climate models that agree with a positive/increase (+) or a negative/decrease (-) change sign for antecedent soil moisture simulated by MGB–SA, considering two future scenarios: RCP4.5 and RCP8.5.

In general, projected changes in antecedent soil moisture from both GHG emissions scenarios are similar. Results show a predominant negative sign north of 20°S, a transitional zone around 25°S, and a positive sign on southeastern South America for RCP4.5 and RCP8.5. However, there is a smaller agreement among RCP4.5 simulations (orange) on the Orinoco Basin, western Amazon and Paraguay Basin, while the negative sign from the RCP8.5 simulations is stronger (red). For the Paraná Basin, the negative sign of the northern catchments is predominant over the wetter regions south of 20°S as the main river maintains the red color even near the river mouth.

A more pronounced decrease in antecedent soil moisture for the RCP8.5 is also demonstrated in Figure 24. Overall, the soil saturation degree prior to an extreme discharge event is lower in future scenarios, especially for RCP8.5. In addition, it was observed no difference in the antecedent soil saturation degree for different catchment sizes.

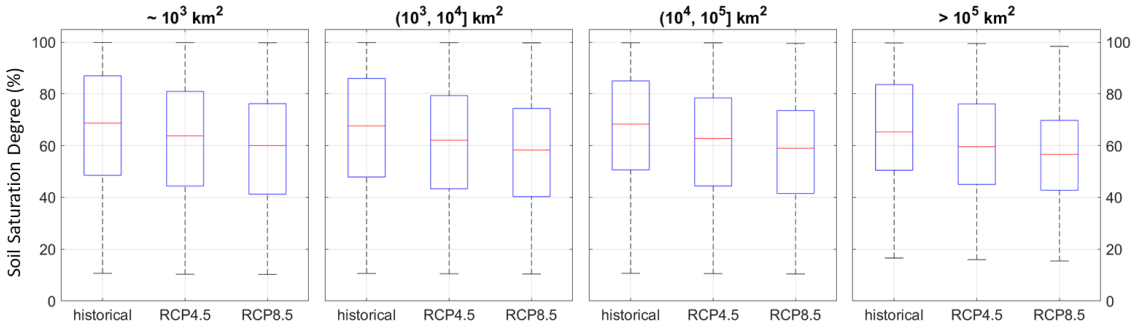

Figure 24. Average soil saturation degree prior to the annual maximum discharge for different scenarios (historical, RCP4.5 and RCP8.5) and catchment sizes.

In theory, a general reduction of soil moisture is expected since higher temperatures intensify evapotranspiration. Our results agree with the literature that points to drier soil in the future due to global warming (Samaniego et al., 2018; Wasko and Nathan, 2019). There is a

positive change sign only in southeastern South America, most likely because this region is expected to become wetter (Brêda et al., 2020; Chou et al., 2014a; Zaninelli et al., 2019), and this precipitation increase will have a stronger impact on the soil moisture compared to the projected evapotranspiration increase.

3.3. Flood Discharge

To assess to what extent climate change will impact floods in South American rivers, we performed projections of annual maximum discharge. Figure 25 shows the relative differences of simulated flood discharges for the historical and future periods. It also shows the upper and lower limits of the MGB–SA simulations ensemble (one simulation for each driven GCM), and how many members (out of 4) agree about the change sign. In regions where more ensemble members agree on the change sign, projections should be more reliable.

The spatial arrangement of flood discharge signs generally follows extreme precipitation results, but projected changes in floods present a clearer delineation and distinction between regions. The maps in Figure 25 show a predominant negative sign in Central and Eastern South America and a positive sign in Southeastern South America and western Amazon. Even for the upper limit of MGB–SA simulations, some rivers, such as the São Francisco and the Tocantins, are projected to face severe reduction (over 20%) for their average annual maximum discharge (RP2). Southern tributaries of the Amazon River are also expected to reduce flood magnitude. The Paraná Basin seems to be a transition zone, presenting a negative sign for the northern tributaries and positive sign for the southern tributaries.

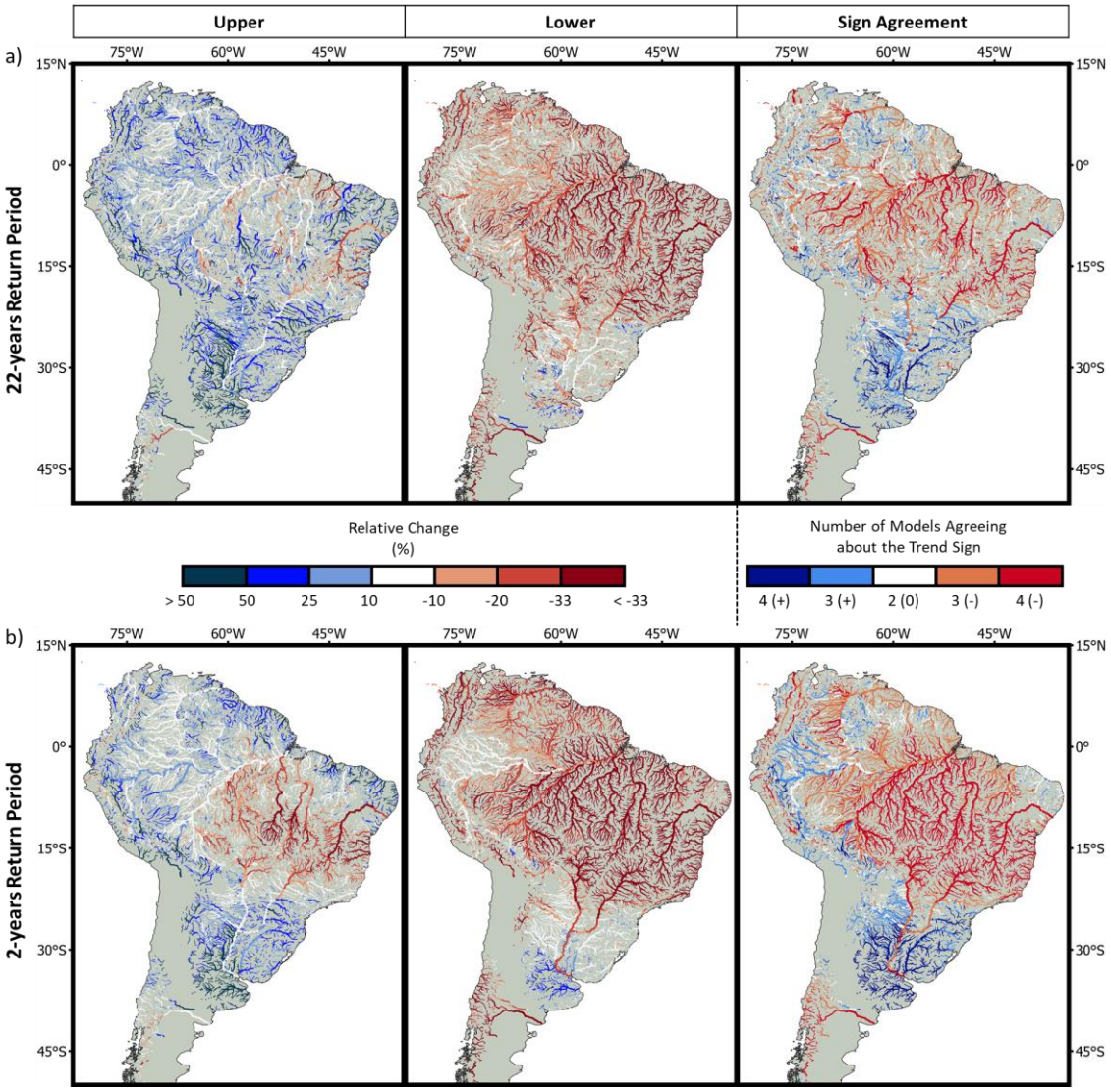

Figure 25. Relative change of flood discharge projections for the RCP4.5 scenario compared to the historical period. The left and center panels show the upper and lower limits related to the ensemble of 4 downscaled climate models, respectively, while the right panel indicates the agreement between these models regarding the change sign. Relative differences are shown for the second-highest (a) and median (b) annual maximum discharges from the future and historical periods.

As for extreme precipitation, a subtle difference between the change signs of RP2 and RP22 can be observed for flood discharges. This can be explained by the randomness of rarer events and the limited sample size (44 years) for estimating the return period. For example, the Paraná and Magdalena rivers present a negative sign for RP2 but no clear sign for RP22. However, studies have provided some evidence that less extreme flood events are expected to decrease, particularly in larger catchments, while rarer floods are likely to become more intense (see Sharma et al., 2018). So, it is possible that some regions indeed present opposing signs for RP2 and RP22.

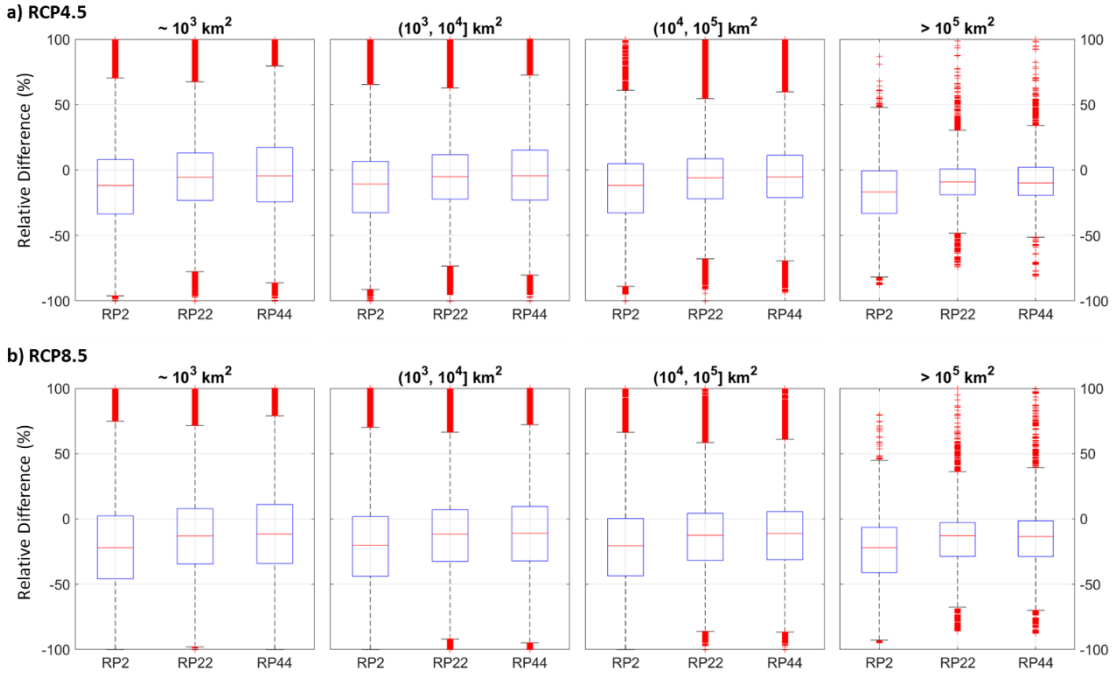

Figure 26. Relative differences between flood discharges simulated for historical and future periods. Results are shown for RCP4.5 (a) and RCP8.5 scenarios, considering different catchment sizes and return periods (2, 22, and 44 years).

Figure 26 summarizes the results for estimated climate impacts on flood discharge. Overall, results suggest a reduction of extreme discharge for most catchments in South America as the boxplot medians are negative. However, climate change apparently has a different impact on ordinary floods (2-year return period) and extraordinary floods (22 year return period). In scenario RCP4.5, 66% of the catchments present a negative sign for RP2, while only 60% and 59% present a negative sign for RP22 and RP44, respectively. These numbers increase to 75%, 69%, and 68% respectively on the scenario RCP8.5. Therefore, at least in 7% of the catchments, it is likely that rarer floods, up to a return period of 44 years, will become more intense while the average annual maximum discharge is expected to decrease.

Also, there were slight differences related to the catchment sizes. Very large catchments are more likely to present extreme discharge reductions than medium to large catchments. This is mostly explained by the climate impact on extreme precipitation (see Section 3.1), as the projected changes for antecedent soil moisture do not depend on the catchment size (Section 3.2). (Do et al., 2017) already have observed decreasing trends in floods with catchment size. The authors have detected a positive trend only for groups of catchments smaller than 400 km2, which were not assessed in this article due to the discretization of the hydrological model (area threshold of 1,000 km2) and the Eta cell size (400 km2).

Thus, our results partially support previous findings. The model outcomes point to a general reduction of extreme discharges in South America. Also, there are a few regions where the average annual maximum discharge is expected to decrease while greater floods

are expected to increase. These outcomes agree with previous studies that claim floods will decrease due to global warming, especially because of reduced soil moisture (Do et al., 2020; Sharma et al., 2018; Wasko and Nathan, 2019; Wasko and Sharma, 2017). On the other hand, it contradicts (Hirabayashi et al., 2021), which projected extreme discharge using GCMs outputs and concluded that floods will increase in magnitude for most South American River Basins. Although (Hirabayashi et al., 2021) have used a larger return period for their evaluation (100 years), it is unlikely that their results would be significantly different for 44-year floods.

3.4. Flood Drivers Analysis

Finally, we aim to connect the outcomes described in the previous sections through a graphical contingency table (Figure 27), considering results from all 4 climate models and all catchments. In Figure 27, the size of the circles represents the number of catchments in a sample and their color indicates the percentage of catchments with a positive/negative sign for RP2 discharge. The y-axis is associated with the change sign of RP2 precipitation (P), while the x-axis refers to the change sign of the median antecedent soil moisture (W) that can be either positive (+), negative (-), or neutral (0), whereas neutral means a relative difference between present and future within 5% and -5%.

For example, given that RP2 precipitation is supposed to increase in the future (P+) and the antecedent soil moisture is supposed to decrease (W-), 60 to 70% of the catchments will present a negative change sign for flood discharge in the RCP4.5 scenario, symbolized by the darkish yellow color on the top left corner. In this example, the size of the circle indicates that nearly 15,000 catchments present P+ and W- signs simultaneously.

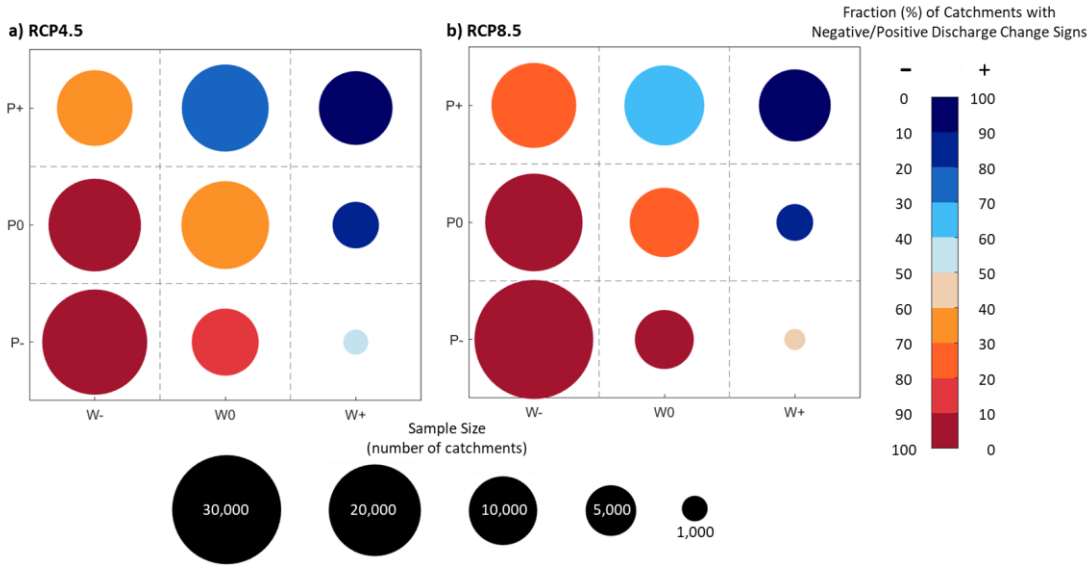

Figure 27. Graphical contingency table relating change signs of RP2 flood discharge, RP2 extreme precipitation (P), and antecedent soil moisture (W) for (a) RCP4.5 and (b) RCP8.5 scenarios. The size of the circle refers to the number of catchments in a sample, and the color is related to the fraction of catchments with a positive/negative change sign.

This contingency table reflects the influence of flood drivers. It can be observed that the largest circles are on the bottom left corner, colored in dark red. This position on the contingency table indicates a negative sign for RP2 precipitation and antecedent soil moisture (P- ∩ W-), and its color means that in most catchments, flood discharge will be reduced in such conditions. On the other hand, the smallest circles are in the bottom right corner (P- ∩ W+) with a light color, light blue for RCP4.5 and light orange for RCP8.5, which indicates a similar number of rivers with positive and negative signs for flood discharge. On the top right corner, RP2 precipitation and antecedent soil moisture present a positive sign (P+ ∩ W+), and consequently, is also expected an increase in flood discharge (dark blue). These results indicate that when P and W present the same sign, it is very likely that flood discharge will follow the same change.

Some considerations can be made on the size of the circles: a) circles colored from dark yellow to red are larger than those in blue, which means that RP2 discharge will decrease in the future for most catchments; b) the number of catchments that present P+, P0 and P- are approximately the same (sum of columns); c) the circles of column W+ are smaller than circles of column W-, thus antecedent soil moisture will be reduced for most catchments. Overall, while there is no clear change sign for extreme precipitation, flood discharge and antecedent soil moisture are expected to decrease. This suggests that the reduced soil moisture is the main responsible for negative change signs of RP2 discharge.

On the top line (P+) the circles have similar sizes, which means that when RP2 precipitation is expected to increase, there is no indication of what will happen to antecedent soil moisture. However, when RP2 precipitation is expected to decrease (P-), it is expected a reduction in antecedent soil moisture (W-) for most of the catchments, or a neutral sign (W0) at least. This reinforces the projections of drier soils, as W can equally present a negative sign even if extreme precipitation is expected to increase. In other words, the negative effects of higher temperatures and consequently greater evaporation might surpass the positive effect of increased precipitation on the soil moisture in nearly half of the cases: number of P+ ∩ W+ ≈ number of P+ ∩ W-.

In addition, there are small differences between the climate scenarios, mainly related to antecedent soil moisture. For example, circles in column W- for the RCP4.5 scenario are smaller than those in W- for the RCP8.5 scenario. This can be explained by the higher temperatures expected for RCP8.5, which will intensify evaporation and consequently reduce the soil moisture more than the RCP4.5 scenario.

Finally, we can see that for a P+ ∩ W- condition, 60 to 70% (70 to 80%) of the catchments will present a negative sign for flood discharge, and for a P- ∩ W+ condition, 50 to 60% (40 to 50%) of the catchments will present a positive sign on scenario RCP4.5 (RCP8.5). These results imply that the sign of antecedent soil moisture is predominant over the sign of RP2 precipitation in most cases. We can take the same conclusions when analyzing neutral signs (P0 and W0). Our findings agree with other studies that show that

antecedent soil moisture is the main driver of recurrent annual floods (Ivancic and Shaw, 2015; Sharma et al., 2018; Wasko et al., 2020), at least for river basins of 1000 km2 or larger. However, we cannot extend our conclusions to rarer floods as a more detailed analysis would be necessary.

4. CONCLUSIONS

Global warming is expected to intensify the hydrological cycle at a global scale. Projected intensification of extreme rainfall generally led to the suggestion that floods would also increase. However, more recent analyses showed that projected changes in floods are less straightforward than initially thought. The climate alterations present different impacts on floods for different regions of the world and depend on processes like antecedent soil moisture and the size of the river basins. In this paper, we assessed climate change impacts in antecedent soil moisture, extreme precipitation, and flood discharge in South America and evaluated how these projections are related. We used outputs from a regional climate model (Eta) nested in four global models and a continental-scale hydrologic-hydrodynamic model for the analysis.

There is a clear indication of reduced soil moisture for most of South America due to global warming, as suggested in the literature (Sharma et al., 2018; Wasko et al., 2020). For the RCP8.5 scenario, the reductions of soil moisture are even more pronounced due to higher increases in temperature. We observed a positive change sign in soil moisture only in Southeastern South America (SESA), as this region is expected to become significantly more humid (Brêda et al., 2020; Zaninelli et al., 2019).

In general, the average annual maximum precipitation is expected to increase in western Amazon and SESA and decrease mainly in Central South America (CSA), especially in the São Francisco and Tocantins Basins. For rarer precipitation events (over 20 years of return period), a clear spatial pattern in the change sign was not detected, probably because of the greater randomness of rarer events and the small sample size (45 years) for frequency analysis. Nevertheless, catchments over 100,000 km² were shown to be more susceptible to negative signs for extreme precipitation, suggesting that extreme rainfall events that lead to floods in large rivers are expected to decrease in South America.

The spatial arrangement of the change signs of flood discharge is similar to extreme precipitation. There is also a positive sign in SESA and western Amazon and a negative sign in CSA and Eastern South America, which outlines the influence of extreme precipitation in floods. However, the number of catchments exhibiting a negative sign for flood discharge was larger than that for extreme precipitation. While the fraction of catchments showing positive/negative signs was 50%/50% for extreme precipitation, this relation moved to 30%/70% for flood discharge. This can be attributed to the projected reduction of soil moisture in most of South America. When the average annual maximum precipitation and

antecedent soil moisture present different change signs, it is more likely that the average annual maximum discharge follows the same sign as soil moisture (over 60% of the time).

In addition, there were slight differences related to the frequency of flood events. Although for most of the catchments in South America, the maximum (RP44) and median (RP2) simulated floods presented a reduced magnitude in the future period, at least in 10% of the cases, there is a positive sign for the maximum flood despite a negative sign for the median annual flood. However, because (i) there was a limited sample size for the distribution function (45 years) and (ii) we used a bias removal method that affects the precipitation maxima, we cannot be sure if these change signs would remain negative for even rarer floods (e.g. 100 or 1,000 years return period).

5. REFERENCES

Alejandro Martinez, J., Dominguez, F., 2014. Sources of atmospheric moisture for the La Plata River Basin. J. Clim. 27, 6737–6753. https://doi.org/10.1175/JCLI-D-14-00022.1

Alfieri, L., Bisselink, B., Dottori, F., Naumann, G., de Roo, A., Salamon, P., Wyser, K., Feyen, L., 2017. Global projections of river flood risk in a warmer world. Earth's Futur. 5, 171–182. https://doi.org/10.1002/2016EF000485

Asadi Zarch, M.A., Sivakumar, B., Malekinezhad, H., Sharma, A., 2017. Future aridity under conditions of global climate change. J. Hydrol. 554, 451–469. https://doi.org/10.1016/j.jhydrol.2017.08.043

Avila-Diaz, A., Abrahão, G., Justino, F., Torres, R., Wilson, A., 2020. Extreme climate indices in Brazil: evaluation of downscaled earth system models at high horizontal resolution. Clim. Dyn. 54, 5065–5088. https://doi.org/10.1007/s00382-020-05272-9

Bates, P.D., Horritt, M.S., Fewtrell, T.J., 2010. A simple inertial formulation of the shallow water equations for efficient two-dimensional flood inundation modelling. J. Hydrol. 387, 33–45. https://doi.org/10.1016/j.jhydrol.2010.03.027

Beck, H.E., Van Dijk, A.I.J.M., Levizzani, V., Schellekens, J., Miralles, D.G., Martens, B., De Roo, A., 2017. MSWEP: 3-hourly 0.25° global gridded precipitation (1979-2015) by merging gauge, satellite, and reanalysis data. Hydrol. Earth Syst. Sci. 21, 589–615. https://doi.org/10.5194/hess-21-589-2017

Beck, H.E., Wood, E.F., Pan, M., Fisher, C.K., Miralles, D.G., Van Dijk, A.I.J.M., McVicar, T.R., Adler, R.F., 2019. MSWep v2 Global 3-hourly 0.1° precipitation: Methodology and quantitative assessment. Bull. Am. Meteorol. Soc. 100, 473–500. https://doi.org/10.1175/BAMS-D-17-0138.1

Berghuijs, W.R., Aalbers, E.E., Larsen, J.R., Trancoso, R., Woods, R.A., 2017. Recent changes in extreme floods across multiple continents. Environ. Res. Lett. 12. https://doi.org/10.1088/1748-9326/aa8847

Blöschl, G., Gaál, L., Hall, J., Kiss, A., Komma, J., Nester, T., Parajka, J., Perdigão, R.A.P., Plavcová, L., Rogger, M., Salinas, J.L., Viglione, A., 2015. Increasing river floods: fiction or reality? WIREs Water 2, 329–344. https://doi.org/10.1002/wat2.1079

Blöschl, G., Hall, J., Viglione, A., Perdigão, R.A.P., Parajka, J., Merz, B., Lun, D., Arheimer, B., Aronica,

G.T., Bilibashi, A., Boháč, M., Bonacci, O., Borga, M., Čanjevac, I., Castellarin, A., Chirico, G.B., Claps, P., Frolova, N., Ganora, D., Gorbachova, L., Gül, A., Hannaford, J., Harrigan, S., Kireeva, M., Kiss, A., Kjeldsen, T.R., Kohnová, S., Koskela, J.J., Ledvinka, O., Macdonald, N., Mavrova-Guirguinova, M., Mediero, L., Merz, R., Molnar, P., Montanari, A., Murphy, C., Osuch, M., Ovcharuk, V., Radevski, I., Salinas, J.L., Sauquet, E., Šraj, M., Szolgay, J., Volpi, E., Wilson, D., Zaimi, K., Živković, N., 2019. Changing climate both increases and decreases European river floods. Nature 573, 108–111. https://doi.org/10.1038/s41586-019-1495-6

Borges de Amorim, P., Chaffe, P.B., 2019. Towards a comprehensive characterization of evidence in synthesis assessments: the climate change impacts on the Brazilian water resources. Clim. Change 155, 37–57. https://doi.org/10.1007/s10584-019-02430-9

Brêda, J.P.L.F., de Paiva, R.C.D., Collischon, W., Bravo, J.M., Siqueira, V.A., Steinke, E.B., 2020. Climate change impacts on South American water balance from a continental-scale hydrological model driven by CMIP5 projections. Clim. Change 159, 503–522. https://doi.org/10.1007/s10584-020-02667-9

Byrne, M.P., O'Gorman, P.A., 2018. Trends in continental temperature and humidity directly linked to ocean warming. Proc. Natl. Acad. Sci. U. S. A. 115, 4863–4868. https://doi.org/10.1073/pnas.1722312115

Byrne, M.P., O'Gorman, P.A., 2016. Understanding decreases in land relative humidity with global warming: Conceptual model and GCM simulations. J. Clim. 29, 9045–9061. https://doi.org/10.1175/JCLI-D-16-0351.1

Cannon, A.J., Sobie, S.R., Murdock, T.Q., 2015. Bias correction of GCM precipitation by quantile mapping: How well do methods preserve changes in quantiles and extremes? J. Clim. 28, 6938–6959. https://doi.org/10.1175/JCLI-D-14-00754.1

Chou, S.C., Lyra, A., Mourão, C., Dereczynski, C., Pilotto, I., Gomes, J., Bustamante, J., Tavares, P., Silva, A., Rodrigues, D., Campos, D., Chagas, D., Sueiro, G., Siqueira, G., Marengo, J., 2014a. Assessment of Climate Change over South America under RCP 4.5 and 8.5 Downscaling Scenarios. Am. J. Clim. Chang. 03, 512–527. https://doi.org/10.4236/ajcc.2014.35043

Chou, S.C., Lyra, A., Mourão, C., Dereczynski, C., Pilotto, I., Gomes, J., Bustamante, J., Tavares, P., Silva, A., Rodrigues, D., Campos, D., Chagas, D., Sueiro, G., Siqueira, G., Nobre, P., Marengo, J., 2014b. Evaluation of the Eta Simulations Nested in Three Global Climate Models. Am. J. Clim. Chang. 03, 438–454. https://doi.org/10.4236/ajcc.2014.35039

Chou, S.C., Nunes, A.M.B., Cavalcanti, I.F.A., 2000. Extended range forecasts over South America using the regional eta model. J. Geophys. Res. Atmos. 105, 10147–10160. https://doi.org/10.1029/1999JD901137

Chylek, P., Li, J., Dubey, M.K., Wang, M., Lesins, G., 2011. Observed and model simulated 20th century Arctic temperature variability: Canadian Earth System Model CanESM2. Atmos. Chem. Phys. Discuss. 11, 22893–22907. https://doi.org/10.5194/acpd-11-22893-2011

Clark, E.A., Sheffield, J., van Vliet, M.T.H., Nijssen, B., Lettenmaier, D.P., 2015. Continental runoff into the oceans (1950-2008). J. Hydrometeorol. 16, 1502–1520. https://doi.org/10.1175/JHM-D-14-0183.1

Collins, W.J., Bellouin, N., Gedney, N., Halloran, P., Hinton, T., Hughes, J., Jones, C.D., 2011. Model Development Development and evaluation of an Earth-System model – HadGEM2 1051–1075. https://doi.org/10.5194/gmd-4-1051-2011

Cook, B.I., Smerdon, J.E., Seager, R., Coats, S., 2014. Global warming and 21st century drying. Clim.

Dyn. 43, 2607–2627. https://doi.org/10.1007/s00382-014-2075-y

Cunha, A.P.M.A., Zeri, M., Leal, K.D., Costa, L., Cuartas, L.A., Marengo, J.A., Tomasella, J., Vieira, R.M., Barbosa, A.A., Cunningham, C., Cal Garcia, J.V., Broedel, E., Alvalá, R., Ribeiro-Neto, G., 2019. Extreme drought events over Brazil from 2011 to 2019. Atmosphere (Basel). 10. https://doi.org/10.3390/atmos10110642

Dai, A., 2013. Increasing drought under global warming in observations and models. Nat. Clim. Chang. 3, 52–58. https://doi.org/10.1038/nclimate1633

de Abreu, R.C., Cunningham, C., Rudorff, C.M., Rudorff, N., Abatan, A.A., Tett, S.F.B., Dong, B., Lott, F.C., Sparrow, S.N., 2019. Contribution of Anthropogenic Climate Change to April–May 2017 Heavy Precipitation over the Uruguay River Basin. Bull. Am. Meteorol. Soc. 100, S37–S41. https://doi.org/10.1175/BAMS-D-18-0102.1

Debortoli, N.S., Camarinha, P.I.M., Marengo, J.A., Rodrigues, R.R., 2017. An index of Brazil's vulnerability to expected increases in natural flash flooding and landslide disasters in the context of climate change. Nat. Hazards 86, 557–582. https://doi.org/10.1007/s11069-016-2705-2

Dereczynski, C., Chan Chou, S., Lyra, A., Sondermann, M., Regoto, P., Tavares, P., Chagas, D., Gomes, J.L., Rodrigues, D.C., Skansi, M. de los M., 2020. Downscaling of climate extremes over South America – Part I: Model evaluation in the reference climate. Weather Clim. Extrem. 29. https://doi.org/10.1016/j.wace.2020.100273

Do, H.X., Mei, Y., Gronewold, A.D., 2020. To What Extent Are Changes in Flood Magnitude Related to Changes in Precipitation Extremes? Geophys. Res. Lett. 47, 1–10. https://doi.org/10.1029/2020GL088684

Do, H.X., Westra, S., Leonard, M., 2017. A global-scale investigation of trends in annual maximum streamflow. J. Hydrol. 552, 28–43. https://doi.org/10.1016/j.jhydrol.2017.06.015

Donat, M.G., Lowry, A.L., Alexander, L. V., O'Gorman, P.A., Maher, N., 2016. More extreme precipitation in the world's dry and wet regions. Nat. Clim. Chang. 6, 508–513. https://doi.org/10.1038/nclimate2941

Ehret, U., Zehe, E., Wulfmeyer, V., Warrach-Sagi, K., Liebert, J., 2012. HESS Opinions "should we apply bias correction to global and regional climate model data?" Hydrol. Earth Syst. Sci. 16, 3391–3404. https://doi.org/10.5194/hess-16-3391-2012

Espinoza, J.C., Garreaud, R., Poveda, G., Arias, P.A., Molina-Carpio, J., Masiokas, M., Viale, M., Scaff, L., 2020. Hydroclimate of the Andes Part I: Main Climatic Features. Front. Earth Sci. 8, 1–20. https://doi.org/10.3389/feart.2020.00064

Feng, H., Zhang, M., 2015. Global land moisture trends: Drier in dry and wetter in wet over land. Sci. Rep. 5, 1–6. https://doi.org/10.1038/srep18018

Fischer, E.M., Knutti, R., 2016. Observed heavy precipitation increase confirms theory and early models. Nat. Clim. Chang. 6, 986–991. https://doi.org/10.1038/nclimate3110

Fowler, H.J., Wasko, C., Prein, A.F., 2021. Intensification of short-duration rainfall extremes and implications for flood risk: Current state of the art and future directions. Philos. Trans. R. Soc. A Math. Phys. Eng. Sci. 379. https://doi.org/10.1098/rsta.2019.0541

Gudmundsson, L., Boulange, J., Do, H.X., Gosling, S.N., Grillakis, M.G., Koutroulis, A.G., Leonard, M., Liu, J., Schmied, H.M., Papadimitriou, L., Pokhrel, Y., Seneviratne, S.I., Satoh, Y., Thiery, W., Westra, S., Zhang, X., Zhao, F., 2021. Globally observed trends in mean and extreme river flow

attributed to climate change. Science (80-.). 371, 1159–1162. https://doi.org/10.1126/science.aba3996

Hagemann, S., Chen, C., Haerter, J.O., Heinke, J., Gerten, D., Piani, C., 2011. Impact of a statistical bias correction on the projected hydrological changes obtained from three GCMs and two hydrology models. J. Hydrometeorol. 12, 556–578. https://doi.org/10.1175/2011JHM1336.1

Hempel, S., Frieler, K., Warszawski, L., Schewe, J., Piontek, F., 2013. A trend-preserving bias correction – The ISI-MIP approach. Earth Syst. Dyn. 4, 219–236. https://doi.org/10.5194/esd-4-219-2013

Hirabayashi, Y., Tanoue, M., Sasaki, O., Zhou, X., Yamazaki, D., 2021. Global exposure to flooding from the new CMIP6 climate model projections. Sci. Rep. 11, 1–7. https://doi.org/10.1038/s41598-021-83279-w

Iizumi, T., Takikawa, H., Hirabayashi, Y., Hanasaki, N., Nishimori, M., 2017. Contributions of different bias-correction methods and reference meteorological forcing data sets to uncertainty in projected temperature and precipitation extremes. J. Geophys. Res. 122, 7800–7819. https://doi.org/10.1002/2017JD026613

Ivancic, T.J., Shaw, S.B., 2015. Examining why trends in very heavy precipitation should not be mistaken for trends in very high river discharge. Clim. Change 133, 681–693. https://doi.org/10.1007/s10584-015-1476-1

Kavetski, D., Kuczera, G., Franks, S.W., 2006. Bayesian analysis of input uncertainty in hydrological modeling: 2. Application. Water Resour. Res. 42, 1–10. https://doi.org/10.1029/2005WR004376

Kundzewicz, Z.W., Kanae, S., Seneviratne, S.I., Handmer, J., Nicholls, N., Peduzzi, P., Mechler, R., Bouwer, L.M., Arnell, N., Mach, K., Muir-Wood, R., Brakenridge, G.R., Kron, W., Benito, G., Honda, Y., Takahashi, K., Sherstyukov, B., 2014. Flood risk and climate change: global and regional perspectives. Hydrol. Sci. J. 59, 1–28. https://doi.org/10.1080/02626667.2013.857411

Lehner, B., Liermann, C.R., Revenga, C., Vörösmarty, C., Fekete, B., Crouzet, P., Döll, P., Endejan, M., Frenken, K., Magome, J., Nilsson, C., Robertson, J.C., Rödel, R., Sindorf, N., Wisser, D., 2011. High-resolution mapping of the world's reservoirs and dams for sustainable river-flow management. Front. Ecol. Environ. 9, 494–502. https://doi.org/10.1890/100125

Lenderink, G., Fowler, H.J., 2017. Hydroclimate: Understanding rainfall extremes. Nat. Clim. Chang. 7, 391–393. https://doi.org/10.1038/nclimate3305

Lenderink, G., Van Meijgaard, E., 2008. Increase in hourly precipitation extremes beyond expectations from temperature changes. Nat. Geosci. 1, 511–514. https://doi.org/10.1038/ngeo262

Liu, Z., Herman, J.D., Huang, G., Kadir, T., Dahlke, H.E., 2021. Identifying climate change impacts on surface water supply in the southern Central Valley, California. Sci. Total Environ. 759, 143429. https://doi.org/10.1016/j.scitotenv.2020.143429

Maity, R., Suman, M., Laux, P., Kunstmann, H., 2019. Bias correction of zero-inflated RCM precipitation fields: A copula-based scheme for both mean and extreme conditions. J. Hydrometeorol. 20, 595–611. https://doi.org/10.1175/JHM-D-18-0126.1

Mamalakis, A., Langousis, A., Deidda, R., Marrocu, M., 2017. A parametric approach for simultaneous bias correction and high-resolution downscaling of climate model rainfall. Water Resour. Res. 53, 2149–2170. https://doi.org/10.1002/2016WR019578

Maraun, D., 2016. Bias Correcting Climate Change Simulations - a Critical Review. Curr. Clim. Chang.

Reports 2, 211–220. https://doi.org/10.1007/s40641-016-0050-x

Marengo, J.A., Chou, S.C., Kay, G., Alves, L.M., Pesquero, J.F., Soares, W.R., Santos, D.C., Lyra, A.A., Sueiro, G., Betts, R., Chagas, D.J., Gomes, J.L., Bustamante, J.F., Tavares, P., 2012. Development of regional future climate change scenarios in South America using the Eta CPTEC/HadCM3 climate change projections: Climatology and regional analyses for the Amazon, São Francisco and the Paraná River basins. Clim. Dyn. 38, 1829–1848. https://doi.org/10.1007/s00382-011-1155-5

Mesinger, F., 1984. A blocking technique for representation of mountains in atmospheric models. Riv. Meteor. Aeronaut. 44, 195–202.

Mesinger, F., Chou, S.C., Gomes, J.L., Jovic, D., Bastos, P., Bustamante, J.F., Lazic, L., Lyra, A.A., Morelli, S., Ristic, I., Veljovic, K., 2012. An upgraded version of the Eta model. Meteorol. Atmos. Phys. 116, 63–79. https://doi.org/10.1007/s00703-012-0182-z

Meza, I., Siebert, S., Döll, P., Kusche, J., Herbert, C., Rezaei, E.E., Nouri, H., Gerdener, H., Popat, E., Frischen, J., Naumann, G., Vogt, J. V., Walz, Y., Sebesvari, Z., Hagenlocher, M., 2020. Global-scale drought risk assessment for agricultural systems. Nat. Hazards Earth Syst. Sci. 20, 695–712. https://doi.org/10.5194/nhess-20-695-2020

Milly, P.C.D., Wetherald, R.T., Dunne, K.A., Delworth, T.L., 2002. Increasing risk of great floods in a changing climate. Nature 415, 514–517. https://doi.org/10.1038/415514a

Monte, B.E.O., Goldenfum, J.A., Michel, G.P., Cavalcanti, J.R. de A., 2021. Terminology of natural hazards and disasters: A review and the case of Brazil. Int. J. Disaster Risk Reduct. 52. https://doi.org/10.1016/j.ijdrr.2020.101970

Muerth, M.J., Gauvin St-Denis, B., Ricard, S., Velázquez, J.A., Schmid, J., Minville, M., Caya, D., Chaumont, D., Ludwig, R., Turcotte, R., 2013. On the need for bias correction in regional climate scenarios to assess climate change impacts on river runoff. Hydrol. Earth Syst. Sci. 17, 1189–1204. https://doi.org/10.5194/hess-17-1189-2013

Myhre, G., Alterskjær, K., Stjern, C.W., Hodnebrog, Marelle, L., Samset, B.H., Sillmann, J., Schaller, N., Fischer, E., Schulz, M., Stohl, A., 2019. Frequency of extreme precipitation increases extensively with event rareness under global warming. Sci. Rep. 9, 1–10. https://doi.org/10.1038/s41598-019-52277-4

Netto, A.L.C., Sato, A.M., de Souza Avelar, A., Vianna, L.G.G., Araújo, I.S., Ferreira, D.L.C., Lima, P.H., Silva, A.P.A., Silva, R.P., 2013. January 2011: The Extreme Landslide Disaster in Brazil BT - Landslide Science and Practice: Volume 6: Risk Assessment, Management and Mitigation, in: Margottini, C., Canuti, P., Sassa, K. (Eds.), . Springer Berlin Heidelberg, Berlin, Heidelberg, pp. 377–384. https://doi.org/10.1007/978-3-642-31319-6_51

New, M., Lister, D., Hulme, M., Makin, I., 2002. A high-resolution data set of surface climate over global land areas. Clim. Res. 21, 1–25. https://doi.org/10.3354/cr021001

Nobre, C.A., Marengo, J.A., Seluchi, M.E., Cuartas, L.A., Alves, L.M., 2016. Some Characteristics and Impacts of the Drought and Water Crisis in Southeastern Brazil during 2014 and 2015. J. Water Resour. Prot. 08, 252–262. https://doi.org/10.4236/jwarp.2016.82022

Nobre, P., Siqueira, L.S.P., De Almeida, R.A.F., Malagutti, M., Giarolla, E., Castelã O, G.P., Bottino, M.J., Kubota, P., Figueroa, S.N., Costa, M.C., Baptista, M., Irber, L., Marcondes, G.G., 2013. Climate simulation and change in the brazilian climate model. J. Clim. 26, 6716–6732. https://doi.org/10.1175/JCLI-D-12-00580.1

O'Gorman, P.A., 2015. Precipitation Extremes Under Climate Change. Curr. Clim. Chang. Reports 1,

49–59. https://doi.org/10.1007/s40641-015-0009-3

Pandey, B.K., Khare, D., Kawasaki, A., Mishra, P.K., 2019. Climate Change Impact Assessment on Blue and Green Water by Coupling of Representative CMIP5 Climate Models with Physical Based Hydrological Model. Water Resour. Manag. 33, 141–158. https://doi.org/10.1007/s11269-018-2093-3

Papalexiou, S.M., Montanari, A., 2019. Global and Regional Increase of Precipitation Extremes Under Global Warming. Water Resour. Res. 55, 4901–4914. https://doi.org/10.1029/2018WR024067

Pasquini, A.I., Depetris, P.J., 2007. Discharge trends and flow dynamics of South American rivers draining the southern Atlantic seaboard: An overview. J. Hydrol. 333, 385–399. https://doi.org/10.1016/j.jhydrol.2006.09.005

Pontes, P.R.M., Fan, F.M., Fleischmann, A.S., de Paiva, R.C.D., Buarque, D.C., Siqueira, V.A., Jardim, P.F., Sorribas, M.V., Collischonn, W., 2017. MGB-IPH model for hydrological and hydraulic simulation of large floodplain river systems coupled with open source GIS. Environ. Model. Softw. 94, 1–20. https://doi.org/10.1016/j.envsoft.2017.03.029

Prein, A.F., Rasmussen, R.M., Ikeda, K., Liu, C., Clark, M.P., Holland, G.J., 2017. The future intensification of hourly precipitation extremes. Nat. Clim. Chang. 7, 48–52. https://doi.org/10.1038/nclimate3168

Riahi, K., Rao, S., Krey, V., Cho, C., Chirkov, V., Fischer, G., Kindermann, G., Nakicenovic, N., Rafaj, P., 2011. RCP 8.5-A scenario of comparatively high greenhouse gas emissions. Clim. Change 109, 33–57. https://doi.org/10.1007/s10584-011-0149-y

Ribeiro Neto, A., da Paz, A.R., Marengo, J.A., Chou, S.C., 2016. Hydrological Processes and Climate Change in Hydrographic Regions of Brazil. J. Water Resour. Prot. 08, 1103–1127. https://doi.org/10.4236/jwarp.2016.812087

Risser, M.D., Wehner, M.F., 2017. Attributable Human-Induced Changes in the Likelihood and Magnitude of the Observed Extreme Precipitation during Hurricane Harvey. Geophys. Res. Lett. 44, 12,457-12,464. https://doi.org/10.1002/2017GL075888

Samaniego, L., Thober, S., Kumar, R., Wanders, N., Rakovec, O., Pan, M., Zink, M., Sheffield, J., Wood, E.F., Marx, A., 2018. Anthropogenic warming exacerbates European soil moisture droughts. Nat. Clim. Chang. 8, 421–426. https://doi.org/10.1038/s41558-018-0138-5

Sharma, A., Wasko, C., Lettenmaier, D.P., 2018. If Precipitation Extremes Are Increasing, Why Aren't Floods? Water Resour. Res. 54, 8545–8551. https://doi.org/10.1029/2018WR023749

Siqueira, V.A., Paiva, R.C.D., Fleischmann, A.S., Fan, F.M., Ruhoff, A.L., Pontes, P.R.M., Paris, A., Calmant, S., Collischonn, W., 2018. Toward continental hydrologic-hydrodynamic modeling in South America. Hydrol. Earth Syst. Sci. 22, 4815–4842. https://doi.org/10.5194/hess-22-4815-2018

Slater, L., Villarini, G., Archfield, S., Faulkner, D., Lamb, R., Khouakhi, A., Yin, J., 2021. Global Changes in 20-Year, 50-Year, and 100-Year River Floods. Geophys. Res. Lett. 48, 1–10. https://doi.org/10.1029/2020GL091824

Sorribas, M.V., Paiva, R.C.D., Melack, J.M., Bravo, J.M., Jones, C., Carvalho, L., Beighley, E., Forsberg, B., Costa, M.H., 2016. Projections of climate change effects on discharge and inundation in the Amazon basin. Clim. Change 136, 555–570. https://doi.org/10.1007/s10584-016-1640-2

Sperna Weiland, F.C., Vrugt, J.A., van Beek, R.L.P.H., Weerts, A.H., Bierkens, M.F.P., 2015. Significant uncertainty in global scale hydrological modeling from precipitation data errors. J. Hydrol. 529,

1095–1115. https://doi.org/10.1016/j.jhydrol.2015.08.061

Sun, Q., Zhang, X., Zwiers, F., Westra, S., Alexander, L. V., 2021. A global, continental, and regional analysis of changes in extreme precipitation. J. Clim. 34, 243–258. https://doi.org/10.1175/JCLI-D-19-0892.1

Taylor, K.E., Stouffer, R.J., Meehl, G.A., 2012. An overview of CMIP5 and the experiment design. Bull. Am. Meteorol. Soc. 93, 485–498. https://doi.org/10.1175/BAMS-D-11-00094.1

Teutschbein, C., Seibert, J., 2012. Bias correction of regional climate model simulations for hydrological climate-change impact studies: Review and evaluation of different methods. J. Hydrol. 456–457, 12–29. https://doi.org/10.1016/j.jhydrol.2012.05.052

Thomson, A.M., Calvin, K. V., Smith, S.J., Kyle, G.P., Volke, A., Patel, P., Delgado-Arias, S., Bond-Lamberty, B., Wise, M.A., Clarke, L.E., Edmonds, J.A., 2011. RCP4.5: A pathway for stabilization of radiative forcing by 2100. Clim. Change 109, 77–94. https://doi.org/10.1007/s10584-011-0151-4

Todini, E., 1996. The ARNO rainfall-runoff model. J. Hydrol. 175, 339–382. https://doi.org/10.1016/S0022-1694(96)80016-3

Utsumi, N., Seto, S., Kanae, S., Maeda, E.E., Oki, T., 2011. Does higher surface temperature intensify extreme precipitation? Geophys. Res. Lett. 38, 1–5. https://doi.org/10.1029/2011GL048426

Wasko, C., Nathan, R., 2019. Influence of changes in rainfall and soil moisture on trends in flooding. J. Hydrol. 575, 432–441. https://doi.org/10.1016/j.jhydrol.2019.05.054

Wasko, C., Nathan, R., Peel, M.C., 2020. Changes in Antecedent Soil Moisture Modulate Flood Seasonality in a Changing Climate. Water Resour. Res. 56, no. https://doi.org/10.1029/2019WR026300

Wasko, C., Sharma, A., 2017. Global assessment of flood and storm extremes with increased temperatures. Sci. Rep. 7, 1–8. https://doi.org/10.1038/s41598-017-08481-1

Wasko, C., Sharma, A., 2015. Steeper temporal distribution of rain intensity at higher temperatures within Australian storms. Nat. Geosci. 8, 527–529. https://doi.org/10.1038/ngeo2456

Wasko, C., Sharma, A., Lettenmaier, D.P., 2019. Increases in temperature do not translate to increased flooding. Nat. Commun. 10, 4–6. https://doi.org/10.1038/s41467-019-13612-5

Wasko, C., Sharma, A., Westra, S., 2016. Reduced spatial extent of extreme storms at higher temperatures. Geophys. Res. Lett. 43, 4026–4032. https://doi.org/10.1002/2016GL068509

Watanabe, M., Suzuki, T., O'Ishi, R., Komuro, Y., Watanabe, S., Emori, S., Takemura, T., Chikira, M., Ogura, T., Sekiguchi, M., Takata, K., Yamazaki, D., Yokohata, T., Nozawa, T., Hasumi, H., Tatebe, H., Kimoto, M., 2010. Improved climate simulation by MIROC5: Mean states, variability, and climate sensitivity. J. Clim. 23, 6312–6335. https://doi.org/10.1175/2010JCLI3679.1

Westra, S., Fowler, H.J., Evans, J.P., Alexander, L. V., Berg, P., Johnson, F., Kendon, E.J., Lenderink, G., Roberts, N.M., 2014. Future changes to the intensity and frequency of short-duration extreme rainfall. Rev. Geophys. https://doi.org/10.1002/2014RG000464

Yin, J., Gentine, P., Guo, S., Zhou, S., Sullivan, S.C., Zhang, Y., Gu, L., Liu, P., 2019. Reply to 'Increases in temperature do not translate to increased flooding.' Nat. Commun. 10, 1–5. https://doi.org/10.1038/s41467-019-13613-4

Yin, J., Gentine, P., Zhou, S., Sullivan, S.C., Wang, R., Zhang, Y., Guo, S., 2018. Large increase in global storm runoff extremes driven by climate and anthropogenic changes. Nat. Commun. 9.

https://doi.org/10.1038/s41467-018-06765-2

Yu, G., Wright, D.B., Li, Z., 2020. The Upper Tail of Precipitation in Convection-Permitting Regional Climate Models and Their Utility in Nonstationary Rainfall and Flood Frequency Analysis. Earth's Futur. 8, 1–18. https://doi.org/10.1029/2020EF001613

Zaninelli, P.G., Menéndez, C.G., Falco, M., López-Franca, N., Carril, A.F., 2019. Future hydroclimatological changes in South America based on an ensemble of regional climate models. Clim. Dyn. 52, 819–830. https://doi.org/10.1007/s00382-018-4225-0

Zheng, H., Chiew, F.H.S., Charles, S., Podger, G., 2018. Future climate and runoff projections across South Asia from CMIP5 global climate models and hydrological modelling. J. Hydrol. Reg. Stud. 18, 92–109. https://doi.org/10.1016/j.ejrh.2018.06.004